Charged Glycopolymer Materials for Epidermolysis Bullosa

A Thesis
SUBMITTED TO THE FACULTY OF
UNIVERSITY OF MINNESOTA
BY

William S. Boyle

IN PARTIAL FULFILLMENT OF THE REQUIREMENTS
FOR THE DEGREE OF
DOCTOR OF PHILOSOPHY

Theresa M. Reineke

September, 2017

Dedication

For my parents.

And for Elyse, whose daily encouragement and support got me through.

Abstract

Improved delivery of therapeutic nucleic acid payloads to cells could lead to dramatically improved clinical outcomes for patients suffering from genetic disorders. This work focuses on the use of a trehalose-containing cationic glycopolymer, termed Tr4, to transfect clinically relevant cell types. In particular, the development of gene delivery methods to improve the transfection of cell types associated with the skin disease epidermolysis bullosa are investigated. The sulfated glycosaminoglycan, heparin, is show to form ternary complexes with pDNA and Tr4 leading to dramatically increased transfection efficiency in primary fibroblasts, induced pluripotent stem cells, HepG2, and U87-MG cells. This increase is not caused by improved uptake, but instead appears to be driven by improved intracellular trafficking of polyplexes compared transfection without heparin. Increasing the size of the plasmid cargo from 4.7 kbp to a more therapeutically relevant 10 kbp leads to the complete loss of transfection efficiency in Tr4-heparin transfection of primary fibroblasts and a reduction in transfection efficiency in iPSCs. Co-transfecting with additives meant to increase nuclear localization of the pDNA recovers the efficiency lost by increasing the plasmid size. These techniques allowed for the development of function transfection methods in iPSCs delivering a synthetic transcription activator of collagen type VII. Finally, nanofiber mats containing chondroitin sulfate were developed to scavenge inflammatory molecules from wound exudate.

Table of Contents

List of Tables

List of Figures

Chapter 1: Introduction of Polymeric Gene Delivery and Epidermolysis Bullosa

Synopsis

This chapter contains background information on polymeric gene delivery, also known as transfection. The process of gene delivery to cells *in vitro* is described, and intracellular and extracellular barriers to gene delivery are described. Cationic polymers have the ability to form electrostatic complexes with DNA. These complexes compact DNA, protect it from degradation, and promote interaction with anionic species on the surface of the cell. Electrostatic and occasionally receptor-specific interactions can drive uptake into the cell. Vehicles can also promote endosomal escape and effect nuclear localization of the DNA. Industrially and academically important polymeric gene delivery vehicles are discussed. Epidermolysis bullosa, a rare skin disease characterized by severe blistering caused by defects in the structural proteins of the basement membrane is also introduced. Specific challenges associate with epidermolysis bullosa gene therapy are discussed.

1.1 Introduction

Nucleic acids such as small interfering RNA (siRNA), and plasmid DNA (pDNA) have shown show promise as potential therapies for many genetic diseases. Manipulation of the genome has the potential to provide control over the most basic processes in the cell that lead to protein expression.[1] Due to the specific control of protein expression that gene therapy affords, cancer treatments could be developed that are more effective than current treatments, and result in fewer, less harmful side effects. The recent development of easy to use gene editing technologies such as CRISPR-Cas9[2-5], TALEN[6-8], and the Sleeping Beauty transposon[9] provide a path towards fixing defects in a patient's genome leading to permanent, side effect free cures to a variety of diseases. Additionally, gene therapy could provide a path to a cure for devastating incurable inherited diseases such as Huntington's disease, as well as viral infections.[1]

One important obstacle to the use of nucleic acids in therapeutic settings is delivery of the gene to the desired target.[10] In order for any nucleic acid-based therapy to be effective, it must be delivered to the cell. Systemic delivery cannot usually be achieved by simply injecting the naked gene into the blood stream.[10] Naked nucleic acid can be cleared by kidney filtration, aggregation with proteins, or clearance by the immune system.[10] Even when complexed with cationic polymers, the salt concentrations (150 mM) found in the in vivo environment can lead to aggregation of cationic complexes which can block blood vessels.[11] In an attempt to overcome these obstacles, the gene delivery field has moved towards delivery vehicles to help stabilize the nucleic acid in the blood, protect it from immune system recognition, and help deliver it across

the cell membrane.[10] While *in vivo* delivery is necessary for many applications, the use of *ex vivo* transfections to develop cell therapies has also shown promise in the clinic. In either case, improved understanding of transfection *in vitro* could lead to the development of improved cell therapies in the short term and the development of more effective in vivo delivery vehicles in the long term. In order for delivery to be successful, nucleic acids (NAs) must be complexed with a carrier, protected from aggregation or decomplexation triggered by salts and serum proteins, delivered across the cell membrane, and trafficked through the cell to the nucleus.[12] Complexation, cellular uptake, and nuclear delivery are all important factors to consider when developing gene delivery vectors, and each provides unique challenges to consider.

Polyplex Formation

Nucleic Acid
(pDNA)

Cationic Glycopolymer

Polyelectrolyte
Complex
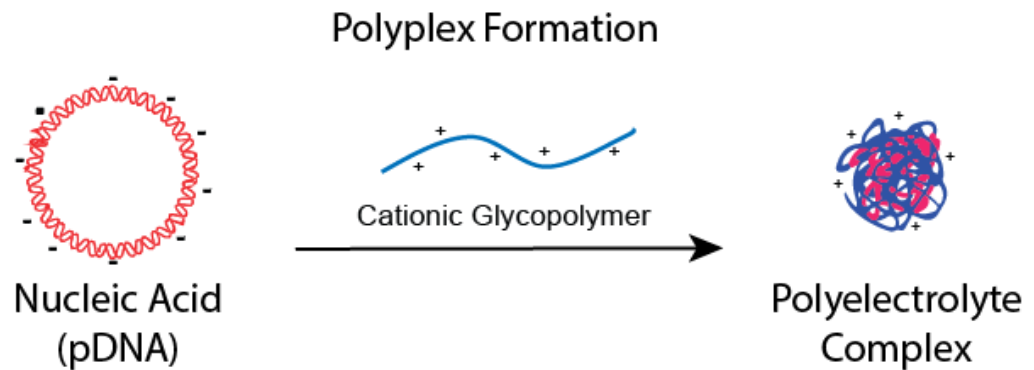
Figure 1.1: Schematic representation of polyelectrolyte complex (polyplex) formation with a polycation and pDNA.

1.2 Complexation

Due to the large size and the highly negative charge of nucleic acids, efficient delivery of free nucleic acids into cells and tissues is nearly impossible in cases where electroporation cannot be used.[12] To overcome this obstacle, the nucleic acid is complexed with a delivery vehicle. (Figure 1.1) The nucleic acid can be complexed with

non-viral vectors such as cationic polymers and nanoparticles, or with viral vectors. Specific types of gene delivery vectors will be discussed in detail in a later section. Nucleic acid complexation serves multiple functions. First, it compresses NAs to a smaller size that is more efficient for delivery.[12] Depending on the method of complexation, NA carriers can range in size from tens to hundreds of nanometers.[12] When polymers are used to complex NAs, the resulting complex is referred to as a "polyplex." Polyplexes can be formed at various ratios of polymer to nucleic acid. The ratio is expressed as the N/P ratio; given by the ratio of nitrogen (from the polymer) to phosphorous (from the nucleic acid) used in the formulation. Condensing the NA to this size contributes to the polyplex's ability to traffic through the cell and penetrate the cell membrane more easily (or the blood stream for *in vivo* applications). Designing delivery vehicles that complex nucleic acids effectively and stably is important to ensure that delivery is achieved.

1.3 Cellular Uptake

After delivery to the surface of the cell, the polyplex must help encourage cellular uptake of the nucleic acid cargo. Cellular uptake can occur via different processes depending on whether or not the polyplex is targeted. For untargeted polyplexes, it has been shown that the driving force to cellular uptake is electrostatic interaction of the cationic delivery vehicle with negatively charged glycosaminoglycans (GAGs) in the cell membrane.[13] However, internalization via GAGs does not necessarily lead to gene expression, indicating that GAGs promote internalization into compartments that do not necessarily lead to gene expression.[14] Positively charged carriers also tend to aggregate in the presence of physiological salt concentrations and serum proteins.[11,15] Other research

4

has shown that untargeted polyplexes can be internalized through a number of other routes. Behr et al. have shown that cellular uptake can occur via a process driven by actin where cationic complexes interact with positively charged proteoglycans which then form cholesterol-rich rafts which are pulled into the cell.[16] Additionally, Pinchon et al showed that HepG2 cells can endocytose polyplexes via either clarthrin-dependent endocytosis, or by macropinocytosis, but that only clathrin dependent endocytosis lead to gene expression..[17] This indicates that clathrin dependent endocytosis should be a focus for gene delivery since it encourages eventual transcription. However, productive endocytic pathways of polyplexes can vary based on cell type and vehicle. Understanding how particles are endocytosed, and what pathways lead to productive expression can be very important for the development of new vehicles for a given cell type.

Polyplexes can also be decorated with encapsulation ligands that bind preferentially to desired cells, and encourage endocytosis. Many encapsulation ligands, including transferrin, asialoglycoprotein, epidermal growth factor, folate, integrin, lactose, and mannose, have been studied.[18] It has been shown that once these ligands bind to the cell's surface, they frequently encourage clathrin dependent endocytosis. This indicates that while the primary benefit of encapsulation ligands is their ability to target and encourage internalization into desired cell lines, they also could encourage encapsulation pathways that eventually encourage gene expression. The use of glycosaminoglycans to modify vehicle interaction with the cell surface has also been studied.[19-21] These molecules have been shown to promote receptor mediated endocytosis

5

in some cell types. However, their effect on how the cells process the polyplexes after internalization has not been extensively studied.

After internalization, the polyplexs are usually trafficked to the endosome. Endosomes are membrane bound vesicles that are responsible for trafficking cargo within the cell after endocytosis.[22] The endosomal environment tends to be acidic compared to the rest of the cell.[23] Usually, the endosome will traffic the polyplex to the lysosome where enzymes and the acidic environment will destroy foreign genetic material, rendering many therapeutic molecules useless.[24] For this reason, encouraging endosomal escape is vital for successful gene delivery. While the mechanism for endosomal escape is not well understood for many polymers, it has been hypothesized that delivery vehicles with amines with low pK_a's such as PEI have the ability to act as a buffer when inside the endosome resulting in swelling, and eventual lysing of the endosome.[25] This is referred to as the proton sponge hypothesis, and it can in some cases provide a good model for future development of polymers for gene delivery.[25] However, later work has shown that it is not applicable in all cases.[26]

1.4 Nuclear localization

After the polyplex has been delivered to the cytoplasm, it must still overcome obstacles before gene expression can take place. (Figure 1.2) Because of its large size, DNA cannot diffuse through the cytosol on its own. Additionally, free NAs can be broken down in the cytoplasm. For these reasons, NAs must frequently remain complexed until they are delivered to the nucleus. To further encourage nuclear localization, nuclear localization sequences (NLS) have been used, but their effectiveness has been shown to be minimal.[27] The nuclear envelope is the final barrier that polyplexes

must cross in order to effect gene expression. Passive diffusion of most polyplexes through the nuclear envelope is not possible due to small size of the pores in the nuclear envelope.[28] However, Dowty et al. have showed that genetic material can be actively transported across the nuclear membrane in a manner similar to proteins.[29] Because of the myriad obstacles to nuclear uptake in postmitotic cells, mitotic cells frequently exhibit higher gene expression. This is likely due to the disruption of the nuclear envelope that occurs during mitosis.[30] While the processes and mechanisms of nuclear localization and uptake are not well understood, they are important to consider when designing a gene delivery vector.
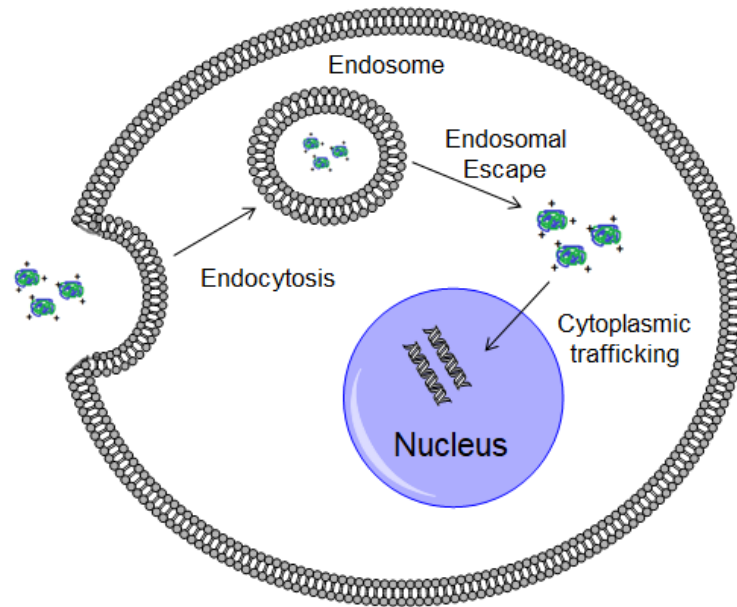
Figure 1.2: Polyplex mediated transfection at the cellular level. Polyplexes enter the cell through endocytosis, must escape the endosomal prior to lysosomal degradation, and then traffic to the nucleus where DNA can be expressed.

1.5 Viral Vectors

Viral vectors have shown remarkably high transfection efficiency, as well as high specificity and have shown promise as gene delivery vehicles in many clinical trials. Even though viral delivery allows for efficient, specific delivery, it suffers from serious drawbacks. Viruses have been known to promote insertional mutagenesis, which has been linked to cancer in clinical trials, and cause severe, potentially fatal, immune responses in patients.[31] Additionally, many viral vectors such as AAV are limited in their ability to deliver large plasmids. The upper limit of plasmid size for AAV is generally considered to be around 5 kb.[32] This limits their ability to deliver Cas9 plasmids which are generally ~10 kb.[3] The complete replacement of large gene like COL7A1 (~30 kb) would not be possible with AAV delivery.[33] In contrast to viruses, polymeric vehicles could be designed to limit interaction with the immune system, and theoretically should be able to complex any size plasmid. For these reasons, extensive research is being conducted into non-viral vectors in spite of their lower delivery efficiency.

1.6 Gene Editing Technologies

In addition to transient protein replacement, the use of gene editing technologies to permanently edit the genome of a cell provides access to the treatment of a variety of diseases that result from errors in the genome.[31] Many different methods of editing the genome have been developed, but most of them still require the delivery of pDNA to express an enzyme, transposon, or nuclease that can then edit the genome.[4,7,9] For CRISPR-Cas9 editing, the Cas9 protein must be present in the cell in order to achieve editing. In many cases, this is achieved via the delivery of pDNA that codes for Cas9 as well as the targeting gRNA.[2,4,5,34] Additionally, if gene editing is desired, the donor

template (also a nucleic acid) must be delivered so that it can be incorporated into the genome via homology directed repair.[5] Plasmids that code for Cas9 enzyme are typically around 10 kB in size[3-5], and donor templates can range from tens of base pairs to many kilobase pairs (kbp) depending on the type of template and the gene being corrected.[7,35,36] Many virus-based delivery vehicles have size limits that make the delivery of large plasmids impossible.[32] The development of non-viral delivery vehicles that can efficiently deliver large plasmids in disease-relevant cell types could lead to improved treatments of many diseases in the clinic. While vehicles that efficiently delivery DNA nonspecifically to most cells could lead to improved therapeutic outcomes, each disease presents different challenges associated with tissue and cell type-specific delivery, and differing genetic payloads. For this reason, a holistic approach to gene delivery in a disease of interest may be appropriate for many applications.

1.7 Disease Target: Epidermolysis Bullosa

The main focus of this work is the skin disease epidermolysis bullosa (EB). Epidermolysis bullosa is a group of rare genetic disorders characterized by loss of integrity of the basement membrane of the skin.[37] Recessive Dystrophic EB (RDEB) is caused by a mutation in the COL7A1 gene which codes for type VII collagen. Both recessive and dominant forms of DEB exist, but the recessive form is generally more severe. Junctional epidermolysis bullosa (JEB) is another variant of the disease that is caused by a mutation in laminin 3. Symptoms of DEB include separation of the dermis, blistering and scarring. These symptoms are present at birth, and patients suffer from severely limited life expectancy. Most RDEB patients eventually develop a particularly

aggressive variety of squamous cell carcinoma known as RDEB-SCC. As of 2016, nearly 80% of patients suffering from RDEB succumb to RDEB-SCC by age 45.[38] The progression of RDEB-SCC is not well understood, and efforts are underway to slow it's progression in patients with RDEB. However, improved treatment of the underlying condition is likely the only way to prevent it entirely. While bone marrow transplant is curative in patients who can find matched donors, physicians are largely limited to palliative care.[37,39] However, promising progress has been made using gene therapy to develop autologous cell therapies and improved strategies for gene editing.[39]

In a clinical study in 2010, the patients presenting with recessive DEB were treated with allogeneic stem cell transplantation in an attempt to encourage proper collagen formation.[39] The patients were treated with stem cells from a sibling donor. Results from the study were quite promising as all 7 patients treated with transplants exhibited improved wound healing. However, transplants from other individuals carry greater risks than infusions of the patients own stem cells. Gene therapy is challenging in EB patients for a variety of reasons. The skin represents the largest organ in the body, and systemic delivery of a therapeutic is difficult. In addition, transfection of primary human fibroblasts, one of the main cell types responsible for secreting basement membrane structural proteins, is challenging compared to other faster dividing cell types. The development of improved transfection methods in patient primary fibroblasts and induced pluripotent stem cells (iPSCs) could provide a path toward effective cell therapies that are safer, cheaper, and less invasive than bone marrow transplant. However, the development

of a gene delivery vehicle capable of efficiently delivering plasmid to the patient's stem cells with minimal toxicity is necessary.

1.8 Polymers for Gene Delivery

Poly(L-lysine) (PLL)
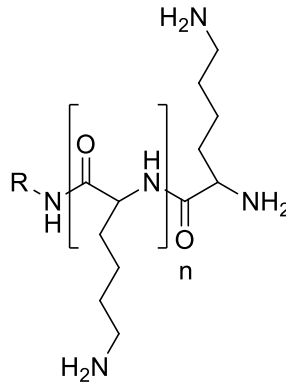
Figure 1.3: Structure of Poly(L-lysine)

Poly(L-lysine) was shown to efficiently complex DNA as early as 1975.[40] Over time, it has been used as a gene delivery vector both *in vitro* and *in vivo*.[41,42] The synthesis of PLL proceeds by a ring opening polymerization that can be controlled by altering the ratio of monomer and initiator present in the reaction pot.[43,44] While PLL has shown promise as a gene delivery vector, it suffers from various drawbacks. Firstly, it does not buffer the endosomal environment, and as a result cannot escape the endosome after uptake, and instead tends to traffic to the lysosome where genetic material is degraded.[45] In addition, PLL exhibits higher than optimal cytotoxicity. This is likely due to disruption of the cell membrane by the cationic polymers as endocytosis occurs.[46] High molecular weight PLL does not promote nuclear penetration, and is only effective at transfecting mitotic cells.[47] Finally, polyplexes formed from PLL tend to aggregate when dispersed in high ionic strength solutions.[48] Many of these drawbacks can be partially or

11

completely overcome by forming copolymers of PLL with PEG.[49] The PEG shields the polyplex from salt-induced aggregations, and prevents digestion by enzymes.[50],[51] The use of PEG and other substances to shield the polyplex has become an important technique for gene delivery that is used in a variety of situations.

Polyethyleneimine (PEI)

$$H_2N \left[\begin{array}{c} \\ \overset{\displaystyle N}{\underset{\displaystyle H}{|}} \end{array} \right]_n NH_2$$
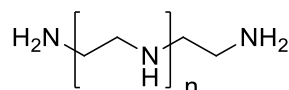
Figure 1.4: Structure of Polyethyleneimine

First used in 1995, polyethyleneimine (PEI) is among the most successful commercial polymeric gene delivery agent that has developed thus far. It can be synthesized in either linear or branched geometry, each of which has different gene delivery properties.[12] Linear PEI is sold commercially as a transfection agent under the trade name jetPEI for use in vitro and in vivo.[52] Linear PEI can be synthesized in a controlled manner by ring opening of 2-ethyl-2-oxazoline.[53] It has been shown to utilize the proton sponge effect to induce endosomal escape.[25] The buffering capacity of the secondary amines in the backbone of PEI leads to swelling, and eventual lysis of the endosome. This leads to improved gene expression compared to PLL. In spite of its wide spread use, PEI does suffer from important drawbacks. First, the proton sponge effect may not hold for all cell types. Additionally, like PLL, it tends to aggregate in serum due to its positive charge, which inhibits its effectiveness *in vivo*.[54] Further, it exhibits very high cytotoxicity which increases as the molecular weight increases.[55] PEI's cyctotoxicity had been attributed to two factors. First, destabilization of the cell membrane during transfection due to PEI's high charge density can lead to cell death. Additionally, free

12

residual PEI left over after transfection can stress cells resulting in cell death.[56] Membrane destabilization can be negated by copolymerizing the PEI with neutral monomers such as carbohydrates.[57] Toxicity due to residual PEI has been addressed by incorporating biodegradable groups, such as disulfide bonds, which are cleaved by glutathione once inside the cell or acid hydrolysable groups such as esters, into the chain.[58] These modifications have shown considerable promise, and provide directions for future research in gene delivery.

Carbohydrate Polymers

Carbohydrate polymers have shown significant promise as drug delivery vehicles. Carbohydrates have been shown to significantly reduce the cytotoxicity of gene delivery vectors by lowering the charge-density along the polymer backbone.[59] It has also been shown that incorporating some carbohydrates into the polymer backbone leads to biodegradable polymers, additionally limiting cytotoxicity, and encouraging gene expression by allowing the release of genetic material once inside the cell.[60] Many different carbohydrates, including glucose, galactose, trehalose, cyclodextrin, and others, when copolymerized with cationic polymers have been used to decrease polyplex toxicity with a minimal decreases in efficiency.[61,62,63,57,59]

Polyglycoamidoamines (PGAAs) represent a particularly successful example of a carbohydrate polymer for gene delivery.[61] In particular, Glycofect[TM] has shown to cause minimal cytotoxicity and transfection efficiency on par with PEI.[61] Interestingly, increasing the buffering capacity of PGAAs does not necessarily result in increased transfection efficiency.[64] This result calls into question the validity of the proton sponge

13

theory. Instead, the driving force for delivery in PGAAs appears to be the biodegradability of the polymers.[60] It appears that the polymers biodegradation at physiological pH results in release of the DNA which then results in transcription.[60] Further work has shown that endocytosis of PGAAs appears to proceed largely via a caveolae-mediated process with some help from clathrin and macropinosomes.[65]

1.9 Step Growth Polymerization

$$A-A \quad + \quad B-B \quad \longrightarrow \quad A-A-B-B \quad \Longrightarrow \quad \left[A-B \right]_n$$
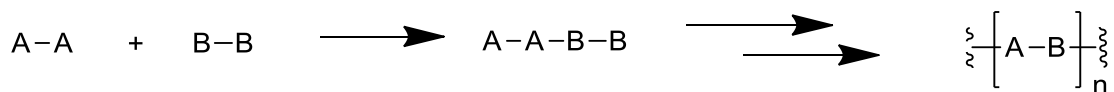
Scheme 1.1: Step Growth Polymerization

Step growth polymerization is a widely used technique for the synthesis of polymers in industry and academia. In a step growth polymerization, two different bifunctional monomers or one bifunctional monomer containing different reactive functional groups are reacted to form a perfectly alternating AB polymer as seen in scheme 1.[66] Step growth polymerization is ideal for the synthesis of polycations for gene delivery because it affords precise control over the number of charged units in sequence on the chain which can have significant impact on the efficacy and toxicity of the polymer.[67] While the reaction cannot afford the degree of control over molecular weight and dispersity seen in living polymerizations such as RAFT or ATRP, some control over the reaction can be attained by using Carother's equation (equation 1) where DP is the degree of polymerization, r is the ratio of monomer A to monomer B, and p is the percent conversion.[66]

$$2DP = \frac{1+r}{1+r-2rp} \quad (1)$$

14

When the ratio of monomer A to monomer B is offset, and conversion goes to 100%, (p=1) equation 1 reduces to equation 2.[66]

$$2DP = \frac{1+r}{1-r} \quad (2)$$

Using this equation, the degree of polymerization can be controlled by controlling the feed ratio of monomer A to monomer B. Because the polymerization control depends on precisely controlling the monomer feed ratio, it is essential that each monomer be as pure as possible.

Due to the kinetics of the reaction, in order for high molecular weight polymers to be synthesized, extremely high conversions (>90%) are required. In order to achieve such high conversions, reactions that proceed efficiently in high yields must be used.[66]

1.10 Azide-Alkyne Huisgen cycloaddition
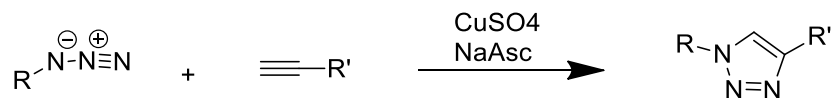
Scheme 1.2: Copper (I) Catalyzed Azide-Alkyne Cycloaddition

One such reaction is the azide-alkyne Huisgen cycloaddition reaction, also known as the azide-alkyne click reaction. This reaction proceeds by the reaction of a terminal alkyne with an azide to give a 1,2,3-triazole.[69] The variant of the reaction used in this work, shown in scheme 2, is catalyzed by copper(I) which is formed from a reaction of copper(II) sulfate and the reducing agent, sodium ascorbate in situ.[70] It is one of the most widely used reactions in click chemistry, and it has been shown to afford nearly quantitative conversion.[70] Since it is such a favorable reaction, it is a fantastic candidate for step growth polymerization using a diazide and a dialkyne. This polymerization has

been shown to be effective in multiple systems.[71,63,72] The use of protected diazido-trehalose and dialkynl oligoamine followed by subsequent deprotection allows for the formation of a cationic, trehalose-containing polymer that has been shown to efficiently transfect many different cell types.[63]
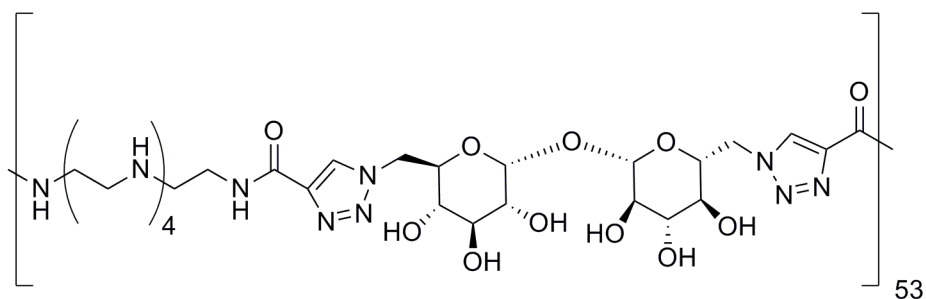
Figure 1.5: Structure of Tr4

1.11 Thesis Outline

This work describes the development of improved gene delivery methods in cell types relevant to epidermolysis bullosa. We use a trehalose-containing polymer containing four charged amines per repeat unit, termed Tr4.[63] Previous work has shown that Tr4 may have promise as a transfection reagent in a wide variety of cell types.[73] The use of Tr4 polymers end-capped with cationic dialkyne monomer has been shown to improve transfection in Hela cells.[71] Based on the promise Tr4 has shown in a variety of in vitro experiments, we investigated a variety of formulations of Tr4 in cell types that are relevant to epidermolysis bullosa. The sulfated glycosaminoglycan, heparin can dramatically increase transfection by coating Tr4 polyplexes leading to improved transfection in primary fibroblasts as well as a variety of other cell types. We also studied the ability of Tr4 to transfect primary fibroblasts and iPSCs as a function of plasmid size with the goal of eventually delivering Cas9 plasmids for gene editing. We further

16

investigate the use of Tr4 and Tr4-heparin polyplexes to deliver therapeutically translatable vehicles, and their ability to transfect the skin when applied topically to a wound in a murine model. Finally, we report the development of glycopolymer-derived nanofiberous materials designed to combat inflammation and slow the progression of RDEB-SCC.

Chapter 2: Heparin Enhances Transfection in Concert with a Trehalose-Based Polycation with Challenging Cell Types

Synopsis

Improving the delivery of nucleic acids to diverse tissue types in culture is important for translating genome editing for regenerative cell therapies. Herein, we examine the effect of transfection media additives, such as the sulfated glycosaminoglycans, in dramatically increasing pDNA delivery efficiency and transgene expression in a wide variety of cell types. Polyplexes formed by combining pDNA and Tr4, a cationic glycopolymer containing repeated trehalose and pentaethylenetetramine groups, were treated with low concentrations of heparin prior to *in vitro* transfection with plasmid DNA. Polyplex formulations were found to be stable and form ternary complexes upon heparin addition according to dynamic light scattering and ethidium bromide dye exclusion assays. Heparin-coated polyplexes offer significant increases (approximately 4-fold) in GFP expression compared to polyplexes prepared with Tr4 only in primary fibroblasts, U87, and HepG2 cells. Heparin was also shown to increase GFP expression in a linear dose-dependent manner. The heparin-treated Tr4 polyplexes exhibited more than 50% higher cellular internalization with HepG2 cells while showing minimal increases with U87 and primary fibroblasts. Pharmacological inhibition was used to further understand the endocytic pathways taken during transfection in the presence and absence of heparin. It was found that heparin-treated polyplexes are endocytosed primarily through macropinocytosis and clathrin-mediated pathways while Tr4 polyplexes without heparin appear to be internalized primarily via caveolae. Heparin

appears to also modify the nuclear localization behavior of Tr4 polyplexes, which likely

contributes to increased efficiency and transgene expression.

This chapter was adapted with permission from the references below. Copyright

2017 American Chemical Society

Boyle, W. S.;Senger, K.;Tolar, J.; Reineke, T. M. *Biomacromolecules*, **2017**, *18* 56-67.

http://pubs.acs.org/doi/abs/10.1021/acs.biomac.6b01297

2.1 Introduction

The cellular delivery of genetic material is central to the advancement of many scientific and medical fields ranging from gene and cell therapies for regenerative medicine to genome engineering of animals and plants to improve research and development of food sources medical treatments.[12] While many advances in the field of gene and cell therapy are resulting in promising clinical outcomes[74-77], the design of effective delivery methods still remains challenging. Many different approaches have shown promise including viral vectors, liposomes, electroporation, and synthetic polymers.[74,77,78] However, no one technique has provided an ideal transfection procedure for this diversity of functions; indeed delivery systems typically need to be optimized for each specific application. Viral vectors, while very effective, are costly to produce on a large scale and in some cases can elicit immune and inflammatory responses.[31,79-81] Electroporation is highly efficient in many cell types, particularly *in vitro,* but frequently results in low cell survival,[82] and the utility of this technique *in vivo* is minimal.[12] To this end, the customizability of nonviral delivery methods such as cationic lipids or polymers provides a unique opportunity to tailor the chemistry of delivery vehicles to specific cell types, applications, and disease targets. To this end, many nonviral methods are being examined to supplement the suite of vehicles for clinical nucleic acid delivery.[74,83]

Polycation transfection agents typically function by forming complexes with negatively charged nucleic acids, which is entropically driven through the release of counterions.[67,84,85] These complexes, termed "polyplexes", compact nucleic acids into positively charged nanocomplexes that protect nucleic acid cargo from aggregation with

serum proteins and degradation and also result in an increased diffusion coefficient[12]. In addition, these complexes facilitate electrostatic interactions with the cell membrane and intracellular transport.[86] Polyplexes may also be functionalized to target receptors on the cell surface to increase specificity in delivery.[74] However, many early polymeric vehicles, such as polyethyleimine have been shown to exhibit significant toxicity, largely due to their high charge density; this can lead to undesired membrane lysis, interaction with/interruption of organelles such as mitochondria, and triggering of apoptotic signaling pathways.[87-90] While most transfection studies and optimization of nonviral vehicles have been conducted on immortalized cell lines, primary cells are a more relevant biological model and of particular importance for the development of regenerative cell therapies.[7,91-93] For example, the transfection of primary fibroblasts is of particular interest for skin grafts.[94] Also, this cell type can be reprogramed to induced pluripotent stem cells (iPSCs) which have a variety of important clinical and research applications.[95]

Previous work in our laboratory has focused on the incorporation of carbohydrates into the backbone of polycations, which leads to a decrease in the toxicity associated with polycations (such as jetPEI) without sacrificing performance.[59] Carbohydrates such as glucose, β-cyclodextrin, and trehalose have all been utilized and shown to promote stable polyplex formation and high transfection of a variety of nucleic acid types.[57,63,96] In particular, trehalose (Tr)-based polycations (denoted by Tr#, where # indicates the number of ethyleneamines between the trehalose units) have achieved high transfection of pDNA and siRNA, and provide the unique ability to stabilize formulations

during lyophilization.[59,97,98] Srinivasachari et al. first created trehalose-based oligoethyleneamine delivery vehicles with 1-4 ethyleneamines between the trehalose groups along the backbone and demonstrated high delivery efficacy of pDNA with motifs containing 3 and 4 ethyleneamines (Tr3 and Tr4).[63] Follow up work by Kizjakina et al. further extended the design motif to 5 and 6 ethyleneamines (Tr5 and Tr6).[59,73] That work concluded that the polymer with 4 ethyleneamine repeat units between trehalose units (Tr4) exhibited high transfection efficiency as well as low toxicity in rat mesenchymal stem cells and HDFn (primary human fibroblast) cells. The Tr4 polymers exhibited the ability to complex pDNA into polyplexes, and were highly stable to aggregation in the presence of serum compared to JetPEI[TM]. In other studies, Anderson et al. were able to show that endgroup functionalization of Tr4 could alter transfection properties and Xue et al. were able to demonstrate efficacy of Tr4 for siRNA delivery.[71,99] Additionally, the low toxicity of Tr4 polyplexes allowed for higher N/P ratios [ratio of ionizable amines (polymer) to negatively charged phosphate (nucleic acid) groups] to be used (e.g., 50). Collectively, these studies have thoroughly demonstrated the high utility and promise of this polymer structure for a variety of nucleic acid delivery applications.

The mechanism of polyplex internalization formed with glycopolymers has also been extensively studied.[65,100] Glycosaminoglycans (GAGs) are negatively charged glycoproteins that make up the glycocalyx on the cell surface. These cell surface receptors have been shown to promote interactions with cationic polyplexes and trigger endocytosis.[14,19,101,102] At high concentrations, GAGs added to cell culture media have been shown to inhibit polyplex internalization. For example, in a study of the interaction

of PEI and polyglycoamidoamine polyplexes with surface GAGs, McLendon et al. showed that many GAGs, including heparin and heparin sulfate inhibit transfection by decomplexing polyplexes. When relatively high concentrations (60 μg/mL) of GAG are added to the polyplexes, they competitively bind the polycation and promote DNA release.[14] Further, Ruponen et al. have shown that hyaluronan and heparan sulfate also both inhibit transfection with JetPEI polyplexes even when they do not decomplex the polyplexes.[102] Conversely, Dreaden et al. have shown that hyaluronan-coated nanoparticles formed using a layer-by-layer process can interact with the CD44 receptor present on some cells to target desired tissues and promote endocytosis.[19] However, the hyaluronan-coated particals were specifically functional in cells that expressed CD44 such as Hep-G2 cells. More recently, other researchers in the Hammond lab have utilized a variety of different anionic polymers, including heparan sulfate, in concert with poly-l-lysine, to deliver drugs and small molecules. These results demonstrate the wide range of potential applications for glycosaminoglycans in gene and drug delivery.[21,103]
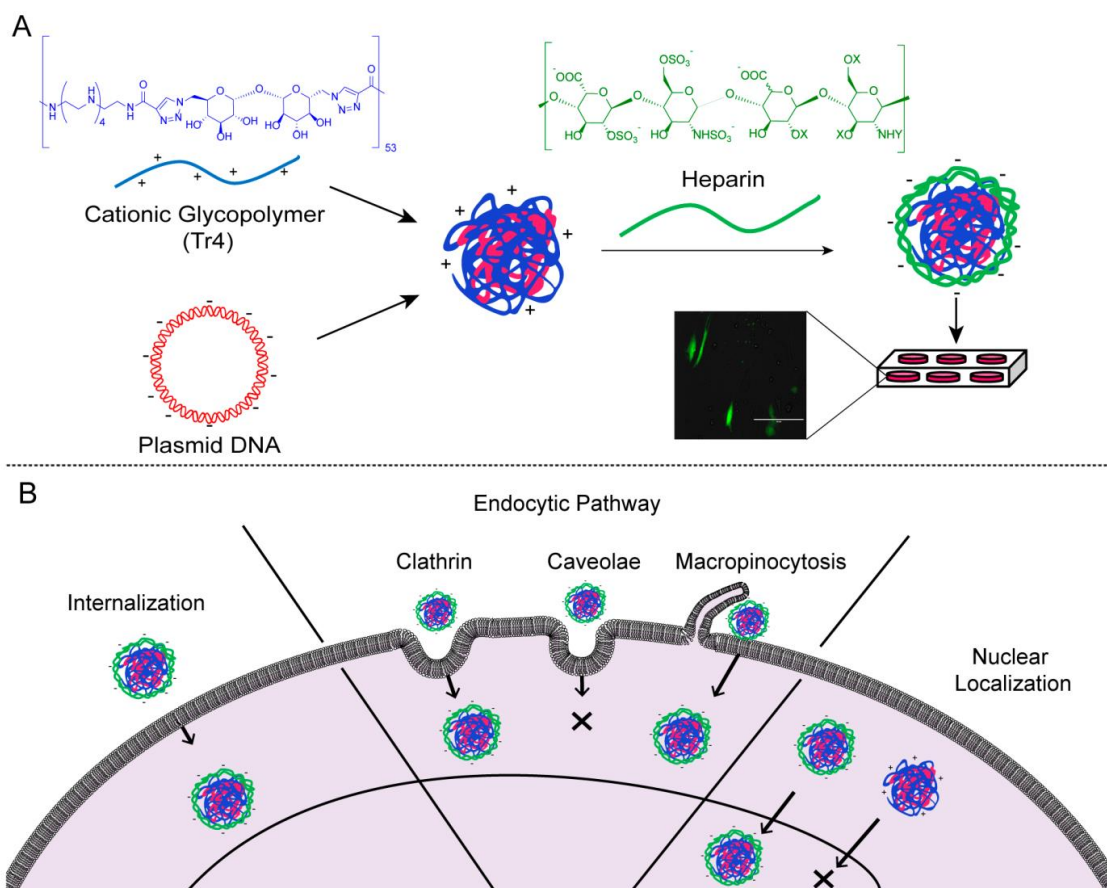
Figure 2.1: Schematic representation of the current study that demonstrates heparin-induced increase in transfection. (A) Polyplexes are formed with Tr4, a trehalose-containing glycopolycation, and then treated with heparin prior to transfection leading to significant increases in transfection efficiency measured by GFP reporter gene. (B) The effect of heparin on internalization, endocytic pathway, and nuclear localization has been studied in detail in PFB, HepG2, and U87 cells.

Herein, we explore the effect of media additives such as heparin, a panel of GAGs, and dexamethasone as enhancers to improve polyplex-based delivery of transgenes to cultured cells. In this work, we demonstrate that low concentrations (10 μg/mL in the dilution media, leading to a final concentration of 6.6 μg/mL) of sulfated GAGs, particularly heparin, increase transfection efficiency in a three diverse cell types: primary human fibroblasts (PFB), human hepatocellular carcinoma (HepG2), and human

glioblastoma (U87) cells) when used in concert with the Tr4 polycation previously developed in our lab (Figure 2.1a). This effect depends on the presence of sulfate groups present on GAGs. We hypothesize that the high polyplex stability afforded by the Tr4 vehicles allows ternary polyplexes to be formed (Tr4-pDNA polyplexes coated with anionic GAGs) at relatively low GAG concentrations. This interaction appears to improve cell surface binding, internalization, and more productive intracellular trafficking mechanisms of polyplexes to the nucleus, all leading to higher transgene expression (Figure 2.1b). This work provides new methodologies for more efficient delivery of plasmid DNA to different tissue types in culture. Indeed, the increased transfection efficiency in primary fibroblasts has potential for translation for improving research and development of regenerative cell therapies for a variety of inherited diseases.

2.2 Materials and Methods
General.

All chemical reagents were purchased from Sigma Aldrich Co. LLC. (St. Louis, MO), and used without further purification unless otherwise specified. D-Trehalose and pentaethylenehexamine were purchased from Acros Organics (Geel, Belgium). The pentaethylenehexamine was distilled prior to use. JetPEI was purchased from Polyplus-Transfection SA (Illkirch, France). PzsGreen GFP expressing plasmid was purchased from Aldeveron (Fargo, ND). Dulbecco's Modified Eagle Medium (DMEM), trypsin, phosphate buffered saline (PBS), UltraPure^{TM} DNase/RNase-Free distilled water (DI H$_2$O), Propidium Iodide (PI), non-essential amino acids (NEAA), fetal bovine serum (FBS), and antibiotic-antimycotic (Ab/Am) were purchased from Life Technologies-

Thermo Fischer Scientific (Carlsbad, CA). Heparin sodium salt from porcine intestinal mucosa (heparin), heparan sulfate sodium salt from bovine kidney, chondroitin sulfate A sodium slat from bovine trachea, dermatan sulfate, and hyaluronic acid were all purchased from Sigma Aldrich Co. LLC. (St. Louis, MO). Cellscrub[TM] was purchased from AMS biotechnology (Abingdon, UK). Human hepatocellular carcinoma (HepG2), and human glioblastoma (U87) cells were purchased from American Type Culture Collection (ATCC) (Manassas, VA). Primary Human Fibroblasts (PFBs) were obtained from skin biopsy of healthy donors using a previously published protocol.[7] All experiments on primary fibroblasts were done on cells below passage 12. Plasmids, (zsGreen and LacZ) were purchased from Aldevron (Fargo, ND)

Instrumentation.

NMR spectra were acquired using a Bruker Avance III HD 500 MHz spectrometer in D_2O (Cambridge Isotope Labrotories Inc., Andover, MD). NMR data was collected using Bruker Top Spin version 3.1. Gel permeation chromatography was performed using an Agilent 1260 High Performance Liquid Chromatograph. The mobile phase was 1.0 wt% acetic acid/0.1 M Na_2SO_4. Chromatography was performed using at a flow rate of 0.4 mL/min on size exclusion chromatography columns [CATSEC1000 (7 μ, 50 x 4.6), CATSEC100 (5 μ, 250 x 4.6), CATSEC300 (5 μ, 250 x 4.6), and CATSEC1000 (7 μ, 250 x 4.6)] (Eprogen Inc, Downers Grove, IL). Signals were obtained using Wyatt HELEOS II light scattering detector (λ=662 nm) and an optilab rEX refractometer (λ=658). Data analysis was performed using the Astra VI software package (version 5.3.4.18, Wyatt Technologies, Santa Barbara, CA). Polyplex size and

surface charge were analyzed using a Malvern Zetasizer Nano ZS. Ethidium bromide dye exclusion measurements were collected using a Biotek Synergy H1 plate reader (Biotek Instruments Inc, Winooski, VT). GFP expression and Cy-5 uptake were measured using a BD FACSverse[TM] flow cytometer (Becton Dickinson Biosciences, San Jose, CA) Confocal experiments were performed using a Zeiss Cell Observer SD Spinning Disk confocal microscope (Carl Zeiss AG, Oberkochen, Germany) equipped with a full environmental chamber at 37 °C and 5% CO_2 housed in the University of Minnesota University Imaging Center (UMN IUC).

Synthesis of Trehalose-Based Polymer.

Trehalose polymers were synthesized via a previously published method.[63,71,73] An excess of dialkyne was used to provide an alkyne-capped polymer with a targeted degree of polymerization of 45. The M_w and M_n were 39.2 kDa and 33.2 kDa (Đ=1.2) respectively which translates to an average of 53 repeat units.

Polyplex Formation.

Polyplexes were formed using the same method for every application using methods established by our group. [57,63] All polyplex solutions were formed in in DNase/RNase free water. Polymer solutions of the necessary concentration for the desired N/P ratio (ratio of positively charged nitrogen to phosphate) were slowly added to an equal volume of 0.02 mg/ml plasmid solution using an automatic pipette to yield a final pDNA concentration of 0.01 mg/ml. Polyplexes were allowed to incubate at room temperature for 1 hr prior to analysis or transfection.

Ethidium Bromide (EtBr) Dye Exclusion Assay.

Polyplexes were prepared in water at N/P ratios of 20 for Tr4 and 5 for PEI at a total volume of 100 μl with a DNA concentration of 0.01 mg/ml in a Corning Costar black flat-bottom 96-well plate (Sigma-Aldrich Co. LLC., St. Louis, MO). After a 1 hr incubation (to ensure binding and polyplex formation) at room temperature, the polyplexes were diluted 3x to a final pDNA concentration of 3.3 ng/μl with DMEM containing 4 μM EtBr and heparin. Heparin-containing solutions were formed with heparin at a final concentration of 6.67 ug/ml. Control solutions were also formed without heparin. Emission spectra were collected using a Biotek plate reader (excitation: 285 nm). Dye exclusion was quantified using the following equation[73] where F= maximum fluorescence intensity:

$$Dye\ Exclusion = 1 - \left(\frac{F_{sample} - F_{blank}}{F_{DNA\ only} - F_{blank}} \right)$$

Dynamic Light Scattering.

DLS was performed using a Malvern Zetasizer (Nano ZS) dynamic light scattering instrument (Malvern instruments, Malvern, UK) with a 4.0 mW 633 nm He-Ne laser and a scattering angle of 173°. Polyplexes were formed at the N/P 20 for Tr4 and N/P 5 for PEI in nuclease free H_2O in triplicate with a total volume of 100 μl, and allowed to equilibrate at room temperature for 1 hour. Polyplexes were then diluted with 200 μl DMEM containing 10% FBS with and without 10 μg/mL heparin (final concentration: 6.67 μg/mL). Measurements were taken at t = 0, 1, 2, 3, and 4 hours. Polyplex sizes were reported based the size distribution by intensity.

Zeta Potential.

Zeta potential measurements were taken on a Malvern Zetasizer (Nano ZS, Malvern Instruments, Malvern, UK) using the same settings as above. Measurements were acquired using disposable folded capillary cell cuvette. Polyplexes were formed at the desired N/P at a volume of 300 μl, and allowed to incubate for 1 hr. Following incubation, the polyplexes were diluted with 600 μl nuclease free PBS with and without 10 μg/mL heparin (final concentration: 6.67 μg.mL). After 3 minutes of equilibration, measurements were taken in triplicate and reported as an average.

GFP Expression Assays.

Prior to transfection, PFB, or U87, or HepG2 were plated in either a 24 well plate (U87 MG, HepG2) or a 12 well plate (PFBs) at a density of 5.0×10^5 cells per well. Cells were cultured in the appropriate media (DMEM with 10% FBS and 1% AB/AM for U87 and HepG2, and DMEM with 10% FBS, 1% l-glutamine, 1% NEAA, and 1% penicillin/streptomycin for PFB) for 24 hours at 37 °C at 5% CO_2. Polyplexes were formed at the necessary N/P ratios in H_2O with pzsGreen GFP expressing plasmid and allowed to incubate for 1 hr. Following incubation, polyplexes were diluted with cell culture medium with and without 10 μg/mL heparin. Cells were washed with PBS and treated with 300 ul of solution containing the polyplexes immediately after dilution. The total DNA dose for each well was 1 ug/well. Cells were incubated with polyplexes for 4 hours at 37 ° with 5% CO_2. After 4 hours, 1 mL cell culture media was added, and the cells were returned to the incubator. After 24 hours, media was removed, and replaced with 1 ml fresh media. Cells were then incubated for another 24 hours for HepG2 and

U87 MG cells, and 48 hours for the fibroblasts (48 and 72 hours total respectively). After the transfections were completed, cells were again washed with PBS, and treated with 300 µl trypsin for 3 min. The trypsin was then neutralized with 700 µl media, and the cell suspensions were transferred to BD falcon round bottom tubes. Cells were then pelleted, and media was removed. Pelleted cells were resuspended in 1 ml PBS, pelleted again, and resuspended in 400 µl PBS containing 1.25% v/v 7-AAD. Cells were incubated for 10 min at 0 °C, and analyzed on a BD FACSCalibur. The GFP and 7-AAD positive gates were set based on a cells-only control.

*Heparin Dose-Response Assay***.**

A heparin dose response assay was conducted in the same manner as the GFP assay reported above. Polyplexes were diluted with cell culture media containing 0, 0.5, 1, 2.5, 5, 10, and 15 µg/mL prior to application to the cells. GFP expression was measured by FACS in the same manner as above. A heparin stock was formed at 10 mg/mL in DNase free H_2O. The stock was then diluted into the appropriate volume of media containing 10 µg/mL heparin. The media was then used to dilute the polyplexes prior to addition to the cells.

Glycosaminoglycan Screen.

Various glycosaminoglycans were examined for their capacity to increase transfection efficiency. The assay was conducted in a manner similar to the GFP assay presented above. Polyplexes were diluted with cell culture media containing 10 µg/mL of heparin, heparin sulfate, dermatan sulfate, chondroitin sulfate A, and hyaluronan. GFP expression was measured by FACS. As above, stock solutions of GAGs were formed in

DNase free H_2O at 10 mg/mL, and diluted to 10 µg/mL in cell culture media. The media was then used to dilute the polyplexes prior to addition to the cells (leading to a final concentration of 6.6 µg/mL of GAGs).

Polyplex Internalization.

The effect of GAGs on DNA internalization was examined. Cy5 labeling of gWIZ luciferase plasmid was conducted using a Label IT® DNA labeling kit purchased from Mirus Bio using the manufacturer's protocol with a targeted labeling efficiency of 5%. Cy5-labeled DNA was used to transfect the cells using the same protocol used for the GFP assay with the following modifications. After the 4 h transfection, cells were washed with PBS, CellScrub™, then PBS again. Cells were then trypsinized, washed twice with PBS, and suspended in 400 µl PBS containing 1.25% v/v propidium iodide, and analyzed by flow cytometry for Cy5 uptake and toxicity. Gates for Cy5 uptake and propidium iodide were set based on an untransfected control.

Transfections with Dexamethasone.

GFP expression in the presence of dexamethasone was assessed using the same protocol as above with the addition of 1 µM dexamethasone to the DMEM (used to dilute the polyplexes prior to transfection). A stock solution of dexamethasone in DMSO was formed at 1 mM. The 1 mM stock was then further diluted to 1 µM in media immediately prior to use.

Endocytic Pathway Studies.

The effect on GFP expression of the inhibition of clathrin, caveolae, and macropinocytosis was assessed by treating the cells with chlorpromazine, fillipin III, and

5-(N,N-dimethyl)amiloride hydrochloride (DMA) respectively using a protocol previously published by McLendon et al.[65] Cells were plated in the same manner used in the GFP expression protocol. Prior to transfection, the cell culture media was replaced with cell culture media containing chloropromazine, filipin III, or DMA at concentrations of 10 µg/mL, 1 µg/mL, and 100 µM respectively. The chloropromazine-treated cells were incubated for 30 min, fillipin-treated cells were incubated for 1 hr, and DMA-treated cells were incubated for 5 minutes. After pre-incubation with the appropriate endocytic inhibitor, transfections were carried out in the same manner described in the GFP expression experiments. Media was aspirated from the cells, the cells were rinsed with PBS, and then treated with polyplexes diluted with media in the same manner as above. The media used to dilute the polyplexes also contained chloropromazine, filipin III, or DMA such that the final concentration would equal the concentrations used in the pre-incubation step. After 4 hours, the polyplexes in media were aspirated, the cells were washed with PBS, and 1 mL of fresh cell culture media without inhibitor was added.

Confocal Microscopy.

Confocal experiments were conducted using TAMRA-labeled Tr4. The TAMRA-labeling was performed using TAMRA-NHS purchased from Thermo-Fischer Scientific (Carlsbad, CA) using the manufacturer's protocol. Briefly, a 1 mL of a 10 mg/mL solution of Tr4 was treated a 1:10 ratio of TAMRA-NHS dissolved in DMF, and allowed to stir for 1 hour at room temperature. The TAMRA-labeled Tr4 was when dialyzed against H$_2$O for 24 hours, and lyophilized to yield 9.7 mg of TAMRA-labeled Tr4. FITC-labeled pDNA gWIZ luciferase was made using a Label IT® DNA labeling kit purchased

from Mirus Bio using the manufacturer's protocol with a targeted labeling efficiency of 5%. Confocal experiments were performed on a Zeiss Cell Observer SD Spinning Disk confocal microscope. Cells were plated in Mat-Tek 35 mm glass bottom dishes at a density of 50,000 cells/ plate. Transfections were conducted in the same manner as the above experiments with the TAMRA-labeled Tr4 and FITC-labeled pDNA and dye-free DMEM. Images were collected hourly for 4 hours. Cell boundaries were defined using the DIC channel to restrict analysis to the cell interior. Co-localization between Tr4 and DNA within the cell was determined using JACOP in ImageJ.[104]

2.3 Results and Discussion

We sought to discover polyplex formulations to promote high pDNA delivery to several cell types, particularly primary human fibroblasts. Successful genomic manipulation of cells offers numerous possibilities for cell-based therapeutics.[39,105] Herein, we explore the effect of media additives such as heparin, a panel of GAGs, and dexamethasone as enhancers to improve polyplex-based delivery of transgenes to cultured cells such as primary human fibroblasts harvested directly from patients[7] and other immortalized cell models of various tissue types such as U87 (human astrocytoma), HepG2 (human hepatocellular carcinoma).

Polymer Characterization

Trehalose polymers (Tr4) were synthesized via AABB step growth polymerization via copper-catalyzed azide-alkyne cycloaddition according to our previously published methods.[71,73] A degree of polymerization (n) of 45 was targeted for these step-growth polymers and we obtained polymer with an average n = 53 (M_w = 39.2 kDa, Đ = 1.2). The unusually low dispersity index for these step-growth polymers is

likely from the dialysis purification step of the final polymer structure and low conversion. As previously mentioned, Tr4 has been extensively studied by our group and shown to be a successful delivery vehicle.[63,67,71,73,106] Its high efficiency and low toxicity lend potential for improved gene editing in clinically relevant and hard to transfect cells. Due to the promise of Tr4, we sought to explore methods of further boosting transfection efficiency with this polymer-based delivery vehicle with the addition of media additives.

Heparin-Mediated Enhancement of Transfection

The effect of heparin on transfection efficiency of Tr4 polyplexes was first screened using GFP expression assays on three different cell types (Figure 2.2) that represent a variety of tissues. Cell culture media containing heparin was added directly to the polyplexes immediately prior to the addition of polyplexes to the cells. The concentrations of heparin were kept low (10 μg/mL in the dilution media, leading to a final concentration of 6.6 μg/mL) as high concentrations are known to dissociate polyplexes and completely inhibit delivery efficiency.

The addition of heparin at the low concentrations to the polyplexes results in increased transfection efficiency in each cell type examined compared to the Tr4 polyplex only control. As shown in Figure 2.2, the magnitude of increase varied from 20% in HepG2 cells to 60% in U87 cells. This effect was surprising because heparin has been observed to inhibit transfection at higher concentrations (40 μg/ml) in most cases. [102] We hypothesized that heparin was increasing receptor-mediated interaction of the polyplexes with the cell surface. CD44 is a cell surface receptor that is responsible for the recognition and endocytosis of hyaluronan and other glycosaminoglycans. [107] However,

34

an increase in GFP expression was found even in HepG2 cells, which do not present CD44 [19], suggesting that a specific receptor-mediated interaction is not the reason for the transfection enhancement. Interestingly, when heparin (10 µg/mL) was added to polyplexes formed with JetPEI, gene expression was undetectable (Figure 2.2). This is likely due to polyplex destabilization (competitive binding of heparin to JetPEI at this low concentration promoted pDNA release) as JetPEI polyplexes were formed at the manufacturer-recommended formulation conditions (N/P ratio of 5). Additional experiments were performed with PEI at N/P ratio of 20 with and without heparin. These experiments lead to almost complete cell death, and unstable populations not suitable for analysis by flow cytometry. This effect has been characterized in detail by DLS, zeta potential, and ethidium bromide dye exclusion measurements (Figure 2.3). From these results, Tr4 appears to bind pDNA more effectively and polyplexes with this polycation maintain their stability and activity even in the presence of polyanionic heparin at this low concentration. This effect is observed because of the low toxicity of Tr4, which allows polyplexes to be formulated at relatively high N/P ratios. Indeed, based on trypan blue assays (Figure S2.1a) negligible toxicity was observed with the Tr4 formulations in this study. We thus hypothesized that the increased transfection efficiency was the result of heparin coating the polyplexes, which prompted us to characterize the formulations via a battery of techniques outlined below.
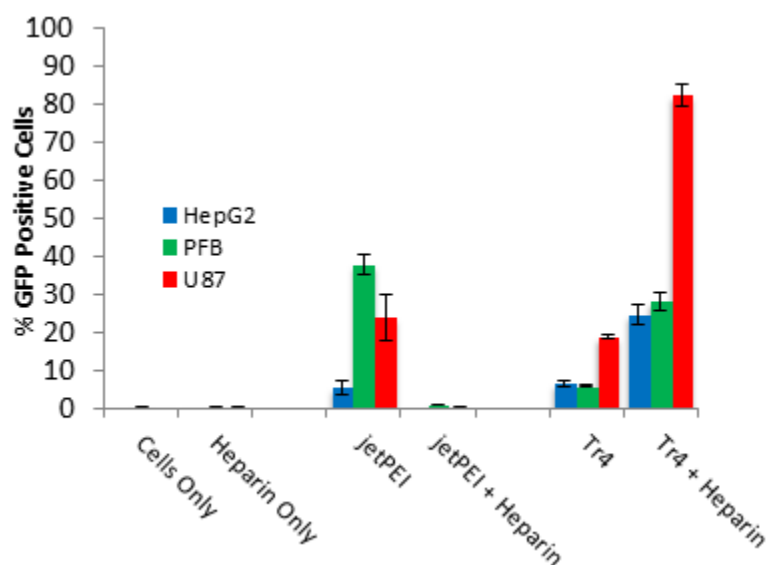
Figure 2.2: Cells treated with 10 μg/mL heparin (final concentration 6.6 μg/mL) and then Tr4 polyplexes formulated with pzsGreen plasmids containing the GFP reporter gene at an N/P=20. Three cell types were explored: HepG2, primary fibroblasts (PFB), and U87 cells. Controls were cells only, cells exposed to heparin and polyplexes formed with JetPEI (N/P=5) in the absence and presence of heparin (10 μg/mL in the dilution media, leading to a final concentration of 6.6 μg/mL). Error bars represent the standard error of 3 measurements.

Polyplex Characterization

Dynamic Light Scattering and Zeta Potential

Dynamic light scattering (Figure 2.3a) was used to investigate and compare polyplex size in the absence and presence of heparin in DMEM with 10% FBS (that reproduce the exact conditions described above with and without heparin). Polyplexes were formed at N/P ratios of 20 for Tr4 and 5 for JetPEI in ultrahigh purity water and were allowed to incubate for 1 hour prior to the addition of DMEM (with 10% FBS containing) and either in the absence or presence of heparin (0 or 10 μg/mL heparin). Measurements were taken immediately after media addition and hourly for 4 hours. Figure 2.3a shows that Tr4 polyplexes aggregate from ~115 nm to ~250 nm over the course of 4 hours regardless of

the presence of heparin. JetPEI polyplexes increased in size from 70 nm to 100 nm in DMEM containing 10% FBS (no heparin). However, heparin-treated JetPEI polyplexes increase in size from 60 nm to 150 nm after only 1 hour. Also, the standard error of the particle size increases over time in the JetPEI polyplexes treated with heparin. Collectively, these results indicate that the addition of low heparin concentrations has a destabilizing effect on JetPEI polyplexes. In contrast, while Tr4 polyplexes appear slightly less stable to media-induced aggregation than JetPEI polyplexes, in general, their aggregation behavior does not appear to change significantly when heparin is added (compared to Tr4 alone). However, it should be noted that the heparin could be destabilizing the polyplex by directly replacing the pDNA binding to the polycation (thus the complexes observed in the presence of heparin could also be polycation binding directly to polyanionic heparin). To this end, further experiments were conducted to more clearly understand this destabilization effect.

Zeta potential measurements (Figure 2.3b) were also conducted to ascertain how heparin affects the surface charge of the polyplexes. The jetPEI polyplexes and Tr4 polyplexes were formed at N/P ratios of 5 and 20, respectively, in water and then diluted by a factor of 2 with PBS containing 0 or 10 μg/mL in a manner consistent with polyplex formulation for transfection. JETPEI polyplexes exhibit a negative surface charge of -12.6 mV immediately with heparin treatment and suggests that the polyplexes could be destabilized/decomplexed, which is likely the cause of the complete diminishment of the delivery efficacy/gene expression. This result is not surprising given the relatively low N/P used to formulate these polyplexes (the manufacturer's recommended formulation

37

condition was used to minimize the well-documented toxic effects of PEI). When these data were compared to that obtained when heparin was added to Tr4 polyplexes, only a slight negative charge (-1.5 mV) was found for those systems. These data could indicate that heparin coats the surface of the polyplexes, forming a ternary complex without actually dissociating the complexes, which is likely due to the higher N/P ratio of polyplex formation. Based on our calculations (Supporting Information, Table S1) the combined negative charge of heparin and DNA is less than the positive charge of polymer system (N/(P+S) = 3.6, where S represents the negative sulfate groups on heparin). This result along with the zeta potential measurements indicates that free heparin does not play a large role this system. A minimal amount of free polymer may still available to play a role in the transfection, but much less than is available at N/P 20 without heparin. A polyanionic coating of heparin could dramatically change polyplex-cell membrane interactions. However, the mechanism of transfection increase was still unclear. To this end, further experiments were conducted in an effort to elucidate the mechanism of the heparin-induced increase in transfection.

Ethidium Bromide Dye Exclusion Assay

Others have shown that heparin has the ability to disassociate polyplexes as it competes for binding to the polycation, thereby dissociating pDNA from polyplexes.[106] An ethidium bromide (EtBr) dye exclusion assay was used to compare the stability of polyplexes with and without heparin. DNA intercalation by EtBr reduces water induced fluorescence quenching leading an increased fluorescence signal in the presence of free DNA. DNA that is bound in polyplexes does not bind EtBr and thus has low fluorescence

signal. Pre-formed polyplexes were treated with varying concentrations of heparin dissolved in serum-free DMEM, and compared to a pDNA only blank control. FBS was not used because it interfered with the control measurements by generating artificially high blank measurements. The relative degree of polyplex dissociation was monitored by calculating the percentage of EtBr dye exclusion compared to free pDNA (full EtBr inclusion) using the following equation where F equals the maximum fluorescence intensity.

$$Dye\ Exclusion = 1 - \left(\frac{F_{sample} - F_{blank}}{F_{DNA\ only} - F_{blank}} \right)$$

As shown in Figure 2.3c, heparin almost completely decomplexes jetPEI polyplexes at the *in vitro* concentration of 10 μg/mL in the dilution media, leading to a final concentration of 6.6 μg/mL. Meanwhile, Tr4 polyplexes are stable up to 10 μg/mL of added heparin, however, at 15 μg/mL decomplexation is noted. This result supports our hypothesis that PEI transfection efficiency is lost because the polyplexes are decomplexed by heparin before cellular transfection. Meanwhile, the Tr4 polyplexes are much more stable to treatment with heparin. They not only maintain their efficacy, but show a significant increase in transfection efficiency that is driven by the presence of heparin. Further experiments were performed to better understand the effect heparin has on transfection.
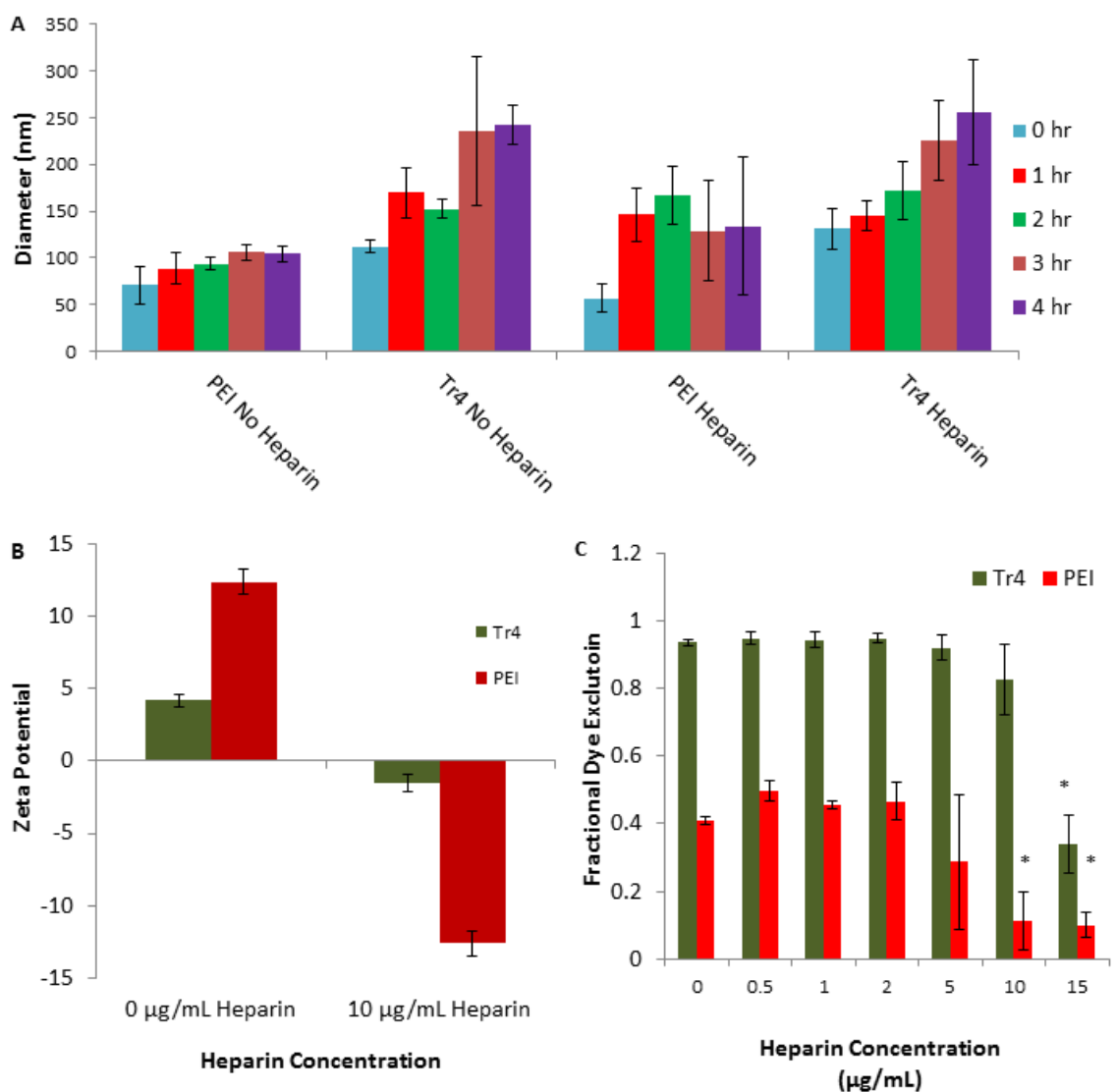
Figure 2.3: Stability of polyplexes at various N/P ratios in the absence and presence of heparin. A) Size of Tr4 (N/P 20) and PEI (N/P 5) polyplexes over time with and without heparin in DMEM containing 10% FBS. B) Zeta potential measurements of Tr4 (N/P 20) and PEI (N/P 5) polyplexes with and without heparin in phosphate buffered saline. C) EtBr dye exclusion of Tr4 (N/P 20) and PEI (N/P 5) polyplexes as a function of heparin concentration. Data represent the average of three replicates. Data exhibiting a significant difference (P<0.05) compared to [heparin] = 0 μg/mL for each polymer is denoted by an asterisk.

Heparin Dose Response

To understand the role of heparin dose on enhancing Tr4 polyplex transfection and gene expression we selected primary human fibroblasts due to their clinical utility and potential for reprogramming to iPSCs. As shown in Figure 2.4, transfection efficiency was found to increase linearly with increased concentration up to 10 μg/mL of added heparin with primary fibroblasts. A subsequent drop in efficacy is observed at 15 μg/mL of added heparin, however, this can be attributed to the loss of polyplex stability observed in the dye exclusion assay at his heparin concentration (Figure 2.3c). We considered the possibility that heparin was improving intracellular DNA release by destabilizing the polyplexes leading to improved DNA release. However, the linear dose response curve, combined with the dye exclusion results (no apparent change in observed in polyplex stability prior to 10 μg/mL of added heparin) indicates that heparin is likely increasing transfection efficiency through another mechanism. While this result does not rule out the potential for heparin to enhance DNA release within the cell, it does indicate that other factors may be at play. Indeed, collectively, these results suggest that heparin may form ternary complexes with Tr4 polyplexes at low concentrations and aid in cell surface binding and intracellular transport of these polyplexes.
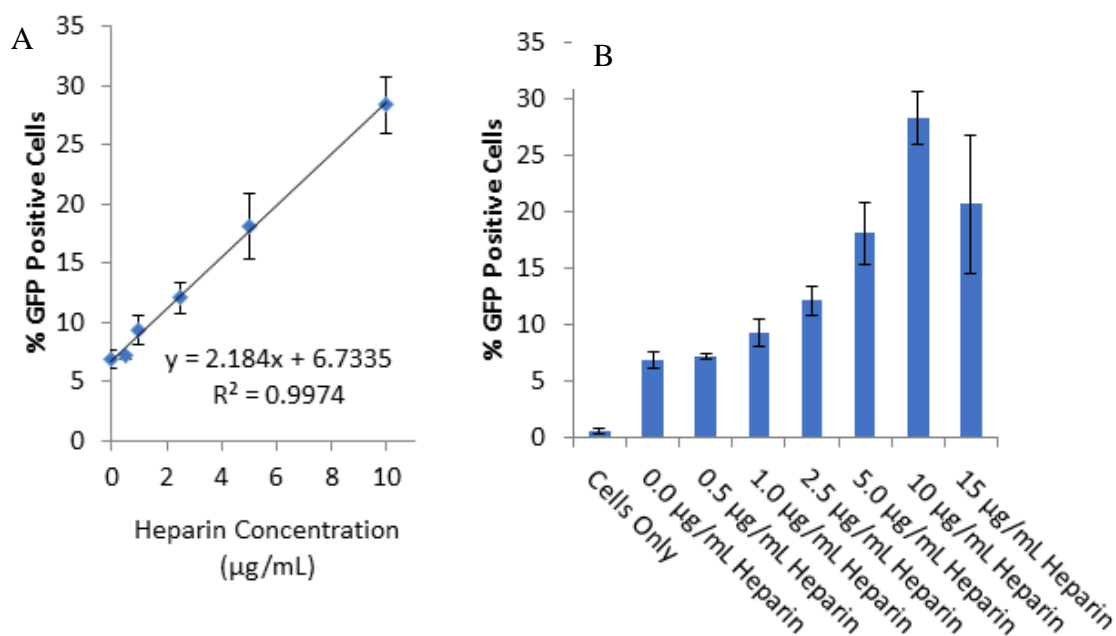
Figure 2.4: GFP expression in primary fibroblasts treated with Tr4 polyplexes at N/P 20 as a function of heparin concentration. Error bars represent the standard deviation of 3 separate sample measurements.

Glycosaminoglycan Specificity

Heparin is a highly sulfated GAG that also contains carboxylates and thus, due to its high anionic character, is likely to form ternary complexes with the Tr4 polyplexes primary due to charge. To this end, we hypothesized that other GAGs may also show a similar transfection enhancement. To assess the specificity in the transfection increase of heparin, the potential of other GAGs to increase transfection, such as heparan sulfate, chondroitin sulfate B, dermatan sulfate, and hyaluronan, was examined. It should be noted that hyaluronan differs in general structure to the other GAG moieties in that the anionic charge groups are all carboxylates (no sulfates are present on this GAG). Primary fibroblasts U87, and HepG2 cells were transfected using a similar procedure as indicated above with the five different GAGs. As shown in Figure 2.5, heparin was found to boost

42

Tr4 transfection to the highest degree in U87 cells, however, heparan sulfate, chondroitin sulfate, dermatan sulfate, all increased transfection efficiency compared to the Tr4 only control. However, in primary fibroblasts, the four GAGs boosted pDNA transfection to about the same degree (with the exception of hyaluronan). This indicates that the increase in transfection efficiency is not necessarily due to a sequence-specific binding of the GAGs to a particular receptor (since GAG type does not appear to have an effect on transfection efficiency). Interestingly, hyaluronan did not promote an increase in transfection efficiency. This result supports our hypothesis that GAG-interaction with a specific receptor such as CD44 is not likely the cause of the observed transfection increase (since hyaluronan showed lower activity yet is the main ligand for CD44 [19]). These results also indicate that the sulfated form of a GAG is essential to boosting transfection efficiency. This could be due in part to the 'hard charge' provided by the sulfate group allowing for stronger ternary interaction with the polycations in the polyplex formulations. To further assess the role of a plain sulfated polycation versus the need for a sulfated GAG molecule to boost transfection, transfections were also performed with an equal charge ratio of a model polyanion, polystyrene sulfonate, to examine if the presence of sulfate groups alone were enough to increase the transfection efficiency. Treatment with PSS had an extreme inhibitory effect on the transfection indicating that the presence of carbohydrate motifs is necessary to transfection enhancement (Figure S2.2).
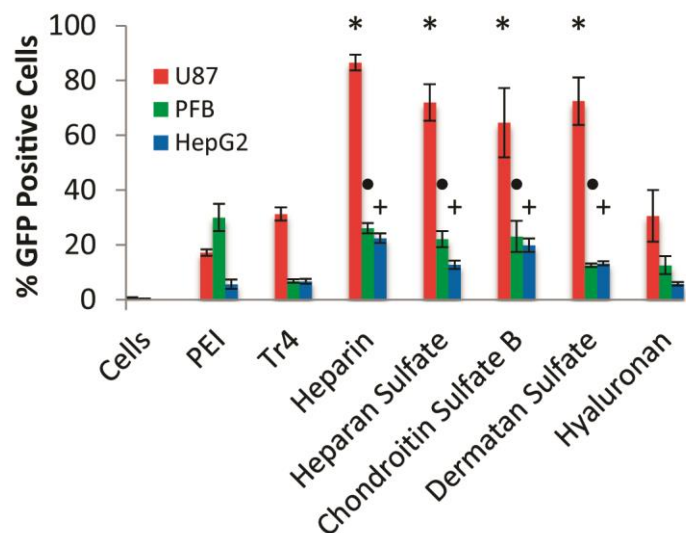
Figure 2.5: GFP expression of primary fibroblasts, HepG2, and U87 cells treated with Tr4 polyplexes at N/P 20 and a library of different GAGs. Error bars represent the standard error of 3 sample replicates. Significance compared to the Tr4 alone control is denoted (P<0.05) Polystyrene sulfonate showed inhibition of transfection with Tr4 (Figure S2.2). Data with hyaluronan was not statically different than Tr4 only.

Polyplex Internalization

The previous data demonstrates that anionic GAGs (namely heparin) play a role in potentially coating polyplexes and enhancing gene expression in the three cell types examined above. We sought to further understand the action of GAGs towards promoting cellular internalization. Thus, its effects on increasing cellular uptake of Tr4 polyplexes was examined in U87, HepG2, and PFBs. Cells were incubated with polyplexes formed with Tr4 and Cy5-labelled pDNA for 4 hours. Following, cells were washed with Cellscrub (removes cell surface-bound polyplexes), and analyzed by flow cytometry to quantitate Tr4 polyplex internalization in the absence and presence of heparin. As shown in Figure 2.6, we found that U87 and PFB cell types exhibited highly efficient polyplex internalization (>95% of cells were Cy5 positive for U87, >85% for

PFB) regardless of the presence of heparin. However, the fluorescence intensity of the Cy5 cells, was found to increase when heparin was added. These data indicate that while the vast majority of cells internalize pDNA, the addition of heparin increases the average amount of pDNA delivered to each cell. The increase in MFI for is a modest 20 percent for fibroblasts and 70 percent for U87 cells relative to Tr4 alone (Figure 2.6). HepG2 cells, which do not have CD44 receptors on the surface,[19] showed lower uptake of Tr4 polyplexes alone, and a more pronounced (4-fold) increase in MFI and 2 fold increase in percent uptake when heparin was added. These results indicate that heparin plays a role in only slightly increasing the amount of pDNA that is internalized into some cell types, which could be the cause for a portion of the increased transgene gene expression, particularly in HepG2. However, these small increases in uptake do not fully explain the increase in gene expression observed in Figure 2.2, particularly in U87 and PFBs. The nature of the heparin-induced transfection was further probed by examining its effect on the intracellular trafficking mechanisms such as endocytic pathway and nuclear localization/entry.
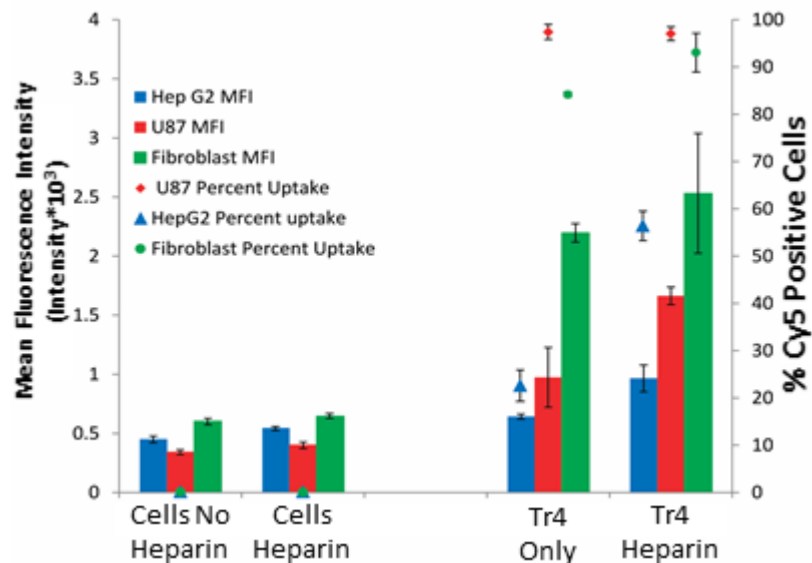
Figure 2.6: Cellular internalization of Cy5 labeled DNA in U87 and primary fibroblasts increases when Tr4 polyplexes are treated with heparin. Cy5 uptake is displayed as fluorescence intensity (MFI)*10^3) and indicated by the bar graph (left axis) while percent uptake is represented by the points (blue triangles, HepG2; red diamonds, U87; green circles, fibroblasts) on the plot (right axis).

Endocytosis Inhibition

To examine how heparin affected the endocytic pathway and eventual gene expression, the cells were treated with 3 different endocytic pathway inhibitors; filipin III, chlorpromazine, and 5-(N,N-dimethyl)amiloride, which inhibit caveolae, clathrin, and macropinocytosis, respectively. Cells were transfected with polyplexes formed with pDNA encoding EGFP and either JetPEI, Tr4, or Tr4 and heparin. After a 4 hr transfection in the presence of the endocytosis inhibitors, the polyplexes and additives were removed and replaced with fresh media and the cells were assayed for EGFP expression after 24 or 48 hours (Figure 2.7).
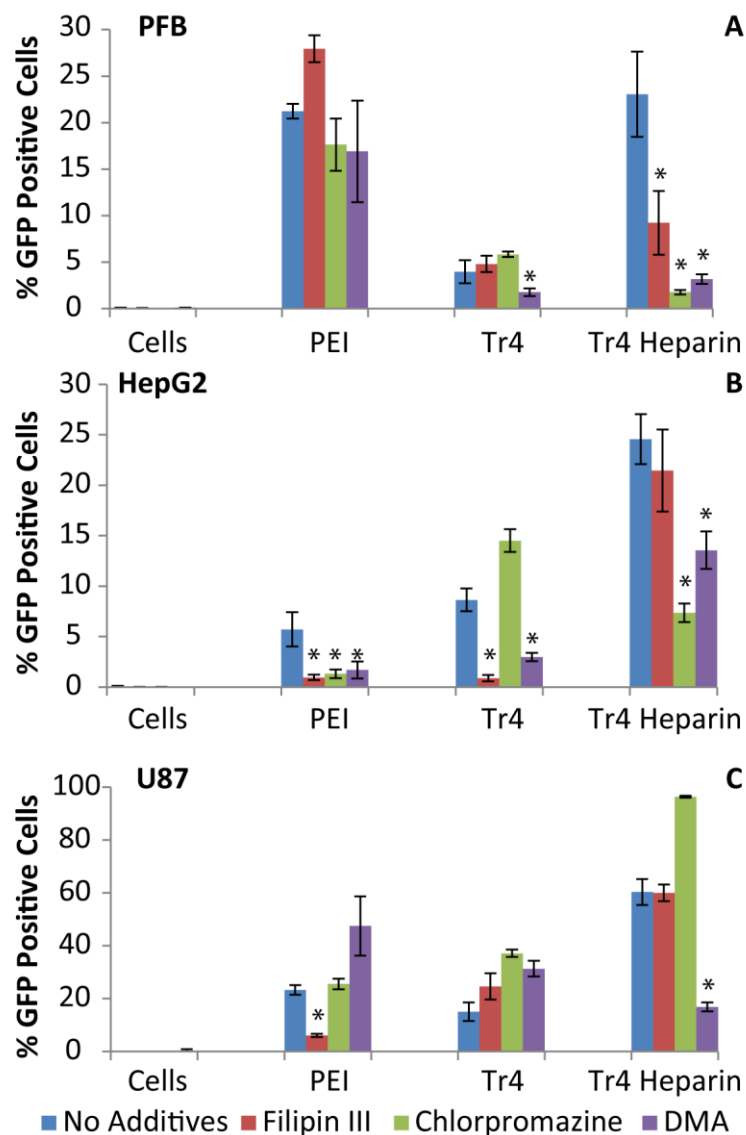
Figure 2.7: GFP expression of a) PFBs, b) HepG2, and c) U87 cells were treated with JetPEI (N/P 5) and Tr4 (N/P 20) polyplexes and endocytic inhibitors in conditions with and without heparin. Filipin III was used to inhibit caveolae (red bars), chlorpromazine was used to inhibit clathrin (green bars), and 5-(N,N-dimethyl) amiloride was used to inhibit micropinocytosis (purple bars). A control transfection without additives (blue bars) was also performed for comparison under the same conditions. Error bars represent the standard deviation of three separate experimental replicates. Significant inhibition compared to no additives is denoted by * (P<0.05)

It should be noted that in general, the transfection efficiency in these endocytosis inhibition experiments were found to be slightly lower than the transfection efficiency observed in the previous transfection experiments (Figures 2.1, 2.4, 2.5, and 2.7), which is due to the removal of the polyplexes after 4 hours. This step was necessary because treating the cells with the inhibitors for longer periods of time lead to significant cytotoxicity and decreased cell counts. At the conditions used, no additional toxicity was observed by FACs. While it is probable that inhibitors did have a toxic effect on the cells, cell count rates were consistent with the no-additive controls, so toxicity was considered to be minimal. The endocytic pathway for each vehicle is highly cell type dependent. However, looking at each cell type independently reveals some interesting insights.

For transfection of primary fibroblasts with Tr4, inhibition of macropinocytosis leads to a decrease in GFP expression, indicating that macropinocytosis is a main pathway for internalization and trafficking with this vehicle. Previous studies have indicated that inhibition of one endocytic pathway can upregulate other pathways. [108,109] In this case, inhibition of unproductive pathways could be causing an increase in transfection efficiency by increasing the rate of more efficient pathways such as macropinocytosis. The heparin treated polyplexes exhibit different behavior (Figure 2.7). With heparin-Tr4 in PFB cells, inhibition of clathrin causes the most drastic reduction in transfection efficiency followed by macropinocytosis for this cell type.

The transfection behavior with HepG2 cells in the presence of the inhibitors appears to exhibit somewhat similar behavior to that observed with PFBs. Tr4 transfection (without heparin) was strongly inhibited by Filipin III and DMA (yet

chlorpromazine appeared to increase transfection), indicating that caveolae and macropinocytosis are both important pathways for Tr4 alone and blocking clathrin may up regulate these pathways with HepG2 cells. Of most interest, heparin-treated Tr4 polyplexes are most strongly inhibited by chlorpromazine followed by DMA. This indicates that, like PFBs, HepG2 cells transfected with heparin-treated polyplexes depend on clathrin-mediated endocytosis and micropinocytosis for successful transfection.

Like the previous transfection data (Figures 2.2 and 2.5), the inhibition experiments with U87 cells differed slightly from that observed with the other two cell types. Cells transfected with Tr4 in the presence of the inhibitors were found to exhibit varying degrees of enhancement in transfection efficiency. This could be due to upregulation of the other endocytic pathways (that are not inhibited) after treatment with each drug inhibitor. The transfection data with the heparin-treated polyplexes also showed a different trend than the other two cell types. Inhibition of clathrin actually caused a significant increase in transfection and gene expression was significantly inhibited by DMA. This result indicates that macropinocytosis is the main endocytic pathway for U87 cells in the presence of heparin.

Taken together, these results support our hypothesis that heparin has a profound effect on the endocytic pathways taken to internalize Tr4 polyplexes. Collectively, these results indicate that in the absence of heparin, that caveolae and macropinocytsis appear to be the main endocytosis routes. These results are consistent with literature, for example, Rejman et al. have previously shown that polycationic PEI polyplexes transfect A549 cells through caveolae.[110] Our results show that in the presence of heparin, clathrin

coated pits (in PFBs and HepG2 cells only) and macropinocytosis (all three cell types) appear to be the main two pathways for cellular uptake that leads to successful transgene expression. A previous report has indicated that macropinosomes do not traffic to lysosomes and instead traffic to irregularly sized vesicles called macropinosomes.[111].[52] While this does not hold for all cell types and delivery vehicles[53,54], an increased reliance on macropinocytosis may be leading to higher gene expression due to decreased lysosomal degradation. Thus, an increased reliance on this pathway may be leading to high gene expression possibly due to less lysosomal degradation.

DNA and Polymer Tracking Within Cells

Confocal microscopy experiments were conducted to further observe how heparin affects the transfection process at the subcellular level. Tr4 polymers were labeled with TAMRA-succinimidyl ester using the manufacturer's protocol. The TAMRA-Tr4 was used to form polyplexes with FITC-labeled plasmids. For this set of experiments, we focused our efforts on U87 cells as a model because heparin treatment promoted the largest increase with this cell type. Polyplexes were added to the cells with and without the addition of heparin, and images were collected hourly for 4 hours. Some differences can be observed in the number of polyplexes visible in solution during the transfection. This is likely due to slight differences in the focal plane used to collect the images. Polyplexes external to the cells were ignored for all image analysis. Figures 2.8a and 2.8b show cells transfected with polyplexes formed with TAMRA-Tr4 and FITC-pDNA after immediate addition (t = 0) in the presence (Figure 2.8a) and absence (Figure 2.8b) of heparin. At this time point, minimal endocytosis has occurred in both conditions (with

and without heparin). However, the samples that have been treated with heparin show very large polyplex aggregates on the cell surface. While the DLS data did not conclusively show that the addition of heparin lead to aggregation, it appears the interaction of the heparin-treated polyplexes with the cells in culture media leads to aggregation compared to untreated polyplexes. Also, the presence of heparin appears to decrease the degree to which the polymer coats the cell membrane. As can be seen in Figures 2.8c and 2.8d, after four hours, the cells have endocytosed a considerable amount of polymer and pDNA (both images display transfections in the absence and presence of heparin). This data agrees with the previously discussed Cy5 uptake experiments (Figure 6) that showed ~100% cell uptake regardless of heparin treatment, however again, the polyplex aggregates were larger in the images with added heparin (large particles are more amenable to internalization by macropinocytosis, which agrees with the data in Figure 2.7).

We investigated the possibility that heparin may help to dissociate polyplexes after internalization leading to DNA release. Colocalization between TAMRA-labeled Tr4 and FITC-labelled pDNA was monitored over 4 hours. Manders coefficients were used to quantify colocalization between pDNA and Tr4 over 4 hours (Table 1). In the presence of heparin, M2 (the DNA-Tr4 localization coefficient) decreases from 0.95 to 0.16 over 4 hours. This can be observed in Figure 2.8c. The DNA signal appears to become more diffuse throughout the cell. This suggests that pDNA is released from the polymer over the course of the 4 hour transfection when heparin is added. In contrast, untreated polyplexes exhibit a low degree of colocalization between polymer and pDNA

throughout the course of the transfection. This is due to the increased amount of free polymer coating the surface of the cell. More notably, pDNA-polymer colocalization remains high throughout the transfection. This could indicate that heparin is contributing to pDNA release. However, based on the other results discussed in this paper, it could also suggest that heparin causes the pDNA to be trafficked away from the polymer via another process. The colocalization of pDNA and polymer in the untreated cells could imply that the polymer and pDNA has trouble escaping endosomes.

Table 2.1: Colocalization of TAMRA-labeled Tr4 and FITC-labeled pDNA

	Heparin	
Time (hr)	M_1 (Tr4-DNA)	M_2 (DNA-Tr4)
0	0.40	0.95
1	0.44	0.97
2	0.74	0.95
3	0.69	0.67
4	0.63	0.16

	No Heparin	
Time (hr)	M_1 (Tr4-DNA)	M_2 (DNA-Tr4)
0	0.50	0.71
1	0.11	0.93
2	0.19	0.97
3	0.31	0.96
4	0.43	0.91
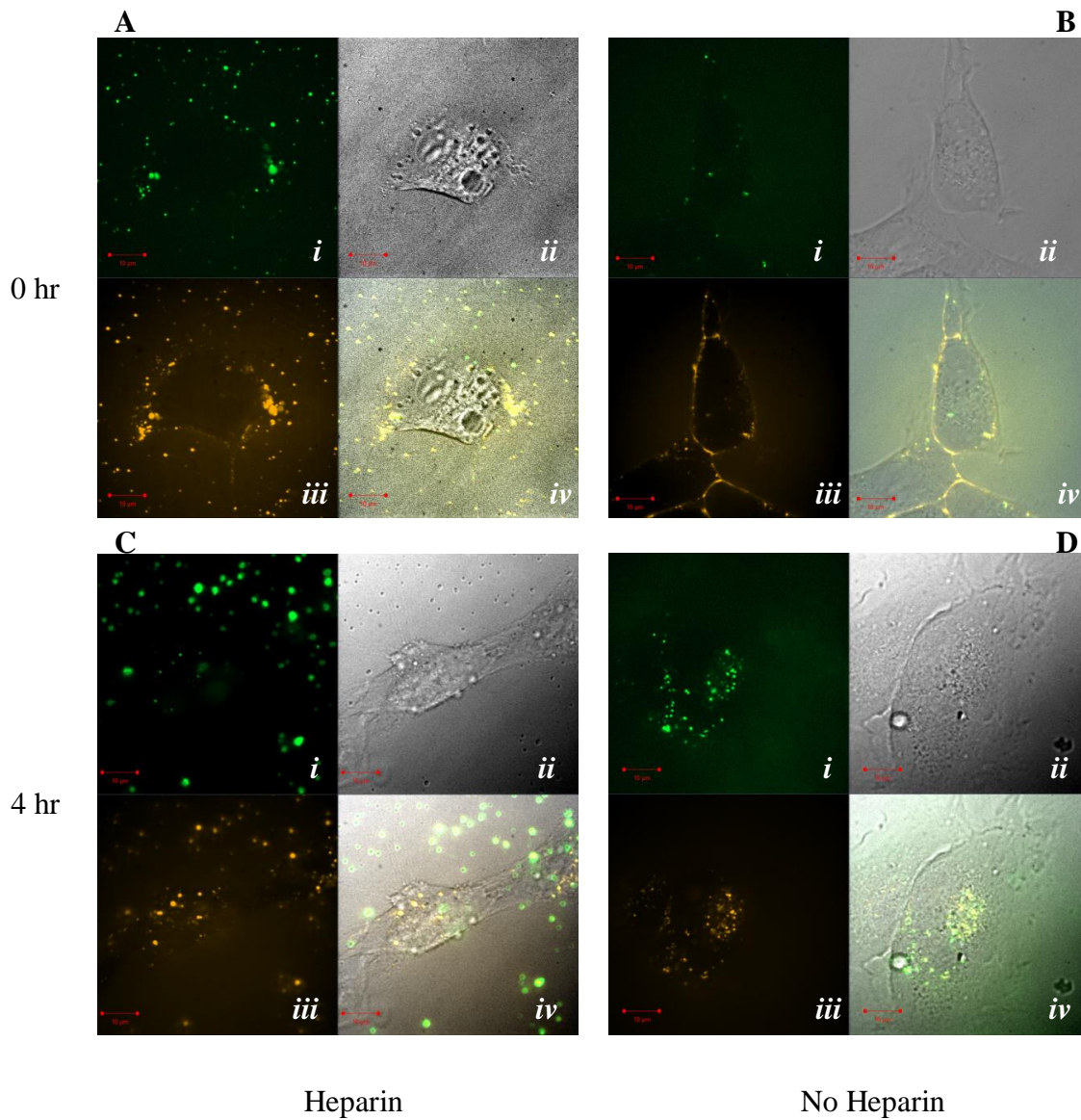
Figure 2.8: Confocal micrographs of U87 cells treated with polyplexes formed from TAMRA-Tr4 (orange) and FITC-pDNA (green) treated with heparin (A and C) and without heparin (B and D). Images were acquired immediately after the addition of polyplexes (0hr, A and B), and after 4 hours of transfection time (C and D). Channels are (in clockwise order) are FITC (*i*), transmitted (*ii*), TAMRA (*iii*), and overlay (*iv*).

Transfection with Dexamethasone

Nuclear localization/internalization of the pDNA payload is the final and most important step in the process of transfection to promote gene expression. Due to the relatively slow rate of mitosis in primary fibroblasts compared to cancerous cell types, we hypothesized that nuclear localization and entry is likely the key barrier to improving delivery efficiency. Our data herein suggests that cell surface binding and polyplex internalization is high and heparin appears to be further increasing internalization primarily through macropinocytosis, which has a positive effect on transgene expression. We hypothesized that heparin may be affecting the nuclear localization pathways in transfection carried out with Tr4. To test this hypothesis, we performed transfections on primary fibroblasts, HepG2 and U87 cells with dexamethasone (dex), a potent glucocorticoid and anti-inflammatory drug, which has been shown to dilate nuclear pores and have anti-apoptotic effects. [112,113] Previous work has shown this small molecule can aid nuclear passage and accumulation of various cargo and biomolecules. [112-114] To probe heparin's effect on nuclear localization, cells were transfected with JetPEI and Tr4. The polyplexes were treated with culture media containing 10 μg/mL of added heparin, leading to a final concentration of 6.6 μg/mL, 1 μM dexamethasone, and both additives.
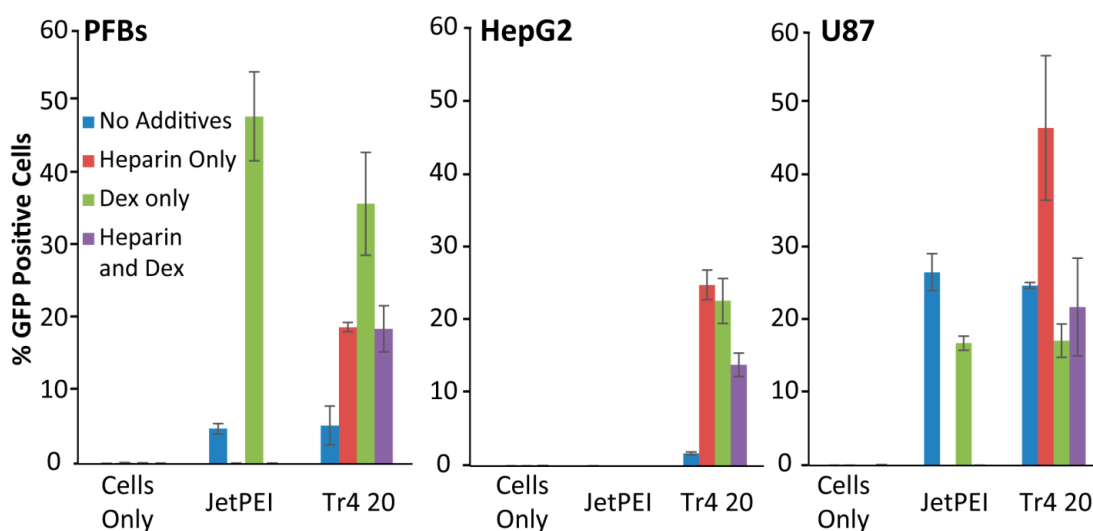
Figure 2.9: GFP expression of primary fibroblasts, HepG2, and U87 cells transfected with JetPEI (N/P 5) and Tr4 (N/P 20) in the absence (blue bars) and presence of 10 μg/mL added heparin, leading to a final concentration of 6.6 μg/mL (red bars), 1 μM dexamethasone (green bars), and both additives (purple bars) combined at these same concentrations. The cell culture media was supplemented with the additives, which was then added to the solution containing the polyplexes. Note: HepG2 transfection was unsuccessful with PEI. Error bars represent the standard deviation of three separate experimental replicates.

As shown in Figure 2.9, the presence of heparin completely inhibits transfection with JetPEI as it appears to decomplex this vehicle at this concentration (Figures 2.2 and 2.3). However, the addition of dexamethasone alone results in a large increase in transfection efficiency in the presence of both PEI and Tr4 polyplexes in PFBs. With primary fibroblasts, dexamethasone does not increase the transfection efficiency of heparin treated polyplexes. These results could indicate that polyplexes treated with heparin are trafficked to the nucleus in manner that cannot be improved by the passive mechanism promoted with dexamethasone. of the heparin-induced transfection increase were caused solely by increased uptake or increased unpacking efficiency, the addition of heparin and dexamethasone should lead to an additive effect caused by the increase in

available pDNA translocating to the nucleus at a higher rate. Instead, the increase provided by heparin is not further aided by the addition of dexamethasone, indicating that heparin may have an impact on the nuclear trafficking in Tr4 transfections.

It is interesting to note that in HepG2 and U87 cells, the effect of dexamethasone is different. HepG2 transfection is enhanced by both heparin and dexamethasone individually, but the heparin-Tr4 transfection is inhibited by the addition of dexamethasone. Transfection of the U87 cells is inhibited by the presence of dexamethasone in all cases while the addition of heparin leads to a 20% increase in transfection efficiency. The lack of increase in U87 cells could be due to the fast rate of mitosis in U87 cells (nuclear membrane breaks down more often allowing polyplex entry) and thus treatment with dexamethasone has no effect. These results, combined with the results in primary fibroblasts reveal that dexamethasone and heparin appear to interfere with each other in a manner that indicates that heparin may be improving the nuclear localization of the pDNA leading to increased transfection efficiency.

2.4 Conclusion

The polycation-based pDNA delivery agents, such as Tr4, show efficiency in hard to transfect cells, which is desirable for the development of cell therapies. Herein, it is shown that the addition of low doses of heparin and other sulfated glycosaminoglycans can significantly increase the pDNA delivery efficiency of Tr4 in a dose responsive manner with a variety of cell types. Tr4 polyplexes are stable to the addition of heparin (up to 10 μg/mL), and heparin-treated polyplexes have a slight negative zeta potential indicating ternary complex formation. Heparin-treated polyplexes are endocytosed more

readily and through different endocytic pathways than untreated polyplexes (no heparin), where clathrin-mediated endocytosis and macropinocytosis was found to be a major trafficking pathway. Furthermore, polyplexes formed with pDNA and Tr4 in the presence of heparin appear to promote enhanced nuclear delivery in a manner that is independent to potential mechanisms influenced by dexamethasone, which was also examined as a media additive. This work demonstrates that the presence of heparin and dexamethasone can significantly enhance gene expression in these cell types but is significantly dependent on the polymer type and formulation concentrations. Collectively, this study provides new methodologies to promote more efficient delivery of plasmid DNA to a variety of tissue types in vitro or ex vivo that can be translated for research and development of regenerative cell therapies.

Chapter 3: Nuclear Destabilization Leads to Dramatically Increased Transfection Efficiency and Functional Cas9 Performance with a Glycopolymer Vehicle in Primary Fibroblasts and Induced Pluripotent Stem Cells

Synopsis

Primary fibroblasts (PFBs) are an important target for regenerative medicine and cell therapies as they are frequently used in the production of induced pluripotent stem cells (iPSCs). Fast, efficient, and inexpensive transfection of primary fibroblasts and induced pluripotent stem cells could lead to the development of improved treatments for skin diseases, including genetic conditions such as epidermolysis bullosa. Successful plasmid-based gene editing (such as CRISPR-Cas9) can require the the delivery of plasmids that are large (~9.5-11 kbp) in comparison to commonly used reporter plasmids (~5-8 kbp). In an effort to develop more efficient delivery vehicles for CRISPR-Cas9 plasmids, we investigated the effect of plasmid size on the transfection of primary fibroblasts and induced pluripotent stem cells using a well-studied trehalose-containing polymer (Tr4). Transfection is almost completely diminished in PFBs and significantly reduced in iPSCs when the plasmid size is increased from 4.7 kbp to 10 kbp, despite equivalent high rates of polyplex internalization of polyplexes formed with both plasmid sizes. Increased gene expression with both the 4.7 kB and the 10 kB plasmid models was achieved under transfection conditions where the nuclear membrane is destabilized such as with the use of dexamethasone or during timed transfection experiments during S phase using synchronized cells. In primary fibroblasts, the fold-increase in the transfection efficiency caused by nuclear permeabilization is significantly higher for the 10 kbp plasmid compared to the 4.7 kbp plasmid. To demonstrate the potential clinical

utility of this delivery system, we utilized Tr4-heparin polyplexes formulated with dexamethasone to achieve successful transcription activation with a dCas9-VP64 synthetic transcription activator targeted to collagen type VII in iPSCs derived from human T-cells. Indeed, functional plasmid transfection efficiency can be significantly improved by nuclear destabilization, which could lead to improved development of nonviral vehicles for ex vivo CRISPR-Cas9 gene editing.

3.1 Introduction

Increased understanding of the human genome and protein function has the potential to revolutionize the treatment of many intractable diseases. The delivery of exogenous genetic material to a patient may replace a defective gene or shut down a defective signaling pathway. The use of novel gene editing technologies such as CRISPR/Cas9[5] and TALEN[7] could allow physicians to permanently fix a defective gene in a patient. However, current technologies lack the ability to safely and efficiently deliver plasmid DNA (which may code for the Cas9 enzyme or a therapeutic protein) to a variety of cell types and tissues. While electroporation and viral vectors work efficiently in vitro, their utility in vivo is often limited by physical access to tissue and potential immune complications, respectively.[79,82] The use of cationic polymers, which can package anionic DNA in polyelectrolyte complexes (termed polyplexes)[12], promotes circulation throughout the patient[97] and DNA internalization, and could provide a cheap, efficient strategy for gene delivery.[115]

Previous work has resulted in the development of cationic glycopolymers that contain positive charges conferred by amines in addition to monomers derived from naturally occurring carbohydrates such as D-glucarate[64], glucose[116], N-acetyl galactosamine[117], cyclodextrin[57], trehalose[63], and many others.[59,61,64,65,96,99] The incorporation of carbohydrate-derived moieties into polycations has been shown to mitigate the cytotoxicity inherent to many polycationic delivery vehicles.[57,64,106] These moieties can also promote stealth properties and colloidal stability due to their ability to form a hydrophilic corona around polyplexes.[97] Glycopolymers containing trehalose, a non-reducing disaccharide known for its lyoprotective properties, have shown particular

promise due to their low in vitro toxicity and high gene delivery efficiency in a variety of cell types.[63,71,97] Tr4, a click-glycopolymer containing four cationic ethyleneamine units alternating with trehalose, has shown the ability to efficiently deliver pDNA, especially when end-functionalized with the cationic monomer.[71] Further work has shown that the addition of heparin to Tr4 polyplexes after complexation can lead to increased transfection efficiency by altering the mechanism through which polyplexes are trafficked within the cells after uptake.[118] The addition of heparin leads to accumulation of the negatively charged glycosaminoglycan on the surface of the polyplex that does not inhibit endocytosis of the particles. It also leads to an increased dependence on macropinocytosis for gene expression, and may impact the nuclear localization behavior of the DNA. Heparin-Tr4 polyplexes have also demonstrated promise in the delivery of a GFP reporter gene to primary human fibroblasts.[118]

The transfection of primary human fibroblasts is essential to the development of gene therapy-based treatment for the skin disease, epidermolysis bullosa. Epidermolysis bullosa is a class of skin disorders characterized by a loss of integrity of the skin at the basement membrane.[37,119] Two severe subtypes of the disease, dystrophic epidermolysis bullosa, and junctional epidermolysis bullosa, Herlitz type are caused by inherited mutations in the genes for collagen type VII (COL7A1) and laminin-332 (LAMA3, LAMB3, or LAMC2).[37,120,121] Currently, the standard of care for these diseases is stem cell replacement therapy via bone marrow transplant.[39] This highly invasive procedure required patients to undergo extensive subsequent care and may suffer from fatal complications such as graft versus host disease. Fibroblasts are the main cell type

responsible for the expression and excretion of collagen type VII and laminin-332 in human skin. The development of efficient editing techniques in induced pluripotent stem cells and primary fibroblasts could lead to autologous cell therapies and/or gene medicine that provide improved clinical outcomes with fewer adverse effects.[7]

Successful gene editing can be achieved via a number of nuclease-based systems, for example, the successful expression of a plasmid coding for Cas9 as well as gRNA and a donor sequence.[4] Due to the size of the protein, Cas9 plasmids range in size from about 9.5 kbp to 14 kbp depending on the presence of other features such as reporter genes and guide sequences.[2-4] This is considerably larger than commonly used reporter plasmids, such as GFP (~5 kbp) that are traditionally used to screen delivery vehicle efficacy. Adeno-associated viruses are known to have a size limit of approximately 5 kbp.[32] Tremblay et al. showed that the polycation PEI can increase this size limit by aiding in complexation with the virus, but transfection efficiency still drops as a function of plasmid size in these vehicles.[122] Yin et al. demonstrated that Lipofectamine 2000 transfection efficiency drops as plasmid size increases from 4.8 to 10 kbp from in a variety of cell types.[123] The efficiency of amine-modified silica nanoparticles also drops considerably when the plasmid size is increased from 6.1 to 8.9 kbp.[124] As CRISPR/Cas9 has gained prominence in the field, researchers have grown more interested in studying the delivery of ~10 kbp plasmids. For example, Kretzmann et al. have shown a ~50% decrease in transfection efficiency for 10 kbp plasmids compared to 5 kbp plasmids when PAMAM dendrimers were used in MCF-7 cells.[125]

In an effort to develop improved strategies for the delivery of large plasmids (e.g., encoding Cas9), herein, we compared the transfection efficiency of a smaller 4.7 kbp GFP plasmid to that of a 10 kbp plasmid. The model plasmids were designed to contain the exact same GFP gene sequence and that same promotor (Figure 3.1) to understand the pure effects of plasmid size on delivery with primary fibroblasts and induced pluripotent stem cells. When compared to the efficacy of small plasmid transfection with our Tr4 vehicle and controls, the transfection efficiency of the large plasmid was almost nonexistent in primary fibroblasts, and significantly reduced in iPSCs. Interestingly, we observed that plasmid size has no significant effect on polyplex internalization in either cell type. Based on these results, we hypothesized that the larger plasmid may be unable to efficiently localize to the nucleus when transfected with Tr4-heparin. To test this hypothesis, we examined transfections in the presence of dexamethasone and during S phase (controlled via cell synchronization) to explore potential delivery efficiency increases in the presence of destabilized nuclear envelope. Indeed, the results revealed that these techniques led to enhanced transgene expression with the large plasmid in primary fibroblasts and induced pluripotent stem cells. While reporter gene expression is useful to evaluate the relative efficiency of delivery vehicles, the expression of a reporter gene may not fully translate to successful delivery of a functional protein. To demonstrate the functional utility of these techniques, we investigated the ability of Tr4-heparin polyplexes administered concurrently with dexamethasone to successfully deliver functional dCas9-based transcription activator leading to increased expression of collagen type VII in iPSCs. These results imply that large plasmid transfection efficiency can be

significantly improved by nuclear destabilization, particularly in hard to transfect cells. These improvements could lead to the development of improved gene delivery vehicles for CRISPR-Cas9 constructs, and improved non-viral gene editing.
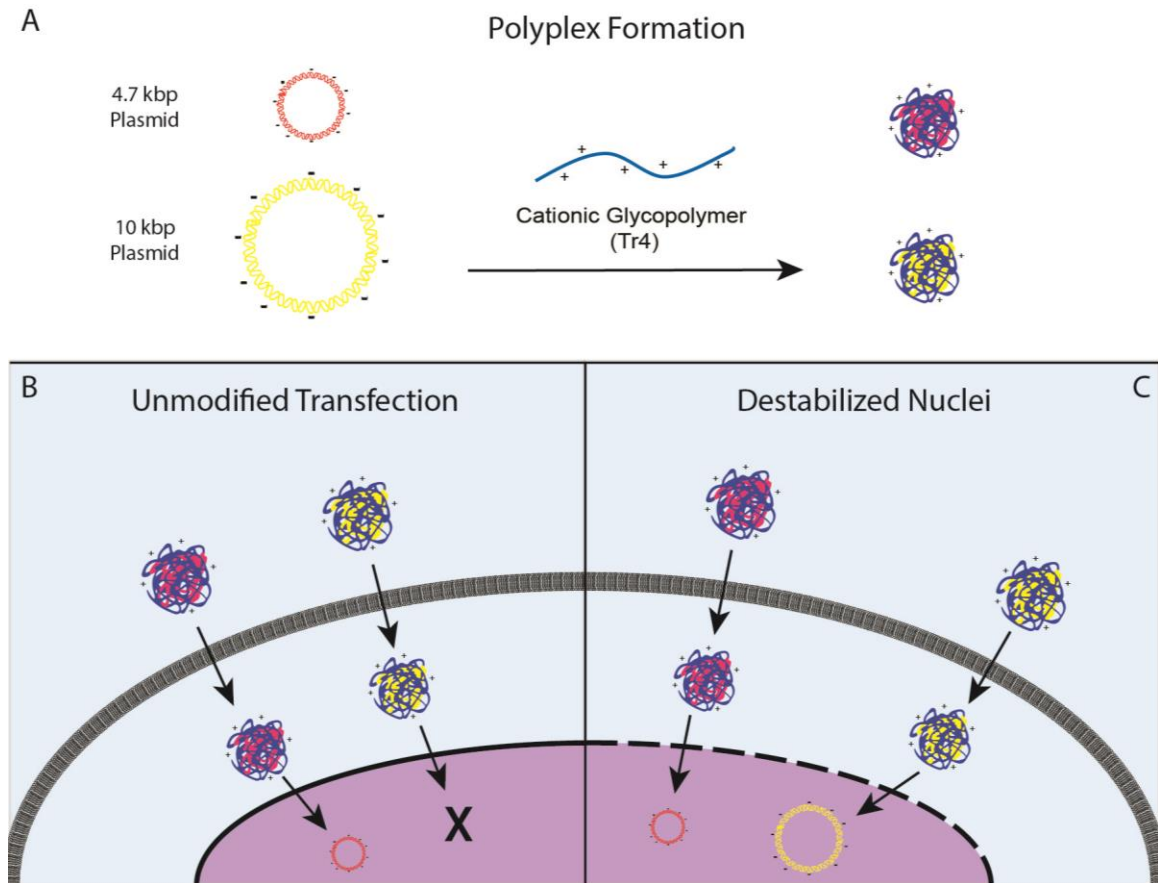
Figure 3.1: A) Schematic of polyplex formulation and B) transfection of both large and small plasmids. The large plasmid transfection is unsuccessful in primary fibroblasts and significantly reduced in induced pluripotent stem cells despite equivalent high cellular internalization. C) Permeabilization of the nuclear membrane by treatment with dexamethasone or via timed transfections via cell synchronization leads to increased transfection efficiency, particularly for the large plasmid.

3.2 Materials and Methods

General

Chemical reagents were purchased from Sigma-Aldrich Co. LLC. (St. Louis, M), and used without further purification unless otherwise specified. PzsGreen GFP and

PzsGreen-10K was purchased from Aldeveron (Fargo, ND). Dulbecco's Eagle Medium (DMEM), trypsin, phosphate buffered saline (PBS), UltraPure™ DNase/RNase-Free distilled water (DI H$_2$O), non-essential amino acids (NEAA), fetal bovine serum (FBS), and penicillin/streptomycin (P/S) were purchased from Life Technologies-ThermoFischer Scientific (Carlsbad, CA). For the culture of iPSCs, mTeSR™1 media was purchased from STEMCELL Technologies (Vancouver, Candada) Matrigel® matrix was purchased from Corning Inc. (Corning, NY) Heparin sodium salt from porcine interstinal mucosa (heparin) was purchased from Sigma Aldrich Co LLC (St. Louis, MO). Cellscrub™ was purchased from AMS biotechnology (Abingdon, UK). Primary Human Fibroblasts (PFBs) were obtained from skin biopsy of healthy donors using a previously published protocol.[7] All transfections were performed on cells below passage 12. Induced pluripotent stem cells were derived from naïve human T-cells using a previously established protocol.[105]

Instrumentation

GFP expression, Ruby intensity, and Cy5 uptake were measured using a BD FACSverse™ flow cytometer Becton Dickinson Biosciences (San Jose, CA). Fluorescence and absorbance measurements were acquired using a Synergy H1 multi-mode plate reader (BioTek, Winooskei, VT). Tissue imaging was performed using an EVOS inverted fluorescence microscope (ThermoFisher Scientific, Carlsbad, CA).

Polymer synthesis

Tr4 polymers were synthesized and characterized as described previously by Anderson et al. and Boyle et al.[71,118] In brief, an alkyne-azide cycloaddition click reaction was performed to yield a polymer with alternating charged and neutral trehalose groups.

Boc-protected dialkynyl oligoethyleneamine and acetylated diazido trehalose were dissolved in dimethyl formamide (DMF). Monomer feeds were controlled so that the dialkyne was in excess to ensure the presence of dialkyne endgroups. Based on Carothers' equation [DP = (1 + r) / (1 - r)] the feed ratio (r) was set to 0.96 to target a degree of polymerization (DP) of ~45. Catalytic amounts of copper sulfate and sodium ascorbate were added, and the reaction mixture was allowed to stir overnight at 70 °C. After 24 hours, 2.5 equivalents of dialkyne monomer were added to ensure complete end capping, and the reaction was allowed to continue for 2 hours. When the reaction was complete, the polymers were isolated by precipitation in cold water. The polymer was then deprotected by stirring in 4 N HCl in dioxane for 18 hrs followed by NaOMe in MeOH for 18 hrs. The deprotected polymer was then dissolved in water, centrifuged to remove insoluble impurities, and dialyzed against water with a 5 kDa membrane (Spectrum Labs, Rancho Dominguez, Ca) for 24 hours with water changes every 4 hours. The resulting water-soluble polymer was characterized by gel permeation chromatography (GPC) according to our previously published procedures to characterize the molecular weight and dispersity.[118] After purification, the polymers had an an average degree of polymerization of 53 (M_w = 39.2 kDa, Đ = 1.2).[118]

Polyplex formulation

Polyplexes were formed using the same previously published protocol.[118] Briefly, plasmid DNA solutions were formed at a concentration of 0.02 µg/µL in 165 µL of DNase/RNase-free water. Tr4 solutions were formed at an N/P ratio of 40 for all experiments in this work (22 µg polymer/µg DNA) in an equal volume of DNase/RNase-free water. The Tr4 solution was then slowly added to the pDNA solution and slowly

triturated to mix. After mixing, the polyplex solutions were allowed to incubate at room temperature for 1 hr before addition to the cells. Polyplex solutions were formed in this manner for all subsequent experiments described herein.

Primary Fibroblast Transfections

Transfections of primary fibroblasts were performed using the method described in Boyle et al.[118] Primary human dermal fibroblasts (PFBs) were obtained from skin biopsy of healthy donors using a previously published protocol.[7] PFBs (below passage 10) were cultured to ~80% confluency for 3 days prior to plating. Cells were then lifted with trypsin, and seeded in 12 well plates at a density of 5×10^4 cells per well with 1 mL of cell culture media (DMEM+10% FBS, 1% L-glutamine, 1% NEAA, 1% P/S). Seeded cells were cultured overnight, and transfected 24 hours after seeding.

Polyplexes were formed using the protocol described above using pzsGreen (4.7 kb) and pzsGreen-10k (10 kb) plasmids. Plasmid maps for pzsGreen and pzsGreen-10K can be seen in Figure S3.1. Lipofectamine complexes were formed in Opti-MEM per the manufacturer's protocol using 5 µL per 1 µg of DNA. Immediately prior to transfection, Tr4 polyplex solutions prepared as described above were diluted by a factor of 3 (to yield a total volume of 990 µL) with cell culture media (DMEM+10% FBS, 1% L-glutamine, 1% NEAA, 1% P/S) with and without heparin (10 µg/mL). Prior to polyplex treatment, the media was aspirated from the cells, and the cells were rinsed with 1 mL PBS. After the removal of the PBS rinse, cells were treated with 300 µL polyplex solution (1 µg of DNA per well). For the lipofectamine samples, the media was replaced with 1 mL of fresh media, and lipofectamine solutions were added directly to the well. All polyplex treated cells and controls were allowed to incubate at 37 °C and 5% CO_2 for 4 hours.

After incubation, 1 mL of cell culture media was added to each well. The cells were then allowed to culture for 72 hours with a media change after 24 hours.

After 72 hours of cell culture, the cells were detached with trypsin (300 µL). The resulting cell suspensions were neutralized with cell culture media (700 µL) and transferred to BD falcon round-bottom tubes. The cells were then centrifuged at 1200 rpm for 4 min, and rinsed with PBS. After the rinse, the cells were again centrifuged, and resuspended in 400 µL PBS containing 1% propidium iodide. Cells were then analyzed for GFP gene expression on a BD FACSverse flow cytometer.

Induced Pluripotent Stem Cells Transfections

Induced pluripotent stem cells were cultured in mTeSR^{TM} serum-free medium (STEMCELL technologies, Vancouver, Ca) on Matrigel (Corning Inc, Corning, NY) in 6-well plates for 3 days (to ~80% confluency). Prior to detachment, cells were rinsed for 5 minutes with PBS. Cells were then treated with 1 mL of fresh mTeSR^{TM}, and lifted mechanically using a cell scraper. To further break up colonies, the cell suspensions were gently triturated with a 1000 µl pipette. Cells were then split by factor of 1/8 (1×10^6 cells) into 12-well plates coated with Matrigel, and incubated at 37 °C and 5% humidity for 24 hours. Cells were then transfected using polyplexes formed as described above. After the polyplexes were formed at a total volume of 330 µL, they were diluted with 660 µL mTeSR^{TM}. Cells were treated with polyplexes formed with either pzsGreen or pszGreen-10k, and treated with 1 µg/well. Immediately after the addition of the polyplexes, the cells were centrifuged in the plate at 1200 rpm for 5 min. After a 4 hour incubation period, 1 mL of mTeSR^{TM} was added to each well. The cells were then cultured for 48 hours with a media change after 24 hours. After 48 hours of incubation,

68

the cells were lifted and analyzed by flow cytometry in the same manner described above.

Cy5 labeling of DNA

To monitor the internalization of DNA into cells and nuclei, both plasmids were labeled with Cy5 using a Label IT® nucleic acid labeling kit (Mirus Bio, Madison, WI). Per the instructions, pDNA solutions were prepared in water at a concentration of 0.1 µg/µL along with labeling buffer A and Label IT reagent provided by the kit. The desired labeling efficiency was 500 bases per molecule of Cy5. The labeling reaction was allowed to proceed at 37 °C for 1 hr. Following the reaction, the labeled DNA was purified by ethanol precipitation, and resuspended in 100 µL water. Labeling was quantified by comparing Cy5 absorbance to A_{260} absorbance as quantified by a Synergy H1 multi-mode plate reader (BioTek, Winooskei, VT). Labelling efficiency was found to be 585 bases/dye for the large plasmid and 526 bases/dye for the large plasmid.

Polyplex Internalization

Transfections were carried out in primary fibroblasts and iPSCs using the same protocol described in the plasmid size comparison assay using the Cy5-labeled pDNA described above. Cy5-labeled pzsGreen and pzsGreen-10k were each diluted to a concentration of 0.02 µg/µL. To 165 µL of the DNA solution, an equal volume of Tr4 solution at N/P 40 was added to form 330 µL of polyplex solution. Polyplexes were then diluted with 660 µL of the appropriate media (DMEM+10% FBS, 1% L-glutamine, 1% NEAA, 1% P/S for PFBs, mTeSR™ for iPSCs). Immediately following the media addition, 300 µL of polyplex solution (1 µg DNA/well) was added to each well. After

transfection, the iPSC plates were centrifuged at 1200 rpm for 5 min, and transferred to the incubator. PFB plates were transferred to the incubator without centrifugation. After 4 hrs of incubation, cells were rinsed with CellScrub™ buffer (AMS Biotechnology, Cambridge, MA) for 15 minutes per the manufacturer's instructions to remove non-internalized polyplexes adhered to the surface of the cells. After CellScrub treatment, the cells were rinsed with PBS, and lifted with 300 µL trypsin. After the cells were lifted, the trypsin was neutralized with 700 µL DMEM, and the resulting cell suspensions were transferred to BD round-bottom falcon tubes. The cells were then centrifuged, rinsed with PBS, and resuspended in PBS containing 1% propidium iodide. Cells were then analyzed on a BD FACsverse flow cytometer for the presence of Cy5.

Transfection of Synchronized Cells

Cells were synchronized using a double thymidine block procedure similar to that described by Männistö et al.[126] Primary fibroblasts were plated at a density of 5×10^4 cells per well in a 12-well plate. Cells were then treated with media supplemented with thymidine (Sigma-Aldrich, St. Louis, MO) at a concentration of 2 mM for 18 hours. The first thymidine block was then released by removing the thymidine-containing media, and rinsing with PBS. The media was replaced with fresh media, and the cells were incubated free of thymidine for 9 hrs. After incubation, the cells were blocked a second time with 2 mM thymidine for 15 hours. To characterize that the cells were successfully blocked, a cell cycle analysis was performed using Ruby stain. Cell cycle analysis (Figure S3.2) showed that >75% of the cells were in S or G2/M phase after the block compared to only about 25% in an unblocked control population. After the second block, the cells were

immediately transfected in the same manner described in the plasmid size comparison assay.

Transfection with Dexamethasone

Transfections with dexamethasone were performed using a similar protocol to that reported in Boyle et al.[118] Polyplexes were formed according to the protocol described above. Tr4 polyplexes were formed in water at an N/P ratio of 40 and a DNA concentration of 0.02 μg/μL. Lipofectamine 2000 complexes were formed in Opti-MEM using 4 μL/ug DNA per the manufacturer's protocol. Cells were pre-incubated with dexamethasone dissolved in cell culture media (5 μM) for 1 hr. After the pre-incubation, the cells were transfected in the same manner described in the plasmid size comparison assay with the addition of 5 μM dexamethasone to the polyplex dilution media. For the Lipofectamine 2000 samples, 100 μL lipoplex solution was added to each well containing the pre-incubation media. For the Tr4 samples, polyplex dilution media was prepared as previously described with the addition of dexamethasone at a concentration of 5 μM. Polyplexes were diluted by a factor of 3 with media, and 300 μL polyplex solution was added to each well. After polyplex addition, iPSC plates were centrifuged for 5 min at 1200 rpm, and transferred to the incubator. Transfections were allowed to incubate for 4 hours. After 4 hours incubation, 1 mL of dexamethasone-free media was added to each well. Primary fibroblasts were incubated for 72 hours post transfection with a media change after 24 hours. iPSCs were incubated for 48 hours post transfection with a media change after 24 hours. After incubation, wells were analyzed for GFP expression by flow cytometry.

Transfections In the Presence of Chloroquine

Transfections were performed as described previously. Primary fibroblasts were seeded in 12-well plates at a density of 5×10^4 cells per well 24 hours prior to transfection. iPSCs were split by factor of 1/8 (~1×10^6 cells) into 12 well plates coated with Matrigel, and incubated at 37 °C and 5% humidity for 24 hours. Polyplexes were formed in DNase/RNase-free water using 1 µg DNA per well at a final concentration of 0.01 µg/µL. Lipofectamine complexes were formed in Opti-MEM using 5 µL per µg DNA. The Tr4 and Tr4-heparin transfections were performed using an N/P ratio of 40. After forming polyplexes in water, and immediately prior to transfection, the polyplexes were diluted by a factor of 2 with cell culture media containing 25 µM chloroquine with or without 10 µg/mL heparin. For the lipofectamine samples, the media was replaced with media containing 25 µM chloroquine immediately prior to transfection. Transfections were allowed to proceed for 4 hours at 37 °C and 5% CO_2. After 4 hours, 1 mL of cell culture media was added to each well. Cells were allowed to culture for 72 hours with a media change after 24 hours. After 72 hours, the cells were detached with trypsin, and analyzed for GFP expression by flow cytometry.

Transcription Activation in iPSCs

The ability of Tr4-heparin formulated with dexamethasone to effectively deliver a functional protein was investigated using a synthetic transcription activation model. Wild type iPSCs with low collagen type VII transcriptional activity[35] were simultaneously transfected with two plasmids coding for Cas9-VP64 (13 kB) and a truncated gRNA targeted to the collagen type VII promoter (4 kB).[3,127] The dCas9-VP64 plasmid was provided as a gift from the from the laboratory of Prof. Feng Zhang

(Addgene plasmid #61425).[3] A non-targeting decoy gRNA plasmid was also used as a negative control. Guide sequences can be seen in Table S1 (Supporting Information). Each transfection was performed with 0.5 µg of each plasmid (1 µg per well total) using a similar protocol described above with the exception of a few steps described below. Cells were pre-incubated for 1 hr with 5 µM dexamethasone in mTesR. Plasmid solutions were prepared at a total concentration of 0.02 µg/µL (0.01 µg/µL Cas9, 0.01 µg/µL gRNA). Equal volume solutions of Tr4 formulated at N/P 40 were added to the DNA, and polyplexes were allowed to incubate at room temperature for 1 hr. Polyplexes were then diluted with mTesR containing 5 µM dexamethasone with or without 10 µg/mL heparin, and added to the cells. Cells were then centrifuged at 1200 rpm for 5 minutes, and transferred to an incubator. After 4 hours, 1 mL of mTesR was added to each well. Cells were then cultured for 48 hrs with a media change daily. After 48 hours, the collagen type VII expression was quantified. RNA was isolated using the Qiagen RNeasy® Plus Mini Kit (Qiagen (Hilden, Germay) according to the manufacturer's protocol. Collagen type VII mRNA was then amplified using RT-qPCR, and collagen expression was quantified. Collagen expression was normalized to the housekeeping gene glyceraldehyde-6-phosphate dehydrogenase (GAPDH).

3.3 Results and Discussion

GFP expression as a function of plasmid size

To investigate the effect of plasmid size on transfection with Tr4 and Tr4-heparin, primary fibroblasts and iPSCs were transfected with Tr4, Tr4-heparin, and the positive control, Lipofectamine 2000, using a small plasmid (4.7 kb) and a large plasmid (10 kB). For each plasmid, the same dose (1 µg per 50,000 cells) and the same N/P ratio (40 for

Tr4 and Tr4-heparin, 5 µL/µg for Lipofectamine 2000). It should be noted that this effectively cuts the molar dose of the plasmid in half for the large plasmid. However, optimization experiments showed that 1 µg of plasmid yielded the highest transfection efficiency regardless of the plasmid size (Supporting Information, Figure S3.3). Doubling the dose of the large plasmid from 1 µg to 2 µg per well provided no increase transfection efficiency while dramatically increasing the toxicity (Supporting Information, Figure S3.3). Toxicity as quantified by propidium iodide staining is shown in the supporting information (Supporting Information Figure S3.4). All transfections with PFBs exhibited >80% cell survival regardless of plasmid size. For primary fibroblasts, the Lipofectamine 2000 and Tr4-heparin treated formulations resulted in approximately 30% GFP positive cells for the small plasmid. However, when the large plasmid was used, the transgene expression was almost nonexistent for the Tr4-heparin treated cells. In contrast, the Lipofectamine 2000 formulations lost roughly half of their efficacy when plasmid size was increased, but maintained a low level of transfection efficiency not observed in the Tr4-heparin transfections. The total loss of transfection in the Tr4-heparin when the large plasmid was used cannot be explained by changes to polyplex stability as the polyplexes formed with the large and small plasmid are indistinguishable by DLS and dye exclusion assays (Supporting Information Figure S3.5 and Figure S3.6).
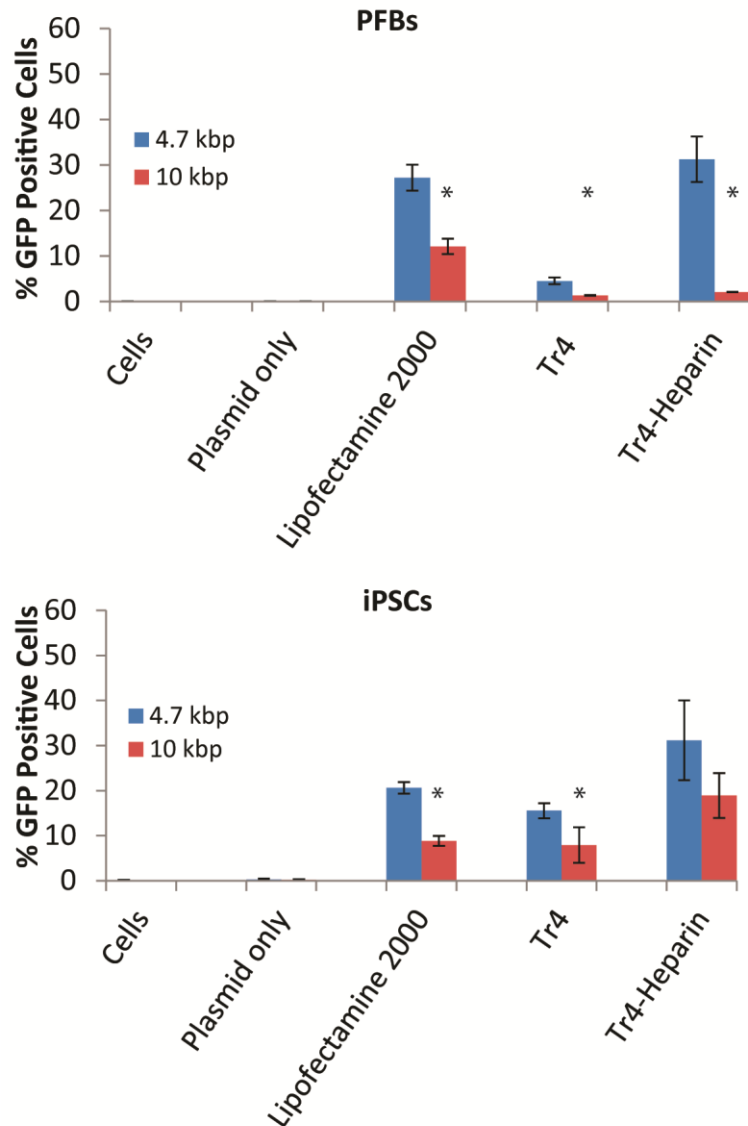
Figure 3.2: GFP expression measured by flow cytometry with pzsGreen (4.7 kbp) and pzsGreen-10Kb (10 kbp) in primary fibroblasts and induced pluripotent stem cells. Error bars represent the standard deviation of three replicates. Significant decrease ($P<0.05$) as calculated by the Student's t-test compared to 4.7 kB transfection are denoted by with an asterisk (*).

In contrast to the PFBs, the transfection results in iPSCs revealed a uniform (~50%) decrease in transfection efficiency as plasmid size was increased. In addition to DLS data and our previously published work[118], this result further illustrates that large plasmid-polyplex instability is not playing a role in the efficacy loss (as efficacy is

dependent on cell type). While the decrease in transfection efficiency in iPSCs would not necessarily prevent the use of Tr4-heparin for some applications, a better understanding of the efficacy loss could lead to the development of better ex vivo gene delivery methods and improved clinical outcomes. Other researchers have examined transfection as a function of plasmid size[123-125], but to our knowledge, a drop this precipitous has not been observed. To this end, we sought to further examine how each of three important cellular transport barriers are affected by the plasmid size for polyplex formulations: i) cellular uptake, ii) endosomal escape, and iii) nuclear internalization. We first examined how plasmid size affects the ability of cells to internalize polyplexes.
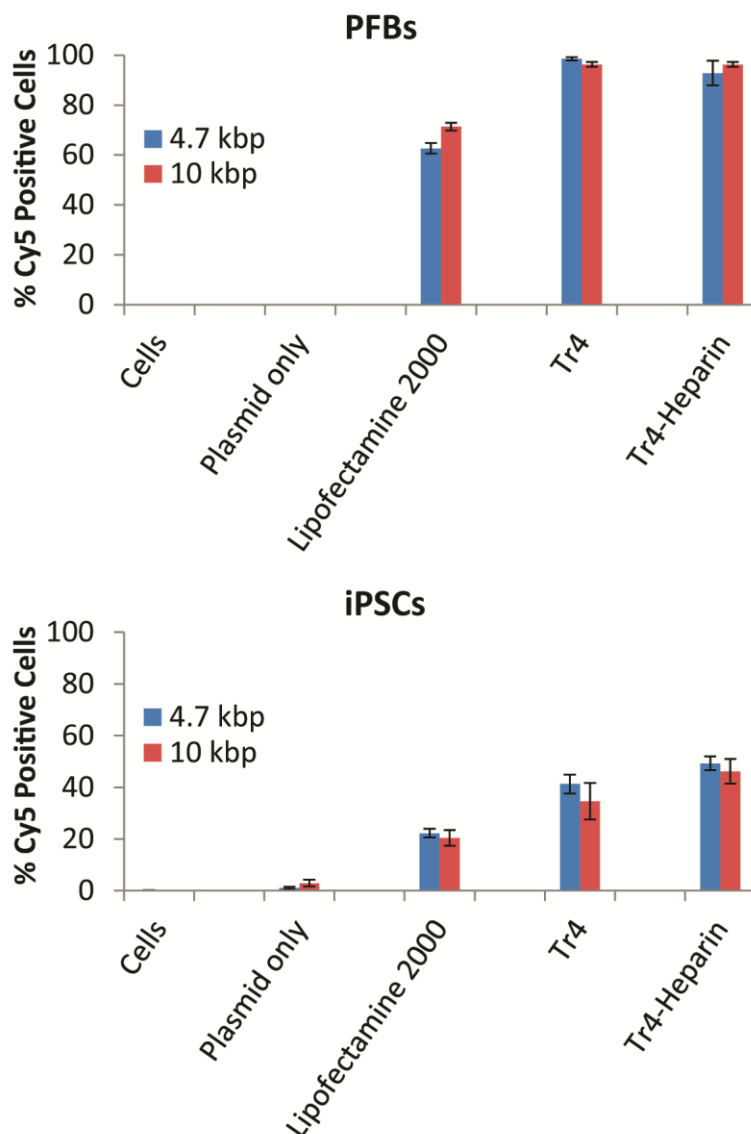
Figure 3.3: Cellular internalization of Cy5-labeled pDNA as a function of plasmid size in primary fibroblasts and induced pluripotent stem cells as determined via flow cytometry. Error bars represent the standard deviation of three replicates. No significant differences were observed between the large and small plasmid for all conditions/formulations.

Cellular Uptake

Primary fibroblasts were transfected with small and large plasmids labeled with

Cy5 using the same transfection conditions described for the GFP expression study. As

shown in Figure 3.3, the data reveals that cellular internalization of the plasmid in the

different formulations does not remarkably differ when comparing the small and large plasmid systems. In this cell type, polyplexes formed with both Tr4 and Tr4-heparin revealed cellular uptake close to 100% and does not show any significant change as a function of plasmid size. However, the transfection efficiency (in terms of gene expression) of Tr4-heparin drops from a functional 31% to an almost non-functional 2% (Figure 3.2) when the plasmid size is increased. With the lipofectamine control, the uptake was slightly lower than the Tr4 and Tr4-heparin polyplexes and increased marginally for the larger plasmid (62% for the small plasmid and 71% for the larger plasmid). However, when comparing GFP expression with lipofectamine complexed with the small and large plasmid (Figure 3.2), a large decrease in expression was noted (by about 50%).

In iPSCs, the overall number of cells positive for plasmid internalization was much lower than that observed in PFBs for all systems. Similar to the data observed with PFBs, no difference in cell internalization was found when comparing small versus large plasmid internalization with all delivery systems. The cells transfected with Lipofectamine 2000 exhibit internalization in 20% of the cells regardless of plasmid size. Similar to PFBs, the Tr4 and Tr4-heparin polyplexes yield higher internalization rates. However, like Lipofectamine 2000, they did not show a dependence on plasmid size. For all delivery vehicle formulations in both iPSCs and PFBs, cellular uptake of DNA alone does not appear to be predictive of successful transfection/transgene expression when comparing plasmid sizes.

Because uptake is roughly the same regardless of plasmid size, it appears that intracellular barriers subsequent to polyplex (or lipoplex in the case of the control) are responsible for the reduction in transfection efficiency when the plasmid size is increased. It is possible that larger plasmids are unable to localize to the nucleus as efficiently as small plasmids. This could explain the cell type dependence of the decrease in transfection efficiency as a function of plasmid size. PFBs have a lower metabolic rate than iPSCs, and consequently a much higher percentage of the cells have intact nuclear membranes during transfection (due to a lower number of cells undergoing mitosis during the experiment). While some iPSC nuclear membranes would remain totally intact during transfection (due to lack of mitosis), many more primary fibroblast membranes likely remain intact, leading to a more dramatic decrease in transfection efficiency as plasmid size is increased. To examine the effect of endosomal and nuclear envelope destabilization on transfection, methods to destabilize intracellular membranes were utilized in an attempt to increase large plasmid transfection efficiency, and better understand the mechanism of decrease with increasing plasmid size.

Endosomal Escape/Destabilization

To further investigate the potential intracellular barrier of endosomal release affecting large plasmid transfection efficacy, primary fibroblasts and iPSCs were transfected with polyplex formulations that were co-delivered with chloroquine. Chloroquine is known to promote endosomal escape of polyplexes by promoting endosomal buffering, leading to endosomal lysis and release of polyplexes. The addition of chloroquine during the transfection leads to a dramatic increase (4.5% to 33% (7 fold) for PFBs, 15% to 47% (3 fold) in iPSCs) in transfection efficiency of the small plasmid

with Tr4 alone. However, it has minimal impact on transfection with Tr4-heparin, which showed no significant increase in small plasmid transfection when comparing transfection results in the absence and presence of chloroquine. This result indicates that Tr4-heparin formulations may be avoiding lysosomal trafficking by increasing reliance on macropinocytosis, which has been shown to avoid lysosomal trafficking in some cell types.[111] Indeed, this theory is supported by our previously published results, which indicate that Tr4-heparin transfection depends largely on endocytosis through macropinocytosis.[118]
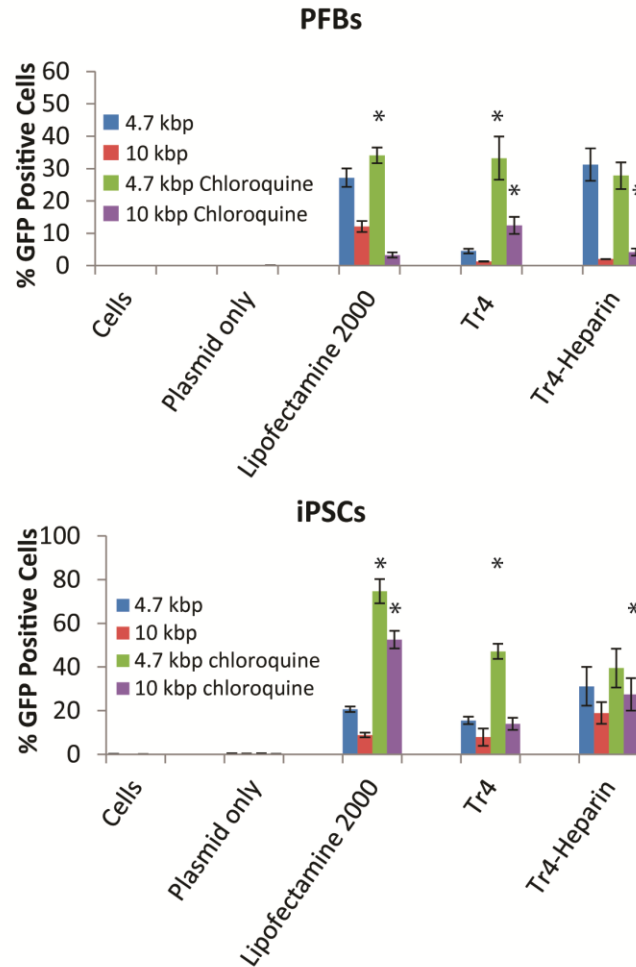
Figure 3.4: Effect of endosomal destabilization by chloroquine on transfection as a function of plasmid size. Error bars represent the standard deviation of 3 replicates. Significant increase (P<0.05) compared to the unmodified transfection (Figure 3.2) as calculated by the Student's t-test is denoted by *.

Like the small plasmid, the large plasmid transfections mediated with Tr4 are improved (at differing degrees) by the addition of chloroquine. Large plasmid transfections with Tr4 alone increased with the addition of chloroquine (5 μM) from 1.3% to 12.4% (10 fold) for primary fibroblasts and 7.9% to 14% for IPSCs. The fold increase for the chloroquine transfection with Tr4 is similar (~7 and ~10 fold) for both the large and small plasmid, respectively in primary fibroblasts. In iPSCs, the fold

increase in transfection efficiency is lower for the large plasmid (>2 fold) than the small plasmid (~3 fold) for Tr4 alone. For Tr4-heparin, the chloroquine leads to a significant, but slight increase in large plasmid transfection for both cell types. This increase is much less than the increase observed in Tr4 alone the increases observed with the small plasmid. This indicates that the inhibited transfection caused by increasing plasmid size is not mitigated by chloroquine treatment. The lipofectamine transfection follow a similar trend. Treatment with chloroquine does provide a significant increase in transfection efficiency for the small plasmid in PFB, and for both plasmid sizes in IPSCs. However, the fold increase is similar regardless of plasmid size. Collectively, these data indicate that endosomal-lysosomal trafficking does not appear to be the major barrier that contributes to the decrease in expression activity with the increase in plasmid size. Although, lipofectamine appears to have a different trend than the Tr4 formulations in that chloroquine increased expression with both the small and large plasmid, indicating endosomal escape is a barrier for this vehicle in general. To this end, nuclear envelope penetration was explored as a means to improve transfection when plasmid size is increased, which is studied below.

Nuclear Internalization

　　Transfection of Cells Synchronized in S Phase. Others have shown that transfection of synchronized cells during mitosis leads to increased transfection efficiency due to increased nuclear localization of the plasmid.[126] If nuclear localization of the large plasmid was limiting transfection efficiency, we hypothesized that transfection of synchronized cells would provide a more significant improvement in transfection efficiency in the large plasmid than the small plasmid. Due to the relatively

low rate of mitosis in primary fibroblasts, we hypothesized that nuclear delivery may be a more significant barrier for those cells, leading to the dramatically reduced transfection in those cells as plasmid size was increased.
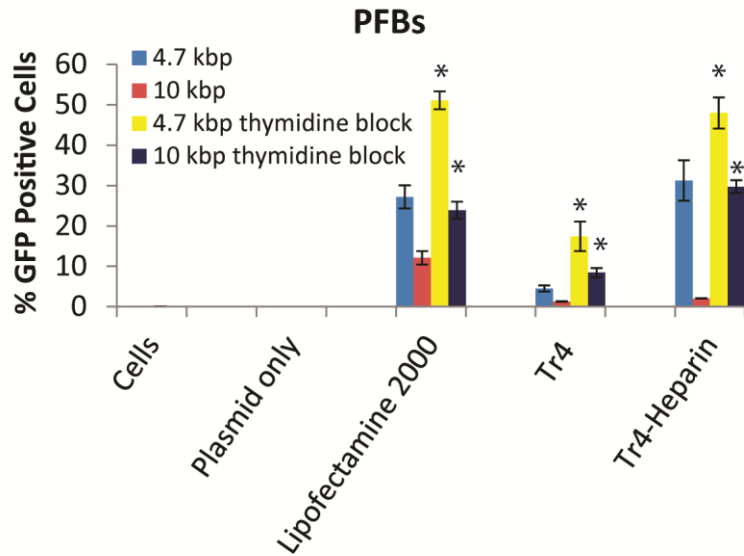
Figure 3.5: GFP expression measured by flow cytometry on primary fibroblast cells synchronized via thymidine block . Error bars represent the standard deviation of three replicates. As denoted by *, all conditions show a significant increase (P<0.5) compared to unblocked cells based on the Student's T test. This assay was not able to be performed on iPSCs as the cells did not survive the thymidine block experiment and transfection.

To synchronize the cells into S phase, cultures were treated with a double thymidine block as described by Mannisto et al.[126] In brief, primary fibroblasts were plated into a 12-well plate, and treated with thymidine for 12 hours. The block was then released, and the cells were cultured for 8 hours. The cells were then blocked again for 16 hours. After the second block, the thymidine was removed, and the cells were transfected immediately after block removal with polyplex and control formulations containing the small and large GFP plasmids as described previously. According to a Ruby[TM] stain

assay (Fig S2), 28% of the cells were in G2/M phase at the start of the transfection after block release.

With the small plasmid, the thymidine block leads to an increase in transfection efficiency compared to the unblocked control for transfections performed with Tr4, Tr4-heparin, and Lipofectamine 2000 in primary fibroblasts. The magnitude of the increase (1.5 and 1.8 fold) is similar for Tr4-heparin and Lipofectamine 2000 for the small plasmid. Transfections with Tr4 generally showed about a 3-fold improvement regardless of plasmid size. For the large plasmid, the trends are similar but more dramatic. For Tr4-heparin, blocking the cells provides a 14.5 fold increase compared to the unblocked cells (compared to a 1.5 fold increase for the small plasmid). Interestingly, the transfection efficiency of the blocked cells for the large plasmid almost exactly matches the unblocked small plasmid transfection efficiency. The ability of the thymidine to recover the transfection efficiency lost when plasmid size is increased strongly indicates that the nuclear envelope barrier plays a large role in the Tr4 transfection of primary fibroblasts and thus timed transfections that traffic during mitosis may aid transfection efficiency. Unfortunately, with some cell types, there is a cost of toxicity; indeed the double thymidine block was too toxic to yield consistent results with iPSCs.

Transfection in the Presence of Dexamethasone. Dexamethasone is a corticosteroid that is known to dilate nuclear pores.[112,113,128] To investigate an alternative method of nuclear membrane disruption, we utilized dexamethasone to perturb the permeability of the nucleus in cultures of primary fibroblasts and iPSCs during transfection. Cells were prepared as described previously in the GFP expression section.

Each well of cells was then pre-incubated with 5 μM dexamethasone for 1 hour prior to transfection. Following pre-treatment, the cells were transfected as previously described with the exception that the polyplex solutions were also supplemented with 5 μM dexamethasone. With Tr4, the addition of dexamethasone at 5 μM leads to 12% GFP positive cells in the large plasmid transfection. This represents a 16-fold increase in transfection efficiency compared to Tr4 alone. With the small plasmid, 5 uM dexamethasone provided a 6 fold increase (from 5 percent to 27 percent GFP positive cells). In contrast, dexamethasone resulted in an approximately 2-fold increase in transfection efficiency regardless of plasmid size for the Lipofectamine formulations in PFBs. Small plasmid Tr4-Heparin transfections are not improved by the addition of dexamethasone. However, dexamethasone does increase large plasmid transfection efficiency from 2% to 14.5% (~7 fold). Overall, these results indicate that disruption of the nuclear envelope has the capacity to recover the transfection efficiency lost when a larger plasmid is used in primary fibroblasts. Further, since the effect on small plasmid transfection is limited compared to large plasmid, it appears that nuclear localization may be a larger barrier to transfection as plasmid size is increased.
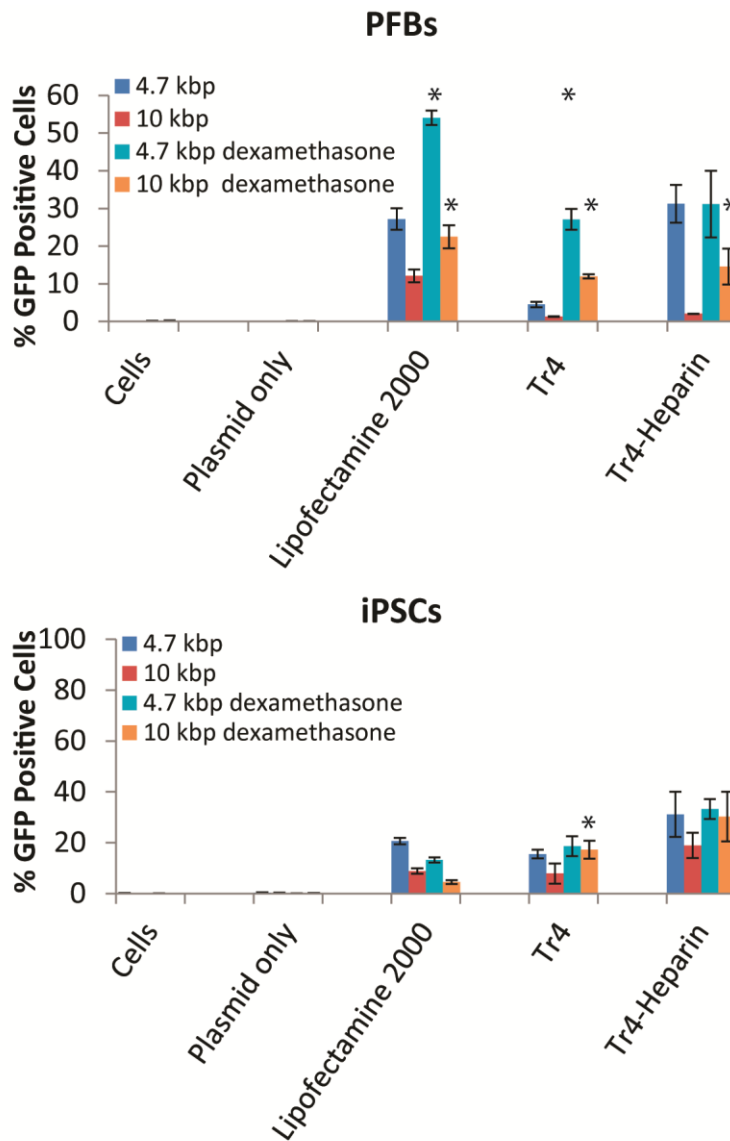
Figure 3.6: GFP expression measured by flow cytometry of primary fibroblasts and induced pluripotent stem cells treated with dexamethasone. Error bars represent the standard deviation of 3 replicates. Significant increase (P<0.05) compared to the unmodified transfection (Figure 3.2) as calculated by the Student's T-Test is denoted by *.

In iPSCs, the dexamethasone transfection results yielded different trends. Treatment of cells with dexamethasone did not provide an increase in transfection efficiency for polyplex and control formulations containing the small plasmid.

Dexamethasone increases the transfection efficiency in the large plasmid to the level that is achieved with the small plasmid in Tr4 and Tr4-Heparin. This could indicate that the loss of transfection efficiency observed in iPSCs for polyplex and control formulations including the large plasmid is due to decreased nuclear localization that can be rescued using dexamethasone. Interestingly, dexamethasone does not have the same effect on the Lipofectamine 2000 treated cells, which could indicate that the trafficking mechanism and nuclear localization pathway for Lipofectamine 2000 may be different from that of Tr4 and Tr4-heparin in iPSCs. Based on propidium iodide staining, treatment with dexamethasone at the experimental concentrations do not appear to have an effect on the toxicity compared to an unmodified transfection.
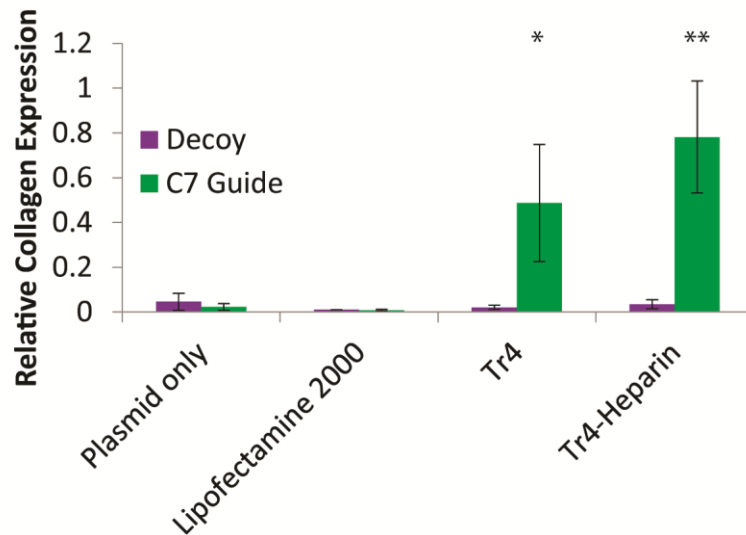
Figure 3.7: Increase in collagen type VII expression driven by targeted dCas9-VP64 in induced pluripotent stem cells. Cells were transfected in mTesR supplemented with 5 μM dexamethasone. Tr4 and Tr4-Heparin transfections were done at an N/P of 40. Lipofectamine 2000 transfections were done using 5 µl/µg DNA. Relative Collagen VII expression is normalized to GAPDH. Error bars represent the standard deviation of three replicates. Significance compared to decoy gRNA was determined. * denotes $P<0.05$ by Student's t-test. ** denotes $P<0.01$.

Transcription Activation using dCas9-VP64

Following the success of utilizing dexamethasone in combination with the transfection formulations with iPSCs, we sought to translate these fundamental findings to functional transfection of iPSCs with a synthetic transcriptional activation system targeted to collagen type VII originally developed by Konermann et al.[3] For these experiments, the collective optimized conditions (i.e., Tr4-Heparin, N/P 40, 5 µM dexamethasone along with controls) were utilized to deliver a two plasmid synthetic transcription activation system previously described by Konermann et al[3] targeted to the promotor for collagen type VII (COL7A1) (Table S1, Supporting Information).[3] The system utilized a dCas9-VP64 fusion protein with a gRNA targeted to the promotor of Col7A1. In these transfections, the dCas9-VP64 plasmid was 13 kbp, and the gRNA plasmid was 3 kbp. In some recessive dystrophic epidermolysis bullosa patients, mutations in COL7A1 produce C7 protein with reduced functional capabilities in establishing the dermal-epidermal basement membrane.[33] In these cases, increasing the total amount of semi-functional C7 protein above a therapeutic threshold may lead to a practical benefit.[7,35] For this reason, this construct could have a direct clinical benefit if delivered efficiently. The two plasmid system encoding both dCas9-VP64 transcriptional activator and the gRNA that targets binding of the correct genomic region were formulated with Lipofectamine, Tr4, and Tr4-heparin according to the methods established aboved and delivered in the presence of dexamethasone. In addition, pDNA only samples were examined as controls (in the presence of dexamethasone). After 48 hours, the resulting cells transfected with both the Tr4 and Tr4-heparin delivery systems in the presence of 5 µM dexamethasone exhibited significantly increased expression of

collagen type VII compared to treatment with dCas9 and decoy gRNA with no target sequence. To control for differences in total protein, all results were normalized to the housekeeping gene glyceraldehyde-6-phosphate dehydrogenase (GAPDH). As shown in Figure 3.7, both vehicles, Tr4 and Tr4-heparin both lead to increased collagen expression with the payload consisting of two plasmids, however the Tr4-heparin system provides slightly higher amplification. Conversely, transfection with Lipofectamine 2000 (also in the presence of dexamethasone) is not sufficient to drive increased collagen expression with this set of plasmids. This result indicates that the use of Tr4-heparin with dexamethasone can functionally transfect iPSCs to enhance collagen expression with a therapeutic dCas9 system, even in a scenario where Lipofectamine 2000 is unsuccessful.

3.4 Conclusions

In this study, we aimed to characterize the effect of plasmid size and delivery vehicle formulation (Lipofectamine, Tr4, and Tr4-heparin) on the transfection of primary fibroblasts and induced pluripotent stem cells. We also aimed to develop a method for translating a subset of these results to the functional transfection of iPSCs using a dual large plasmid system that may have clinical relevance for the treatment of the skin disease, epidermolysis bullosa. We have demonstrated that large plasmid (>10 kbp) transfection does not correlate well with the efficiency achieved using smaller reporter plasmids (~5 kbp). Increasing plasmid size to 10 kBp leads to a dramatic decrease in transfection efficiency in iPSCs and nearly eliminates transfection efficiency in PFBs. For the transfection systems, the lack of expression with larger plasmids is not driven by a decrease in plasmid internalization as both small and large plasmids are internalized to very similar degrees in both cell types with all delivery vehicle formulations examined in

this study. Promoting endosomal escape by co-transfection with chloroquine leads to increased transfection efficiency using a small plasmid, but has a limited impact on large plasmid transfection efficiency. This indicates that while some polyplexes may be sequestered in the endosome, lack of endosomal/lysosomal escape is not for the cause of the diminished activity of large plasmids. Conversely, transfecting cells during S phase (such that trafficking occurs during mitosis when the nuclear membrane is breaking down) or addition of dexamethasone (dialates nuclear pores) revealed that the nuclear envelope is a major barrier and methods to improve nuclear membrane transport leads to significant increases in transfection efficiency for polyplex and control systems carry the large plasmid in both iPSCs and PFBs. These results strongly indicate that a lack of nuclear localization/internalization with the large plasmid drives the decrease in transfection efficiency. We utilized these results to inform the use of Tr4 in a potentially clinically useful application. The ability of Tr4-heparin polyplexes formulated with dexamethasone to successfully deliver a two plasmid system coding for the synthetic transcription factor, Cas9-VP64 targeted to the promoter of collagen type VII. This result indicates that Tr4-Heparin coformulated with dexamethasone has the ability to efficiently delivery a large plasmid cargo resulting in a potentially useful clinical benefit. Collectively, these results inform the design and optimization of future non-viral vehicles to promote successful delivery of functional genome editing systems.

Chapter 4: Ternary composite nanofibers containing chondroitin sulfate as chemokine scavenging wound dressings

Synopsis

Recessive dystrophic epidermolysis bullosa (RDEB), an inherited disease characterized by painful blistering wounds caused by a mutation in collagen type VII leads to a constant state of inflammation in patient skin, and the eventual development of an aggressive form of squamous cell carcinoma (SCC). Inflammatory cytokines such as MCP-1 and Il-8 have been implicated in the development of RDEB-SCC as well as persistent inflammation in other chronic wounds. Herein, we report the fast, efficient production of ternary composite nanofiber mats containing pullulan, chondroitin sulfate, and tannic acid. After crosslinking, the swellable hydrophilic fibers are stable to hydration and can absorb up to 600% their weight in water. The ability of the fibers to scavenge the model cytokine, MCP-1, was also quantified. After 2 hours of incubation, the fibers were able to remove most of the MCP-1 from a solution of cell culture media.

4.1 Introduction

Recessive dystrophic epidermolysis bullosa (RDEB) is an inherited disease characterized by a defect in collagen type VII. From birth, patients are afflicted with painful blistering wounds.[1,2] Most patients eventually develop a particularly aggressive form of squamous cell carcinoma (SCC) known as RDEB SCC. By age 45, 78.7% of patients with severe generalized RDEB succumb to metastatic SCC.[3] The pathogenesis of RDEB SCC and how it differs from SCC in the observed non-RDEB population is an area of active research. The constant state of inflammation in the skin is partially to be blamed for the high incidence of cancer in patients suffering from RDEB.[4,5] Recently, a set of inflammatory chemokines, including MCP-1 and IL-8, were identified as being overexpressed in patients suffering from RDEB.[6] Accumulation of these chemokines leads to a cycle of inflammation in chronic diabetic wounds.[7] MCP-1 and IL-8 have also been implicated in the progression of SCC as well as other cancers such as leukemia.[8-10] We hypothesize that the use of scavenging materials to remove inflammatory chemokines from RDEB wounds would reduce inflammatory signaling, and potentially slow the progression of RDEB SCC.

To this end, we hypothesized that nanofibers containing the glycosaminoglycan, chondroitin sulfate, which has been shown to efficiently bind many chemokines including IL-8 and MCP-1[11] may scavenge inflammatory chemokines from RDEB wounds leading to reduced inflammation and slowing the development of RDEB-SCC. Others have recently shown that a hydrogel composed of the glycosaminoglycan, heparin and PEG could efficiently scavenge chemokines leading to improved healing in diabetic wounds.[12] However, those materials required the chemical functionalization of heparin followed by

crosslinking to form the hydrogel. The fast, efficient development of nanofibrous wound dressings from readily available materials may better serve patients who require bandage changing every other day. The use of GAG-based materials for wound healing has been an area of extensive research.[13-15] Yergoz et al have recently shown that GAG-mimicking nanofibers can promote improved healing in burn victims.[16]

The Forcespinning® method allows for the development of cost effective large-scale fabrication of nonwoven nanofibers mats (industrial systems produce hundreds of meters per minute).[17-19] This method allows the development of affordable wound dressings available to a large population of patients.[20] Xu et al have previously demonstrated the use of Forcespinning® to efficiently develop pullulan-supported nanofibers containing chitosan and tannic acid.[17] The goal of this project was the development of antibacterial scaffolds that could simultaneously promote cell growth.

In an effort to improve on these materials, we developed a similar fiber containing varying concentrations of chondroitin sulfate. These fibers can be quickly generated from all natural materials with no chemical functionalization necessary prior to spinning. These fibers efficiently absorb water without losing their structural integrity. To investigate their potential use as anti-inflammatory wound dressings, their ability to scavenge the model chemokine, MCP-1 was quantified. The fibers quickly and efficiently scavenge chemokines from a solution of cell culture media regardless of chondroitin sulfate content. The high surface area conferred by their nanostructure likely promotes fast binding of chemokines in solution. The fibers also exhibited the ability to

quantitatively remove MCP-1 and Il-8 from RDEB-SCC conditioned media. Finally, cell

migration activated by treatment with RDEB SCC conditioned media.
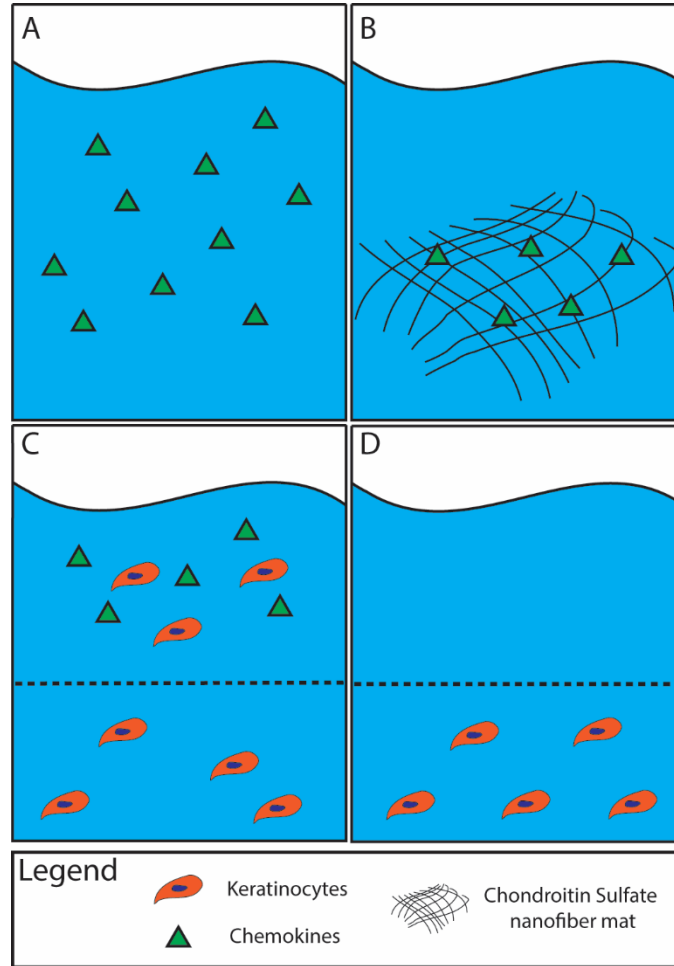
Figure 4.1: Schematic of chemokine scavenging materials. A) Chemokines present in conditioned media derived from RDEB-SCC cells. B) Nanofiber scavenging chemokines from solution. C) Cell migration is activated by RDEB-SCC conditioned media. D) Cell migration is inhibited by scavenged RDEB-SCC conditioned media

4.2 Experimental Methods

General

Pullulan was purchased from Tokyo Chemical Industry Co. (Tokyo, Japan) Tannic

acid (produced from Chinese natural gall nuts) and citric acid were purchased from

Sigma-Aldrich. RPMI was purchased from Thermo Fisher Scientific. Chondroitin sulfate

was purchased from Sigma-Aldrich. Human MCP-1 and coated MCP-1 ELISA kits were purchased from Sigma-Aldrich. Hospital Grade Gauze Pads (Johnson and Johnson, New Brunswick, NJ) were used as positive controls.

Instrumentation

Nanofibers were generated using a FibeRio Cyclone L-1000 Forcespinning® device (FibeRio, McAllen, TX). SEM images were collected using a Hitachi SU8230 Field Emission Gun SEM (Hitachi, Tokyo, Japan). Sputter coating was performed using a Leica EM ACE 600 sputter coater (Leica Biosystems, Wetzlar, Germany).

Development of Ternary Composite Nanofibers

Nonwoven ternary composite mats were formed using a variation on the protocol first published by Xu et al.[17] Solutions were formed by first adding varying wt% (described in Table 1) of chondroitin sulfate as well as 3 wt% citric acid to 10 mL of H_2O. Solutions were stirred overnight until completely dissolved. After the CS was completely dissolved, 18 wt% pullulan was added to each solution, and stirred until dissolved (ca. 12 hr.) Tannic acid was then added (1 wt%) to the solution and dissolved completely prior to spinning.

Solutions of chondroitin sulfate, pullulan, tannic acid, and citric acid were loaded into a cylindrical spinneret equipped with 30 gauge half-inch regular bevel needles. Fibers were spun and collected in 2 mL aliquots until 10 mL of solution was used. The resulting mats were immediately placed in a vacuum oven at 150 °C, and cured for 12 hours.

Water Absorption Coefficient

Water absorption coefficients were determined using a method similar to that published by Xu et al.[17] Mats were cut to a size of 1 cm x 1 cm, weighed, and submerged in 3 mL DI water for 1 hr. After soaking, the mats were removed from the soaking solution. Excess water was dabbed away using a Kimwipe^{TM}, and the mats were weighed again to determine water absorption. The experiment was conducted on 3 samples for each mat, and averaged. Water absorption was determined using the equation below.

$$Water\ Absorption = 100\ x\ \frac{W_{wet} - W_{dry}}{W_{dry}}$$

Scanning Electron Microscopy

Pristine mats were prepared by cutting a small section of the cured mat and affixing to carbon tape. Soaked mats were prepared by soaking in DI water for 1 hr. After soaking, mats were rinsed once with fresh DI water, and transferred to empty scintillation vials. The soaked mats were then frozen in liquid nitrogen, and lyophilized to dryness. Dried mats were affixed to carbon tape.

Prepared mats were then sputter coated with Pd to a thickness of 5 nm using a Leica EM ACE 600 sputter coater. SEM images were then collected using a Hitachi SU8230 Field Emission Gun SEM.

Chemokine Scavenging

The ability of the nonwoven nanofiber mats to scavenge chemokine from solution was determined using an ELISA assay. Based on a modification of the protocol described by Lohmann et al.[12], solutions of the chemokine, MCP-1, were prepared at a concentration of 24 μg/ml. Mats were cut into squares weighing 0.5 mg, and placed in an

empty 96-well plate. Mats were then treated with 100 µl of the MCP-1 solution. MCP-1 solution was also placed in empty wells as a negative control. The solutions were incubated on the mats with gentle rocking at room temperature for 6 hrs. At each time point, 1 µl MCP-1 solution was removed from the well, and frozen until quantification by ELISA.

MCP-1 concentrations were quantified using a pre-coated MCP-1 ELISA kit purchased from Sigma-Aldrich according to the manufacturer's protocol. In order to prepare samples at an appropriate concentration for ELISA quantification, samples were diluted to yield a control concentration of 1,000 pg/mL. 1 µl samples were diluted with 999 µl RPMI. The resulting solutions were then diluted by a factor of 5 with ELISA dilution buffer. The resulting solutions were incubated on the ELISA plate for 3 hrs at room temperature along with a standard curve of MCP-1 concentrations. After incubation, the plate was washed and treated with developing reagents per the manufacturer's instructions. MCP-1 scavenging was quantified by presenting signal from the scavenged solution as a percentage of the T=0 control at each time point.

Scavenging of Conditioned Media

Conditioned media from RDEB-SCC cells was collected after 24 hours of cell culture. To 4 mL of media, a 20 mg piece of 5% CS nanofiber mat was added, and allowed to incubate at 4 °C for 24 hours. 50 µL samples were removes before and after scavenging for analysis by ELISA assay. For ELISA, samples were diluted by a factor of 12, and MCP-1 and Il-8 concentrations were determined using the manufacturer's protocol.

4.3 Results and Discussion
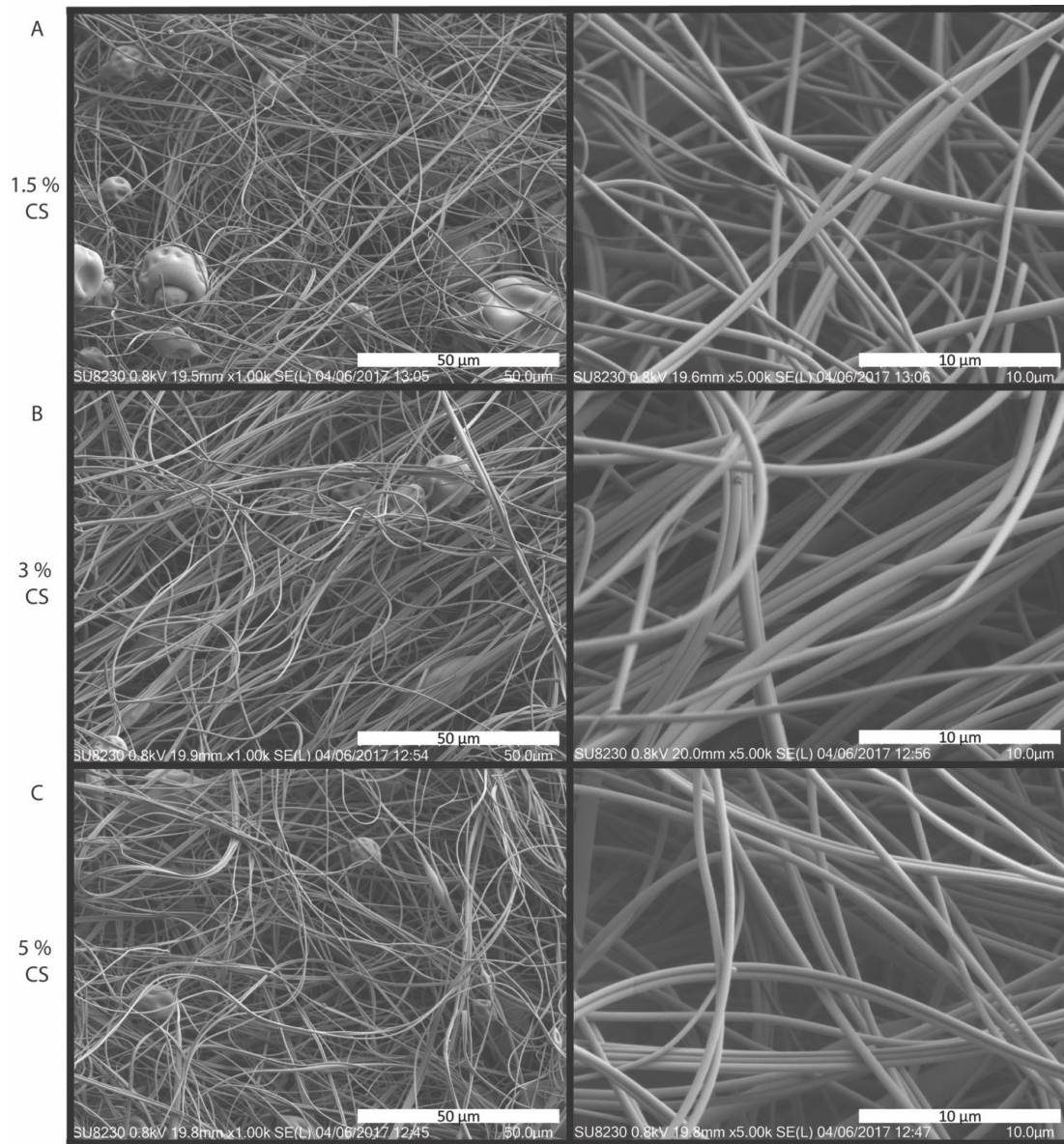
Figure 4.2: SEM micrographs of 1.5% (a), 3% (b), 5% (c) chondroitin sulfate nanofiber mats at 1000x and 5000x magnification. Scale bars equal 50 μm and 10 μm respectively.

Nanofiber mats were formed using the Forcespinning® technique previously described by Xu et al.[17] Formulation conditions can be seen in Table 1.

Table 2: Formulation of Ternary Composite Mats

	Pullulan	Chondroitin Sulfate	Tannic acid	Citric Acid
1.5% CS	18%	1.5%	1%	3%
3% CS	18%	3%	1%	3%
5% CS	18%	5%	1%	3%

Solutions containing 18 wt% pullulan (Pl), varying wt% chondroitin sulfate (CS), 1 wt% tannic acid (TA), and 3 wt% citric acid (CA) were prepared in water and the solutions introduced into the spinneret. The fibers were then formed by spinning at 6500 RPM at room temperature. Fibers were collected using a square collection rack, and formed into nonwoven mats. The resulting mats were then transferred to a vacuum oven at 150 °C for 12 hours.

The morphology of the resulting fibers was characterized by scanning electron microscopy (SEM) (Figure 4.2). The nanofibers have uniform diameter, and form discrete long homogeneous fibers. The average diameter of the nanofibers is <500 nm. The fibers exhibit the same morphology regardless of CS content.
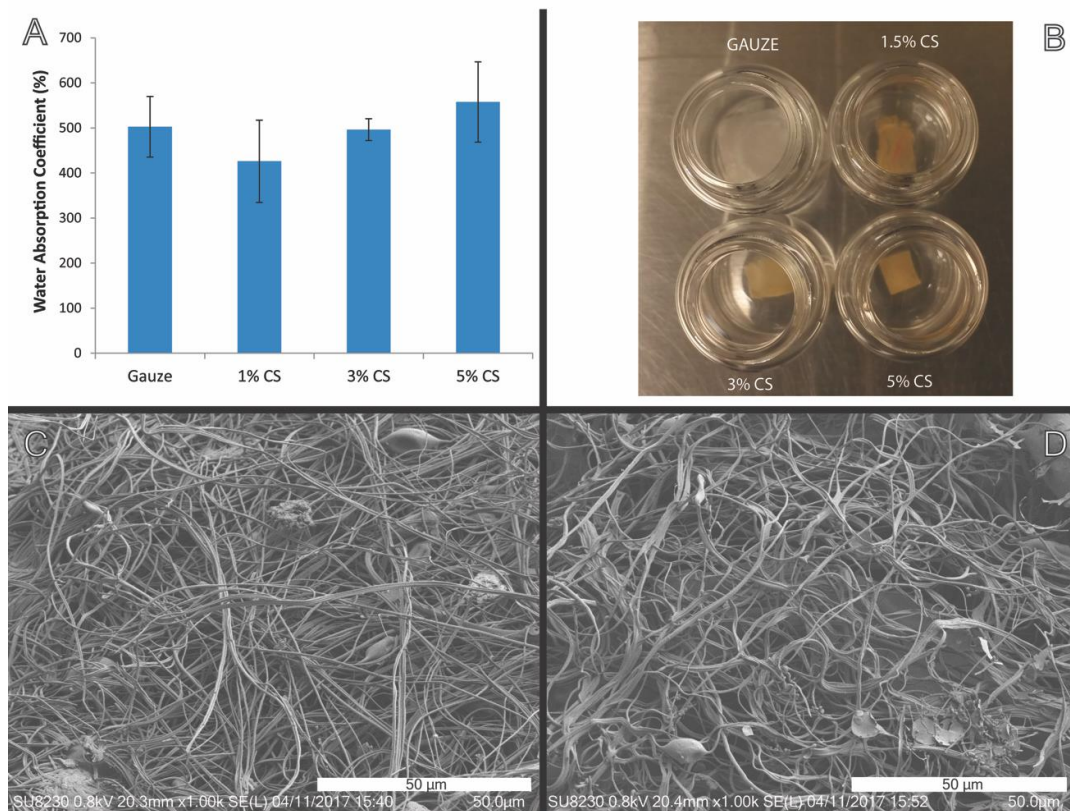
Figure 4.3: A) water absorption coefficient of chondroitin sulfate nanofibers compared to commercially available gauze. B) Nanofiber mats submerged in water. C) SEM micrograph of pristine 5% CS nanofiber mat. D) SEM micrograph of dried 5% CS nanofiber mat after saturation with water.

An important property of wound dressing materials is the ability to efficiently absorb wound exudate to promote an optimal environment for wound healing. To quantify the ability of the mats to absorb excess water, the water absorption coefficient of the mats was determined. Mats were cut to into squares weighing ~4 mg each. Each mat was then submerged in 1 mL of DI water for 60 min. The mats were then removed from solution, and excess water was removed by dabbing with a Kimwipe^TM. The mats were then weighed again to determine the amount of water absorbed. As shown in Figure 4.3a, water absorption was found to be greater than 400% for all samples. These mats show

similar water absorption ability as a commercially available gauze pad. A slight correlation was found between water absorption and CS%, but none of the samples were statistically different from each other. The 5% CS mats exhibited 550% water absorption. Submerged mats maintained their macroscopic structure when treated with water as can be seen in Figure 4.3b. These water absorption properties indicate that mats should be able to efficiently absorb and retain wound exudate when used as wound dressings.

The ability of the mats to maintain their structure on a microscopic level after saturation with water was also investigated. Mats were submerged in water overnight, rinsed, and lyophilized. These swelled mats were compared to pristine mats by scanning electron microscopy (Figure 4.3c and 4.3d). After treatment with water, the resulting mats exhibit no significant change following lyophilization. While some defects can be observed, and the fibers appear to have contracted, the fibers maintain their overall structure, and show no signs of degradation. The developed fibers show promising capabilities to withstand the wet environment of a wound while maintaining their ability to cover the wound.
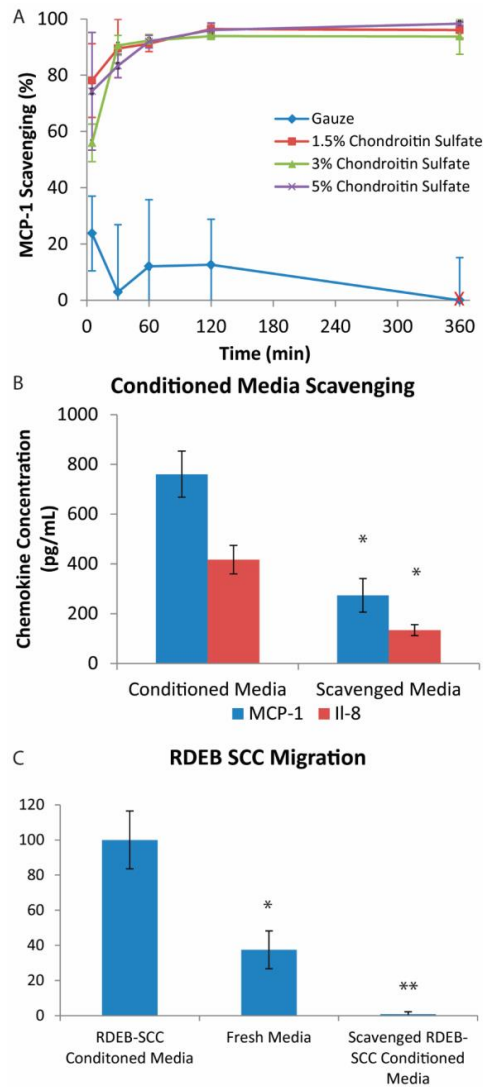
Figure 4.4: Scavenging of MCP-1 from solution by chondroitin sulfate nanofiber mats. Scavenging percentage was determined by quantification of MCP-1 concentration of solution treated with nanofiber mats compared to solution alone over time. Concentrations were quantified by ELISA assay. Error bars represent the standard deviation of 3 replicates. X: After 6 hours, evaporation from the gauze control mats lead a negative apparent scavenging value which has been shown as zero for the purposes of this plot. B) Concentration of MCP-1 and Il-8 in RDEB-SCC conditioned media before and after scavenging with 5% CS nanofibers as determined by ELISA. Error bars represent the average of three replicates. * denotes a significant decrease (P<0.05) compared to unscavenged conditioned media by the Student's T-Test. C) Migration of RDEB-SCC triggered by conditioned media, fresh media, and scavenged conditioned media. Error bars represent the average of 3 replicates. * denotes a significant decrease (P<0.05) compared to the conditioned media. ** denotes a significant decrease (P<0.05) compared to fresh media. Significance was determined using the Student's T-Test.

Chemokines are a class of inflammatory molecules commonly found in wound tissues. In many cases, the buildup of these signaling molecules in tissues can lead to persistent inflammation, and insufficient healing of the wound.[12] MCP-1, IL-8, and other CCL-class chemokines have also been implicated in the progression of RDEB-SCC in patients suffering from epidermolysis bullosa.[6] Sulfated glycosaminoglycans (GAGs) such as chondroitin sulfate have been found to efficiently bind some chemokines, including MCP-1 and Il-8, and materials incorporating GAGs have been shown to reduce inflammation and promote wound healing *in vivo*.[12] To examine the potential anti-inflammatory properties of the CS/PL/TA mats, we investigated the ability of the mats to scavenge the model chemokine, MCP-1, from solution. Mats weighing 0.5 mg each were placed in 96-well plates with 100 μL RPMI medium containing 24 μg/mL MCP-1. Samples were removed from the wells at multiple time points, and MCP-1 concentration was quantified compared to an untreated control solution using an ELISA assay. After only 5 minutes of incubation, the fibers began to scavenge significant amounts (ca. 80%) of MCP-1 from solution. The fibers continued to remove MCP-1 from solution over the course of the incubation. After 2 hours of incubation, 98% of the available MCP-1 had been removed from solution for all tested CS-containing mats. No significant difference was observed in scavenging percentage as a function of chondroitin sulfate percentage. Even 1.5 % CS was sufficient to quickly and almost quantitatively remove MCP-1 from solution. The commercially available gauze mats exhibited little binding of MCP-1 over the course of the experiment. After 6 hours, solvent evaporation from the gauze mats

caused the concentration in the well to increase above the starting concentration, so the scavenging percentage was represented as zero.

The starting concentration of 24 μg/mL is significantly higher than any concentration that would likely be observed in a clinical setting.[12] This indicates that the fibers can quickly remove MCP-1 from solution, and have the capacity to hold high concentrations of chemokine over time. After 24 hours, no MCP-1 was detected in the solution. These results demonstrate the ability of the nonwoven nanofiber mats to successfully scavenge biologically relevant amounts of protein from solution. In a wound environment, the fibers could act as a sink for MCP-1 and other GAG-binding chemokines, leading to reduced inflammation and improved wound healing.

To further test the utility of the nanofibers as chemokine scavengers, the fibers were used to scavenge chemokines from conditioned media derived from RDEB-SCC cells. RDEB-SCC cells were cultured under previously described conditions using Epilife media supplemented with 10% FBS. Conditioned media (4 mL) was then collected from the cells, and placed in a centrifuge tube containing a 20 mg piece of the 5% chondroitin sulfate nanofiber mat. The media was sampled prior to scavenging to determine the starting chemokine concentration. The media was incubated with the nanofibers for 24 hours at 4 °C and gently agitated periodically. After incubation, the fibers were removed, and the chemokine concentration was quantified by ELISA. As can be seen in Figure 4.4b, scavenging reduced the concentration of MCP-1 from 760 pg/mL to 273 pg/mL. The concentration of Il-8 was also reduced from 417 pg/mL to 134 pg/mL. These results differ from the time course scavenging experiment where quantitative reduction of the

chemokine concentration was achieved after only 2 hours. This difference is likely due to the more complex nature of the epilife media after conditioning with RDEB-SCCs compared to the serum free RPMI. Serum proteins, and other excreted molecules may be inhibiting the ability of the fibers to completely remove the chemokines of interest. Additionally, since the starting concentration of the conditioned media is orders of magnitude lower, it is possible that an equilibrium state is being reached with the conditioned media that results in a reduced scavenging percentage. Regardless, these results show that the nanofibers significantly reduce the concentration of inflammatory chemokines associated with RDEB-SCC from complex conditioned media.

To determine whether the chemokine scavenging was sufficient to modify the behavior of RDEB-SCC cells, the scavenged conditioned media was used as a chemoattractant in a cell migration assay. RDEB-SCC cells were plated in a transwell plate, and grown to 60% confluency. The upper chamber of the transwell plate was then treated with RDEB-SCC conditioned media, and the cells were allowed to migrate for 24 hours. After 24 hours, the upper wells were stained with Crystal Violet stain, and cell migration was quantified by counting the cells present on the upper membrane. Migration of the cells towards RDEB-SCC conditioned media was normalized to 100% and migration towards scavenged media and fresh media was plotted as a percentage. The results can be seen in Figure 4.4c. More than twice as many cells migrated towards the conditioned media when compared with the freshly prepared epilife media. In contrast, the migration towards scavenged media is halted almost entirely. The further decrease in migration compared to fresh media could be due to non-specific scavenging of nutrients

105

from the media.   While this effect is undesireable, it is clear that scavenging of conditioned media reverses the migration normally triggered by RDEB-SCC conditioned media. The use of 1.5% CS mats for a reduced amount of time could result in chemokine scavenging without depletion of nutrients. The reduction of RDEB-SCC migration could result in reduced progression of RDEB-SCC in patients treated with nanofiber wound dressings.

4.4 Conclusion

Herein, we have shown that we can form ternary composite nanofibers supported by pullulan containing physiologically-relevant concentrations of chondroitin sulfate and tannic acid. Previous work has indicated that fibers impregnated with tannic acid have antibacterial properties. In addition to these properties, we have shown that these fibers have the potential to efficiently absorb wound exudate. They efficiently scavenge the inflammatory chemokines, MCP-1 and Il-8 from cell culture media. These materials may provide a less inflammatory environment for wound healing in RDEB patients and slow the development of RDEB-SCC. We also expect that the chemokine scavenging properties of these fibers will provide an anti-inflammatory environment necessary for improved healing of a variety of chronic wounds. Additionally, the chemical functionality of pullulan and chondroitin sulfate may provide convenient handles for the production of protein-conjugated materials that can further promote a positive interaction with wound environments.

Chapter 5: Conclusion and Future Directions

Synopsis

This chapter contains concluding remarks and proposed future directions for this work. Based on the conclusions of this work, the development of improved gene delivery vehicles designed to promote increased nuclear localization of cargo are proposed. The delivery of plasmids encoding functional plasmids to skin in order to promote healing of the basement membrane is described. Finally, the implications of chemokine scavenging nanofibers are discussed.

5.1 Concluding Remarks

This work represents a concerted collaborative effort to tailor synthetic delivery vehicles to the needs of translational scientists. The use of Tr4, a synthetic cationic glycopolymer containing 4 charged group copolymerized with trehalose, to deliver plasmid DNA to a variety of cell types was investigated. Cell and tissue types associated with the epidermolysis bullosa were chosen as targets to develop improved treatment strategies for the disease.

The use of heparin to form ternary polyplexes of DNA and Tr4 with heparin decorating the surface yielded dramatically improved transfection efficiency compared to transfection with Tr4 alone. Careful study of the mechanism of transfection with Tr4-heparin polyplexes yielded interesting results. The use of heparin has no significant impact on the uptake of DNA. However, it does modify the uptake pathway, and causes an increased dependence on macropinocytosis compared to Tr4 alone. This increased dependence on macropinocytosis may lead to increased gene expression by avoiding lysosomal trafficking of the polyplexes. These experiments allowed for the efficient transfection with a 4.7 kpb reporter plasmid of patient-derived primary fibroblasts which are difficult to transfect with commercially available reagents.

Continued study of Tr4 and Tr4-heparin transfections showed that Tr4-heparin lost transfection efficiency when the plasmid size was increased from 4.7 kbp to a more clinically applicable 10 kbp plasmid. The decrease in transfection efficiency occurred in spite of high uptake of the large plasmid. To understand this phenomenon, intracellular barriers to transfection were systematically perturbed. Disruption of the nuclear envelope

by the small molecule drug, dexamethasone, or by cell synchronization led to increased transfection efficiency in primary fibroblasts and induced pluripotent stem cells. Conversely while the use of chloroquine to promote endosomal escape caused a pronounced increase in transfection efficiency with the small plasmid with Tr4 alone, its effect on Tr4-heparin, and on the large plasmid transfection was minimal. This further indicates that Tr4-heparin transfection has a positive effect on endosomal escape/avoidance of the polyplexes. It also indicates that the large plasmid transfection is still inhibited by nuclear localization even in situations where the endosomal barriers are circumvented.

The use of dexamethasone as a nuclear destabilization agent was studied in two functional transfection scenarios. First, induced pluripotent stem cells were transfected *in vitro* with a plasmid coding for a synthetic transcription activator targeted to collagen type VII. Transfection with this plasmid may drive increased expression of truncated forms of collagen type VII in certain patients, and lead to recovered basement membrane function. The use of Tr4-heparin and dexamethasone in this transfection produced a significant increase in collagen type VII expression compared to transfection with an untargeted gRNA. To further demonstrate the ability perform clinically useful transfections, Tr4-heparin polyplexes were used to deliver 4.7 kbp plasmid topically to a mouse wound meant to model epidermolysis bullosa. Preliminary experiments showed that mice treated with Tr4-heparin polyplexes exhibited GFP expression within the wound tissue.

To investigate a different facet of epidermolysis bullosa treatment, a ternary composite nanofiber mat containing chondroitin sulfate was developed. The fibers were hydrophilic in nature, and exhibited the ability to absorb 5 times their weight in water. They had an average diameter of approximately 500 nm, and demonstrated the ability to withstand swelling with water. The fibers' ability to scavenge model inflammatory chemokines from cell culture media was investigated. The fibers were able to efficiently scavenge biologically relevant concentrations of MCP-1 out of cell culture media. They also exhibited the ability to remove MCP-1 and Il-8 from conditioned media derived from RDEB-SCC cells. After treatment, the scavenged conditioned media no longer acted as a chemoattractant for RDEB-SCC cells.

This work could have important implications for the development of improved treatments for epidermolysis bullosa. Tr4-heparin polyplexes have shown the ability to efficiently transfect primary fibroblasts and induced pluripotent stem cells. The use of dexamethasone to dilate nuclear pores enhances the ability of Tr4-heparin to deliver large plasmids. However, cotransfection with a small molecule additive may not be useful for all application. The development of trehalose-based polymers which can form drug-loaded polyplexes containing dexamethasone, chloroquine, or both may provide improved transfection in situation where cotransfection is not viable. The delivery of a GFP reporter in an *in vivo* murine model is currently underway, and could represent a promising step toward *in vivo* gene therapy for epidermolysis bullosa. Efforts to perform transfections with a functional laminin beta 3, the protein responsible for junctional epidermolysis bullosa, plasmid are underway. If the expression of laminin beta 3 is high

110

enough for it to integrate into the basement membrane and promote wound healing, this could significantly improve the ability to treat JEB wounds.

Continued research into chemokine scavenging materials is also underway. The fibers have shown the ability to remove chemokines from solution have been confirmed. However, the study of how chemokine scavenging affects wound healing and the progression of RDEB-SCC should continue to be studied.

References

(1) Unciti-Broceta, A.;Jose Diaz-Mochon, J.;Sanchez-Martin, R. M.; Bradley, M. *Acc. Chem. Res.*, **2012**, *45*.

(2) Cong, L.;Ran, F. A.;Cox, D.;Lin, S.;Barretto, R.;Habib, N.;Hsu, P. D.;Wu, X.;Jiang, W.;Marraffini, L. A.; Zhang, F. *Science*, **2013**, *339* 819.

(3) Konermann, S.;Brigham, M. D.;Trevino, A. E.;Joung, J.;Abudayyeh, O. O.;Barcena, C.;Hsu, P. D.;Habib, N.;Gootenberg, J. S.;Nishimasu, H.;Nureki, O.; Zhang, F. *Nature*, **2015**, *517* 583-588.

(4) Ran, F. A.;Hsu, P. D.;Wright, J.;Agarwala, V.;Scott, D. A.; Zhang, F. *Nat. Protocols*, **2013**, *8* 2281-2308.

(5) Chu, V. T.;Weber, T.;Wefers, B.;Wurst, W.;Sander, S.;Rajewsky, K.; Kuhn, R. *Nat Biotech*, **2015**, *33* 543-548.

(6) Boch, J. *Nat Biotech*, **2011**, *29* 135-136.

(7) Osborn, M. J.;Starker, C. G.;Mcelroy, A. N.;Webber, B. R.;Riddle, M. J.;Xia, L.;Defeo, A. P.;Gabriel, R.;Schmidt, M.;Von Kalle, C.;Carlson, D. F.;Maeder, M. L.;Joung, J. K.;Wagner, J. E.;Voytas, D. F.;Blazar, B. R.; Tolar, J. *Mol. Ther.*, **2013**, *21* 1151-1159.

(8) Boch, J.; Bonas, U. *Annu. Rev. Phytopathol.*, **2010**, *48* 419-436.

(9) Aronovich, E. L.;Mcivor, R. S.; Hackett, P. B. *Hum. Mol. Genet.*, **2011**, *20* R14-R20.

(10) Reineke, T. M.; Davis, M. E. In *Comprehensive Polymer Science*; Krzysztof Matyjaszewski, M. M., Ed.; Elsevier: 2012; Vol. 2nd Edition, p 1-31.

(11) Ogris, M.;Brunner, S.;Schuller, S.;Kircheis, R.; Wagner, E. *Gene Ther.*, **1999**, *6*.

(12) Mintzer, M. A.; Simanek, E. E. *Chem. Rev.*, **2009**, *109* 259-302.

(13) Mislick, K. A.; Baldeschwieler, J. D. *Proceedings of the National Academy of Sciences*, **1996**, *93* 12349-12354.

(14) Mclendon, P. M.;Buckwalter, D. J.;Davis, E. M.; Reineke, T. M. *Mol. Pharm.*, **2010**, *7* 1757-1768.

(15) Dash, P. R. R., M L; Barrett, L B;Wolfert, M a; Seymour, L W *Gene Ther.*, **1999**, *6* 643-650.

(16) Kopatz, I.;Remy, J.-S.; Behr, J.-P. *J. Gene Med.*, **2004**, *6* 769-776.

(17) Goncalves, C.;Mennesson, E.;Fuchs, R.;Gorvel, J.-P.;Midoux, P.; Pichon, C. *Mol. Ther.*, **2004**, *10* 373-385.

(18) Molas, M.;Gomez-Valades, A. G.;Vidal-Alabro, A.;Miguel-Turu, M.;Bermudez, J.;Bartrons, R.; Perales, J. C. *Curr. Gene Ther.*, **2003**, *3* 468-485.

(19) Dreaden, E. C.;Morton, S. W.;Shopsowitz, K. E.;Choi, J.-H.;Deng, Z. J.;Cho, N.-J.; Hammond, P. T. *ACS Nano*, **2014**, *8* 8374-8382.

(20) Deng, Z. J.;Morton, S. W.;Bonner, D. K.;Gu, L.;Ow, H.; Hammond, P. T. *Biomaterials*, **2015**, *51* 250-256.

(21) Correa, S.;Choi, K. Y.;Dreaden, E. C.;Renggli, K.;Shi, A.;Gu, L.;Shopsowitz, K. E.;Quadir, M. A.;Ben-Akiva, E.; Hammond, P. T. *Adv. Funct. Mater.*, **2016**, *26* 991-1003.

(22) Russell, M. R. G.;Nickerson, D. P.; Odorizzi, G. *Curr. Opin. Cell Biol.*, **2006**, *18* 422-428.

(23) Mellman, I. *Annu. Rev. Cell Dev. Biol.*, **1996**, *12* 575-625.

 (24) Luzio, J. P.;Rous, B. A.;Bright, N. A.;Pryor, P. R.;Mullock, B. M.; Piper, R. C. *J. Cell Sci.*, **2000**, *113* 1515-1524.

 (25) Behr, J. P. *Chimia*, **1997**, *51* 34-36.

 (26) Van De Wetering, P.;Moret, E. E.;Schuurmans-Nieuwenbroek, N. M. E.;Van Steenbergen, M. J.; Hennink, W. E. *Bioconjugate Chem.*, **1999**, *10* 589-597.

 (27) Boulanger, C.;Di Giorgio, C.; Vierling, P. *European Journal of Medicinal Chemistry*, **2005**, *40* 1295-1306.

 (28) Luby-Phelps, K.;Castle, P. E.;Taylor, D. L.; Lanni, F. *Proceedings of the National Academy of Sciences*, **1987**, *84* 4910-4913.

 (29) Dowty, M. E.;Williams, P.;Zhang, G.;Hagstrom, J. E.; Wolff, J. A. *Proceedings of the National Academy of Sciences*, **1995**, *92* 4572-4576.

 (30) Wilke, M.;Fortunati, E.;Vandenbroek, M.;Hoogeveen, A. T.; Scholte, B. J. *Gene Ther.*, **1996**, *3* 1133-1142.

 (31) Thomas, C. E.;Ehrhardt, A.; Kay, M. A. *Nature Reviews Genetics*, **2003**, *4* 346-358.

 (32) Wu, Z.;Yang, H.; Colosi, P. *Mol. Ther.*, **2010**, *18* 80-86.

 (33) Hovnanian, A.;Hilal, L.;Blanchet-Bardon, C.;De Prost, Y.;Christiano, A. M.;Uitto, J.; Goossens, M. *Am. J. Hum. Genet.*, **1994**, *55* 289-296.

 (34) Shalem, O.;Sanjana, N. E.; Zhang, F. *Nat. Rev. Genet.*, **2015**, *16* 299-311.

 (35) Webber, B. R.;Osborn, M. J.;Mcelroy, A. N.;Twaroski, K.;Lonetree, C.-L.;Defeo, A. P.;Xia, L.;Eide, C.;Lees, C. J.;Mcelmurry, R. T.;Riddle, M. J.;Kim, C. J.;Patel, D. D.;Blazar, B. R.; Tolar, J. *npj Regenerative medicine*, **2016**, *1* 16014.

 (36) Li, Hongmei l.;Fujimoto, N.;Sasakawa, N.;Shirai, S.;Ohkame, T.;Sakuma, T.;Tanaka, M.;Amano, N.;Watanabe, A.;Sakurai, H.;Yamamoto, T.;Yamanaka, S.; Hotta, A. *Stem Cell Reports*, **2015**, *4* 143-154.

 (37) Sawamura, D.;Nakano, H.; Matsuzaki, Y. *Journal of Dermatology*, **2010**, *37* 214-219.

 (38) Krupiczojc, M. A.; O'toole, E. A. *Br. J. Dermatol.*, **2016**, *174* 15-15.

 (39) Wagner, J. E.;Ishida-Yamamoto, A.;Mcgrath, J. A.;Hordinsky, M.;Keene, D. R.;Riddle, M. J.;Osborn, M. J.;Lund, T.;Dolan, M.;Blazar, B. R.; Tolar, J. *New Engl. J. Med.*, **2010**, *363* 629-639.

 (40) Laemmli, U. K. *Proceedings of the National Academy of Sciences of the United States of America*, **1975**, *72* 4288-4292.

 (41) Wu, G. Y.; Wu, C. H. *J. Biol. Chem.*, **1987**, *262* 4429-4432.

 (42) Wu, G. Y.; Wu, C. H. *J. Biol. Chem.*, **1988**, *263* 14621-14624.

 (43) Fuller, W. D.;Verlander, M. S.; Goodman, M. *Biopolymers*, **1976**, *15* 1869-1871.

 (44) Ahn, C. H.;Chae, S. Y.;Bae, Y. H.; Kim, S. W. *J. Controlled Release*, **2004**, *97* 567-574.

 (45) Wolfert, M. A.; Seymour, L. W. *Gene Ther.*, **1998**, *5* 409-414.

 (46) Choi, Y. H.;Liu, F.;Kim, J. S.;Choi, Y. K.;Park, J. S.; Kim, S. W. *J. Controlled Release*, **1998**, *54* 39-48.

 (47) Parker, A. L.;Eckley, L.;Singh, S.;Preece, J. A.;Collins, L.; Fabre, J. W. *Biochimica Et Biophysica Acta-General Subjects*, **2007**, *1770* 1331-1337.

 (48) Liu, G.;Molas, M.;Grossmann, G. A.;Pasumarthy, M.;Perales, J. C.;Cooper, M. J.; Hanson, R. W. *J. Biol. Chem.*, **2001**, *276* 34379-34387.

(49) Wolfert, M. A.;Schacht, E. H.;Toncheva, V.;Ulbrich, K.;Nazarova, O.; Seymour, L. W. *Hum. Gene Ther.*, **1996**, *7* 2123-2133.

(50) Katayose, S.; Kataoka, K. *Bioconjugate Chem.*, **1997**, *8* 702-707.

(51) Harada, A.;Togawa, H.; Kataoka, K. *Eur. J. Pharm. Sci.*, **2001**, *13* 35-42.

(52) Ferrari, S.;Moro, E.;Pettenazzo, A.;Behr, J. P.;Zacchello, F.; Scarpa, M. *Gene Ther.*, **1997**, *4* 1100-1106.

(53) Brissault, B.;Kichler, A.;Guis, C.;Leborgne, C.;Danos, O.; Cheradame, H. *Bioconjugate Chem.*, **2003**, *14* 581-587.

(54) Jiang, D.; Salem, A. K. *Int. J. Pharm.*, **2012**, *427* 71-79.

(55) Fischer, D.;Li, Y. X.;Ahlemeyer, B.;Krieglstein, J.; Kissel, T. *Biomaterials*, **2003**, *24* 1121-1131.

(56) Godbey, W. T.;Wu, K. K.; Mikos, A. G. *Biomaterials*, **2001**, *22* 471-480.

(57) Srinivasachari, S.; Reineke, T. M. *Biomaterials*, **2009**, *30* 928-938.

(58) Gosselin, M. A.;Guo, W. J.; Lee, R. J. *Bioconjugate Chem.*, **2001**, *12* 989-994.

(59) Sizovs, A.;Mclendon, P. M.;Srinivasachari, S.; Reineke, T. M. *Top. Curr. Chem.*, **2010**, *296* 131-190.

(60) Liu, Y.; Reineke, T. M. *Biomacromolecules*, **2010**, *11* 316-325.

(61) Liu, Y. M.;Wenning, L.;Lynch, M.; Reineke, T. M. *J. Am. Chem. Soc.*, **2004**, *126* 7422-7423.

(62) Ren, T.;Zhang, G. S.; Liu, D. X. *Biorg. Med. Chem.*, **2001**, *9* 2969-2978.

(63) Srinivasachari, S.;Liu, Y.;Zhang, G.;Prevette, L.; Reineke, T. M. *J. Am. Chem. Soc.*, **2006**, *128* 8176-8184.

(64) Liu, Y.; Reineke, T. M. *Bioconjugate Chem.*, **2007**, *18* 19-30.

(65) Mclendon, P. M.;Fichter, K. M.; Reineke, T. M. *Mol. Pharm.*, **2010**, *7* 738-750.

(66) Odian, G. *Principles of Polymerization*; 4th ed.; John Wiley & Sons: New York, NY, 2004.

(67) Prevette, L. E.;Lynch, M. L.;Kizjakina, K.; Reineke, T. M. *Langmuir*, **2008**, *24* 8090-8101.

(68) Wei, M.;Xu, Y.;Zou, Q.;Tu, L.;Tang, C.;Xu, T.;Deng, L.; Wu, C. *Eur. J. Pharm. Sci.*, **2012**, *46* 131-141.

(69) Huisgen, R. *Proceedings of the Chemical Society*, **1961**, 357-396.

(70) Meldal, M.; Tornoe, C. W. *Chem. Rev.*, **2008**, *108* 2952-3015.

(71) Anderson, K.;Sizovs, A.;Cortez, M.;Waldron, C.;Haddleton, D. M.; Reineke, T. M. *Biomacromolecules*, **2012**, *13* 2229-2239.

(72) Qin, A.;Lam, J. W. Y.; Tang, B. Z. *Macromolecules*, **2010**, *43* 8693-8702.

(73) Kizjakina, K.;Bryson, J. M.;Grandinetti, G.; Reineke, T. M. *Biomaterials*, **2012**, *33* 1851-1862.

(74) Davis, M. E. *Mol. Pharm.*, **2009**, *6* 659-668.

(75) Maclaren, R. E.;Groppe, M.;Barnard, A. R.;Cottriall, C. L.;Tolmachova, T.;Seymour, L.;Clark, K. R.;During, M. J.;Cremers, F. P. M.;Black, G. C. M.;Lotery, A. J.;Downes, S. M.;Webster, A. R.; Seabra, M. C. *The Lancet*, **2014**, *383* 1129-1137.

(76) Kotterman, M. A.; Schaffer, D. V. *Nat. Rev. Genet.*, **2014**, *15* 445-451.

(77) Singh, H.;Huls, H.;Kebriaei, P.; Cooper, L. J. N. *Immunol. Rev.*, **2014**, *257* 181-190.

(78) Kay, M. A. *Nature Reviews Genetics*, **2011**, *12* 316-328.

(79) Wu, T.-L.; Ertl, H. C. J. *Trends Mol. Med.*, **2009**, *15* 32-39.

(80) Bessis, N.;Garciacozar, F. J.; Boissier, M. C. *Gene Ther.*, **2004**, *11* S10-S17.

(81) High, K. H.;Nathwani, A.;Spencer, T.; Lillicrap, D. *Haemophilia*, **2014**, *20* 43-49.

(82) Stacey, K. J.;Ross, I. L.; Hume, D. A. *Immunol. Cell Biol.*, **1993**, *71* 75-85.

(83) Rahman, M. A.;Amin, A. R. M. R.;Wang, X.;Zuckerman, J. E.;Choi, C. H. J.;Zhou, B.;Wang, D.;Nannapaneni, S.;Koenig, L.;Chen, Z.;Chen, Z.;Yen, Y.;Davis, M. E.; Shin, D. M. *J. Controlled Release*, **2012**, *159* 384-392.

(84) Jewell, C. M.; Lynn, D. M. *Current Opinion in Colloid & Interface Science*, **2008**, *13* 395-402.

(85) Prevette, L. E.;Kodger, T. E.;Reineke, T. M.; Lynch, M. L. *Langmuir*, **2007**, *23* 9773-9784.

(86) Gonzalez, H.;Hwang, S. J.; Davis, M. E. *Bioconjugate Chem.*, **1999**, *10* 1068-1074.

(87) Beyerle, A.;Irmler, M.;Beckers, J.;Kissel, T.; Stoeger, T. *Mol. Pharm.*, **2010**, *7* 727-737.

(88) Khansarizadeh, M.;Mokhtarzadeh, A.;Rashedinia, M.;Taghdisi, S.;Lari, P.;Abnous, K.; Ramezani, M. *Hum. Exp. Toxicol.*, **2016**, *35* 377-387.

(89) Zintchenko, A.;Philipp, A.;Dehshahri, A.; Wagner, E. *Bioconjugate Chem.*, **2008**, *19* 1448-1455.

(90) Grandinetti, G.;Smith, A. E.; Reineke, T. M. *Mol. Pharm.*, **2012**, *9* 523-538.

(91) Tolar, J.;Mcgrath, J. A.;Xia, L.;Riddle, M. J.;Lees, C. J.;Eide, C.;Keene, D. R.;Liu, L.;Osborn, M. J.;Lund, T. C.;Blazar, B. R.; Wagner, J. E. *J Invest Dermatol*, **2014**, *134* 1246-1254.

(92) Wilkins, L. M.;Watson, S. R.;Prosky, S. J.;Meunier, S. F.; Parenteau, N. L. *Biotechnol. Bioeng.*, **1994**, *43* 747-756.

(93) Barry, F. P.; Murphy, J. M. *The International Journal of Biochemistry & Cell Biology*, **2004**, *36* 568-584.

(94) Di, W.-L.;Larcher, F.;Semenova, E.;Talbot, G. E.;Harper, J. I.;Del Rio, M.;Thrasher, A. J.; Qasim, W. *Mol. Ther.*, **2011**, *19* 408-416.

(95) Okita, K.;Nakagawa, M.;Hyenjong, H.;Ichisaka, T.; Yamanaka, S. *Science*, **2008**, *322* 949-953.

(96) Reineke, T. M.; Davis, M. E. *Bioconjugate Chem.*, **2003**, *14* 255-261.

(97) Tolstyka, Z. P.;Phillips, H.;Cortez, M.;Wu, Y.;Ingle, N.;Bell, J. B.;Hackett, P. B.; Reineke, T. M. *ACS Biomaterials Science & Engineering*, **2016**, *2* 43-55.

(98) Sizovs, A.;Xue, L.;Tolstyka, Z. P.;Ingle, N. P.;Wu, Y.;Cortez, M.; Reineke, T. M. *J. Am. Chem. Soc.*, **2013**, *135* 15417-15424.

(99) Xue, L.;Ingle, N. P.; Reineke, T. M. *Biomacromolecules*, **2013**, *14* 3903-3915.

(100) Fichter, K. M.;Ingle, N. P.;Mclendon, P. M.; Reineke, T. M. *ACS Nano*, **2013**, *7* 347-364.

(101) Reitsma, S.;Slaaf, D. W.;Vink, H.;Van Zandvoort, M. a. M. J.; Oude Egbrink, M. G. A. *Pflugers Archiv*, **2007**, *454* 345-359.

(102) Ruponen, M.;Honkakoski, P.;Tammi, M.; Urtti, A. *J. Gene Med.*, **2004**, *6* 405-414.

(103) Correa, S.;Dreaden, E. C.;Gu, L.; Hammond, P. T. *J. Controlled Release*, **2016**.

(104) Bolte, S.; Cordelières, F. P. *Journal of Microscopy*, **2006**, *224* 213-232.

 (105) Tolar, J.;Xia, L.;Riddle, M. J.;Lees, C. J.;Eide, C. R.;Mcelmurry, R. T.;Titeux, M.;Osborn, M. J.;Lund, T. C.;Hovnanian, A.;Wagner, J. E.; Blazar, B. R. *J Invest Dermatol*, **2011**, *131* 848-856.

 (106) Srinivasachari, S.;Liu, Y.;Prevette, L. E.; Reineke, T. M. *Biomaterials*, **2007**, *28* 2885-2898.

 (107) Culty, M.;Nguyen, H. A.; Underhill, C. B. *The Journal of Cell Biology*, **1992**, *116* 1055-1062.

 (108) Damke, H.;Baba, T.;Van Der Bliek, A. M.; Schmid, S. L. *The Journal of Cell Biology*, **1995**, *131* 69-80.

 (109) Perumal, O. P.;Inapagolla, R.;Kannan, S.; Kannan, R. M. *Biomaterials*, **2008**, *29* 3469-3476.

 (110) Rejman, J.;Bragonzi, A.; Conese, M. *Mol. Ther.*, **2005**, *12* 468-474.

 (111) Medina-Kauwe, L. K.;Xie, J.; Hamm-Alvarez, S. *Gene Ther.*, **2005**, *12* 1734-1751.

 (112) Kastrup, L.;Oberleithner, H.;Ludwig, Y.;Schafer, C.; Shahin, V. *J. Cell. Physiol.*, **2006**, *206* 428-434.

 (113) Mishra, D.;Kang, H. C.;Cho, H.; Bae, Y. H. *Macromol. Biosci.*, **2014**, *14* 831-841.

 (114) Kim, H.;Kim, H. A.;Bae, Y. M.;Choi, J. S.; Lee, M. *J. Gene Med.*, **2009**, *11* 515-522.

 (115) Glover, D. J.;Lipps, H. J.; Jans, D. A. *Nat. Rev. Genet.*, **2005**, *6* 299-310.

 (116) Yin, L.;Dalsin, M. C.;Sizovs, A.;Reineke, T. M.; Hillmyer, M. A. *Macromolecules*, **2012**, *45* 4322-4332.

 (117) Dhande, Y. K.;Wagh, B. S.;Hall, B. C.;Sprouse, D.;Hackett, P. B.; Reineke, T. M. *Biomacromolecules*, **2016**, *17* 830-840.

 (118) Boyle, W. S.;Senger, K.;Tolar, J.; Reineke, T. M. *Biomacromolecules*, **2017**, *18* 56-67.

 (119) Horn, H. M.; Tidman, M. J. *Clin. Exp. Dermatol.*, **2002**, *27* 707-710.

 (120) Kiritsi, D.;Has, C.; Bruckner-Tuderman, L. *Cell Adhesion & Migration*, **2013**, *7* 135-141.

 (121) Boeira, V. L. S. Y.;Souza, E. S.;Rocha, B. D. O.;Oliveira, P. D.;Oliveira, M. D. F. S. P. D.;Rêgo, V. R. P. D. A.; Follador, I. *Anais Brasileiros de Dermatologia*, **2013**, *88* 185-198.

 (122) Tremblay, P. C. P. C. S. S.-V. B. M. J. *Gene Ther.*, **2001**, *8* 1387-1394.

 (123) Yin, W.;Xiang, P.; Li, Q. *Anal. Biochem.*, **2005**, *346* 289-294.

 (124) Yu, M.;Niu, Y.;Zhang, J.;Zhang, H.;Yang, Y.;Taran, E.;Jambhrunkar, S.;Gu, W.;Thorn, P.; Yu, C. *Nano Research*, **2016**, *9* 291-305.

 (125) Kretzmann, J. A.;Ho, D.;Evans, C. W.;Plani-Lam, J. H. C.;Garcia-Bloj, B.;Mohamed, A. E.;O'mara, M. L.;Ford, E.;Tan, D. E. K.;Lister, R.;Blancafort, P.;Norret, M.; Iyer, K. S. *Chemical Science*, **2017**, *8* 2923-2930.

 (126) Männistö, M.;Rönkkö, S.;Mättö, M.;Honkakoski, P.;Hyttinen, M.;Pelkonen, J.; Urtti, A. *J. Gene Med.*, **2005**, *7* 466-476.

 (127) Fu, Y.;Sander, J. D.;Reyon, D.;Cascio, V. M.; Joung, J. K. *Nat Biotech*, **2014**, *32* 279-284.

 (128) Choi, J. S.;Ko, K. S.;Park, J. S.;Kim, Y.-H.;Kim, S. W.; Lee, M. *Int. J. Pharm.*, **2006**, *320* 171-178.

(129) Louis, K. S.; Siegel, A. C. In *Mammalian Cell Viability: Methods and Protocols*; Stoddart, J. M., Ed.; Humana Press: Totowa, NJ, 2011, p 7-12.

Appendix 1: Chapter 2 Supporting Information

Toxicity of heparin-Tr4 transfection

Toxicity was monitored using the live-dead stain, propidium iodide during all flow cytometry experiments (Figure S2.1B). No significant toxicity was observed during any of these experiments according to propidium iodide (PI) staining, even for formulations known to cause significant toxicity such as PEI. Due to the length of the experiment, and the need for media changes and phosphate buffered saline (PBS) washes prior to trypsinization, we hypothesized that dead cells were being washed away during the assay, and were not counted during flow cytometry analysis.

To better measure the toxicity of our transfections, a trypan blue dye exclusion assay was performed after transfection of primary fibroblasts with PEI, Tr4, and Tr4-heparin based on an established protocol.[129] Cells were transfected in the same manner described in the green fluorescent protein (GFP) Expression Assays section of the materials and methods. 72 hours after transfection, cells were trypsinized, and transferred to falcon tubes. After centrifugation, each sample was resuspended in 100 µL DMEM. Each sample was then stained for 3 min with trypan blue (Thermo Fisher Scientific), and counted using a hemocytometer. The total number of viable cells was quantified. The results were normalized to a cells only control.

As shown in Figure S2.1A below, PEI was found to be highly toxic while Tr4 and Tr4-heparin were not significantly different from the cells only control.
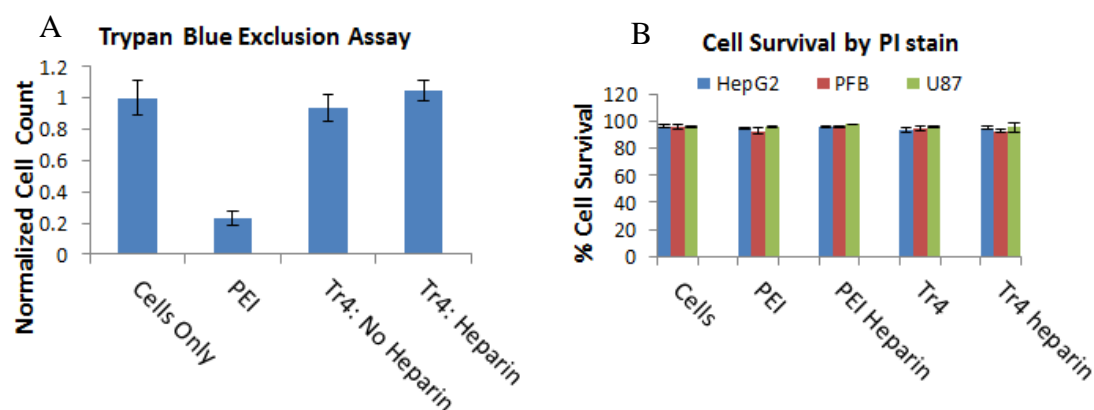
Figure S2.1. A) Trypan blue exclusion assay for cell viability after transfection. Cell count results are normalized to the cells only control. **B)** Percent cell survival measured by propidium iodide stain after GFP expression assay for each cell type. Error bars represent the standard deviation of 3 sample measurements.

Calculation of overall charge ratio

The charge ratio of the polyplexes after heparin treatment were calculated and are shown in Table S1. The charge ratio of the heparin treated polyplexes (N/(P+S), where S = sulfate groups on the heparin) was found to be 3.6.

Table S2.1: Calculation of Charge Ratio.

Component	Mass (g)	Molar Mass per charge (g/mol/Z)	Charge/mol	Charge Ratio (N/P+S)
Tr4 (N)	3.6×10^{-5}	182	2.0×10^{-7}	3.6
Heparin (S)	6.6×10^{-6}	143	4.6×10^{-8}	
DNA (P)	3.3×10^{-6}	330	1.0×10^{-8}	

Transfection with polystyrene sulfonate in primary fibroblasts

Polystyrene sulfonate (PSS) was used as a non-biological analog for heparin. The transfection was performed in the same manner described in the GFP expression assay section of the main manuscript using an equivalent sulfate concentration to 10 µg/mL heparin (6.6 µg after dilution) (12 µg/mL PSS). Sulfate concentrations were determined based on the average sulfate per repeat unit present in heparin and PSS. The transfection

was completed with 30 kDa PSS and 200 kDa PSS purchased from PSS Polymer Standards and used as received.

As shown in Figure S2.2 below, PSS had a strong inhibitory effect on transfection with Tr4 in primary fibroblasts. These results indicate that the carbohydrate moieties present in glycosaminoglycans are essential to increased transfection with Tr4 in primary fibroblasts.

Polystyrene Sulfonate Transfections
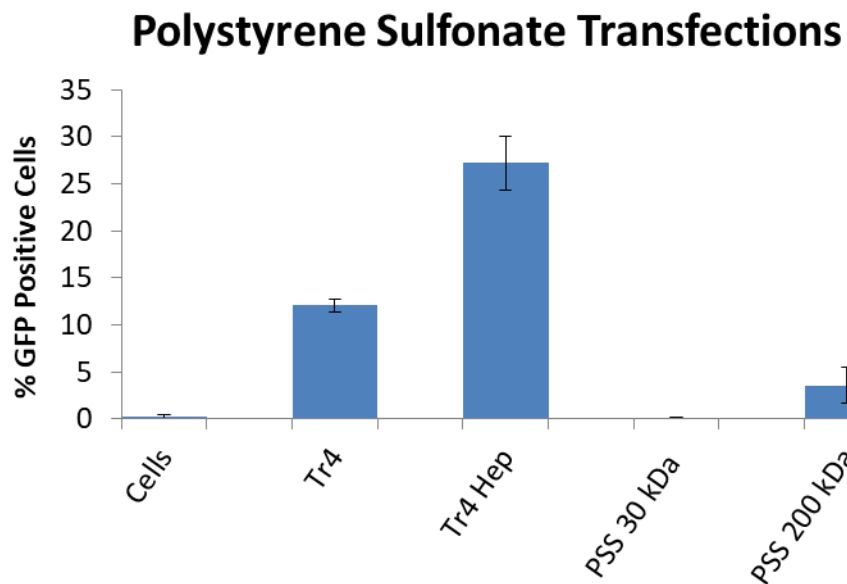
Figure S2.2. Effect of polystyrene sulfonate on transfections with Tr4. PSS was added to the transfection media at a concentration of 12 μg/mL to match the sulfate content used in the heparin transfections. Error bars represent the standard deviation of 3 samples.

Transfection with PEI and 2 μg/mL heparin

Because PEI polyplexes were unstable at higher heparin concentrations, we transfected PFBs and HepG2 cells with PEI at an N/P ratio of 5 with and without heparin at a concentration of 2 μg/ml.

The addition of 2 μg/ml inhibits PEI transfection efficiency in both cell types. However, it does not completely diminish transfection in the manner observed using 10

µg/ml of added heparin (in the dilution media, leading to a final concentration of 6.7 µg/mL). These polyplexes retain their stability at this formulation. Because low level transfection is observed, it appears heparin is unable to provide the same benefit to PEI that it offers to Tr4.
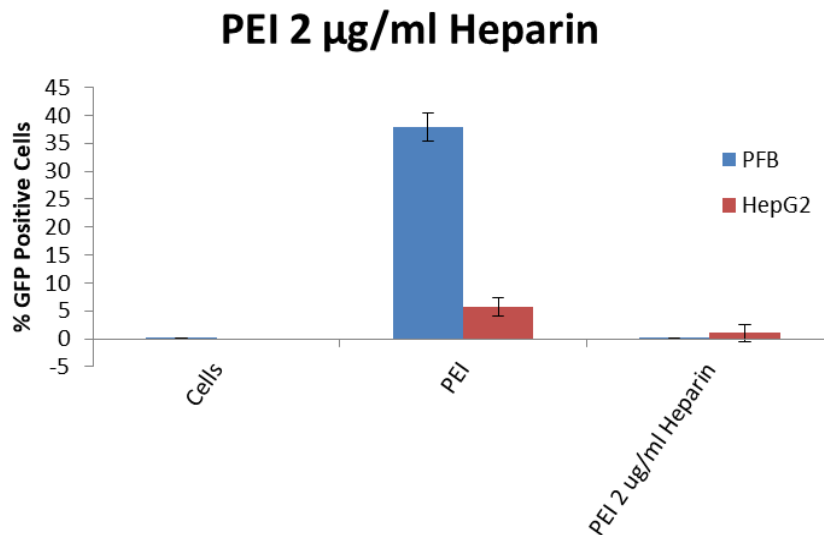

Figure S2.3: Transfection with PEI and 2 µg/ml heparin. Cells were transfected with PEI at an N/P ration of 5 using the same protocol used for the GFP expression experiments, but with 2 µg/mL heparin (1.3 µg/mL after dilution). Analysis was performed 48 hours post-transfection of the HepG2 cells and 72 hours post-transfection for PFBs. Error bars represent the standard deviation of 3 replicates.

Polymer-heparin complexes

Complexes formed from only polymer and heparin were produced to examine the effect of polymer-heparin complexes on DLS and zeta potential measurements. Measurements were taken on a Malvern Zetasizer Nano ZS using the same protocol used for polyplex characterization. These interpolyelectrolyte solutions were formed in water using the same conditions used in polyplex formulation, but without the addition of DNA. The polymer solutions were then diluted by a factor of 2 using PBS containing 10 µg/mL heparin. The resulting formulations were then analyzed by DLS and zeta

potential. The results can be seen in Figure S2.4. Heparin and polymer are able to form

complexes that could contribute the signal acquired during DLS and Zeta potential of
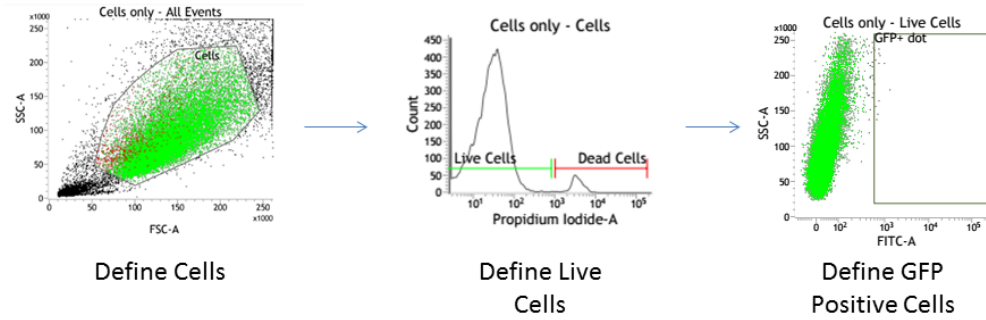
ternary complexes.
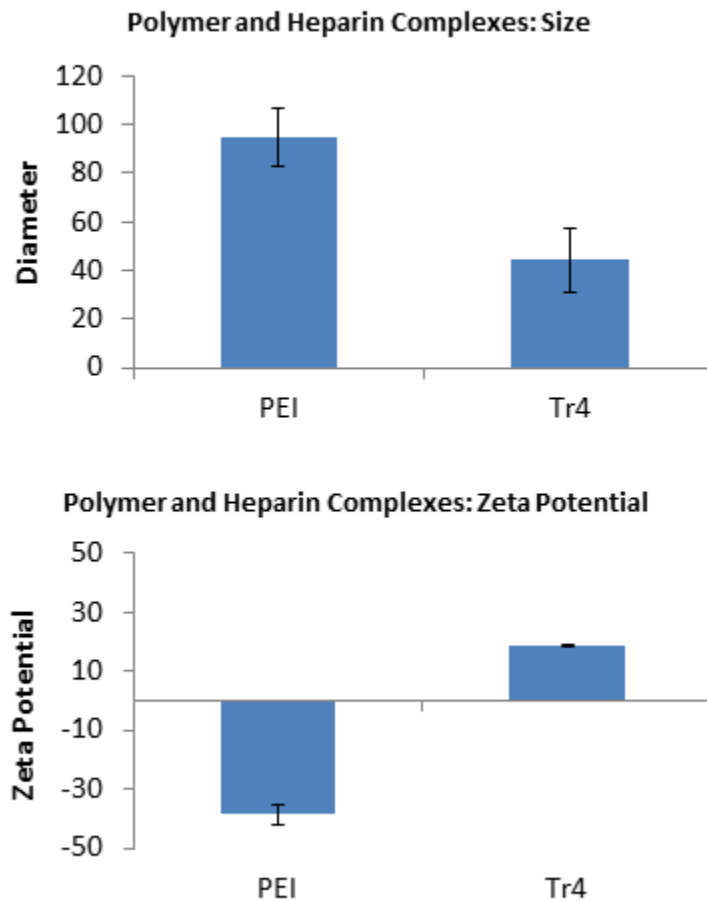
Figure S2.4: DLS and Zeta Potential collected on a Malvern Zetasizer Nano ZS of complexes formed from only polymer and heparin using the equivalent amount of polymer and heparin used in polyplex formulations (N/P = 5 for PEI and 20 for Tr4). Error bars represent the standard deviation of 3 replicates.

Gating strategy and representative dot plots

The gating strategy used for all experiments can be seen in Figure S2.5a-b. The cell population was defined in the forward scatter side scatter (FSC SSC) plot. Debris (represented by small SSC and FSC values) were gated out. From the cell population, live cells were selected based on lack of PI staining. As can be seen in Figure S2.1B, these populations consisted of almost all cells (dead cells are washed away). Finally, from the live cells, GFP or Cy5 positive cells were selected against a cells only negative control. The positive gates were set so that no more than 0.05% of untransfected cells were counted positive, and so that cells transfected with a positive control were contained within the gate. PEI was used as a positive control to set voltages and to help define the GFP/Cy5 positive gate. Representative dot plots for each cell type and each transfection condition can be seen in Figure S2.5c-e.
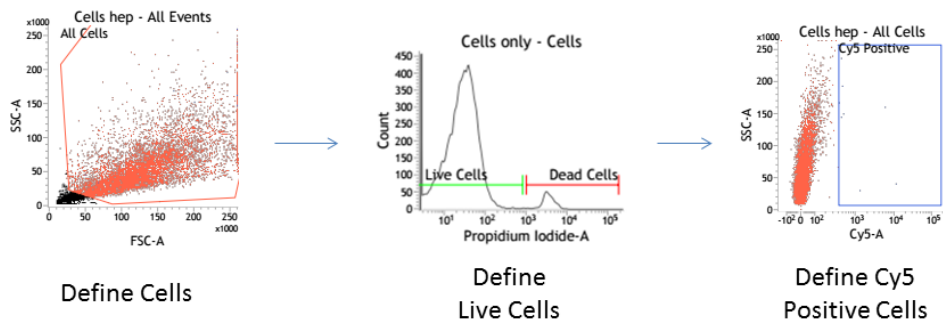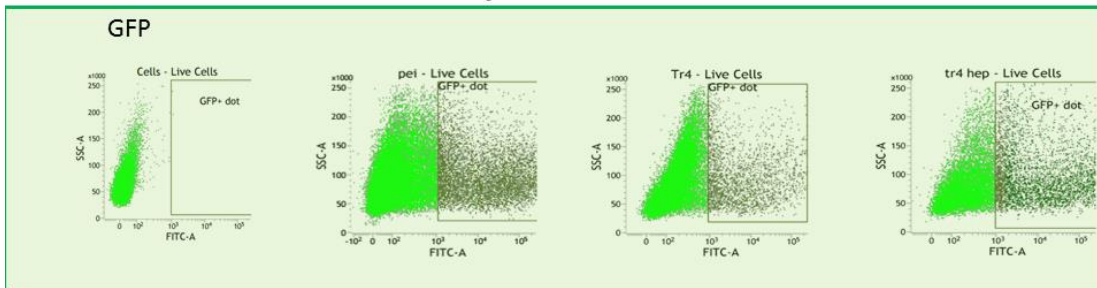
A

Gating Scheme: GFP

Define Cells   Define Live Cells   Define GFP Positive Cells

B

Gating Scheme: Cy5

Define Cells   Define Live Cells   Define Cy5 Positive Cells

124

C

Primary Fibroblasts

GFP

Cells Only   PEI   Tr4   Tr4-Heparin
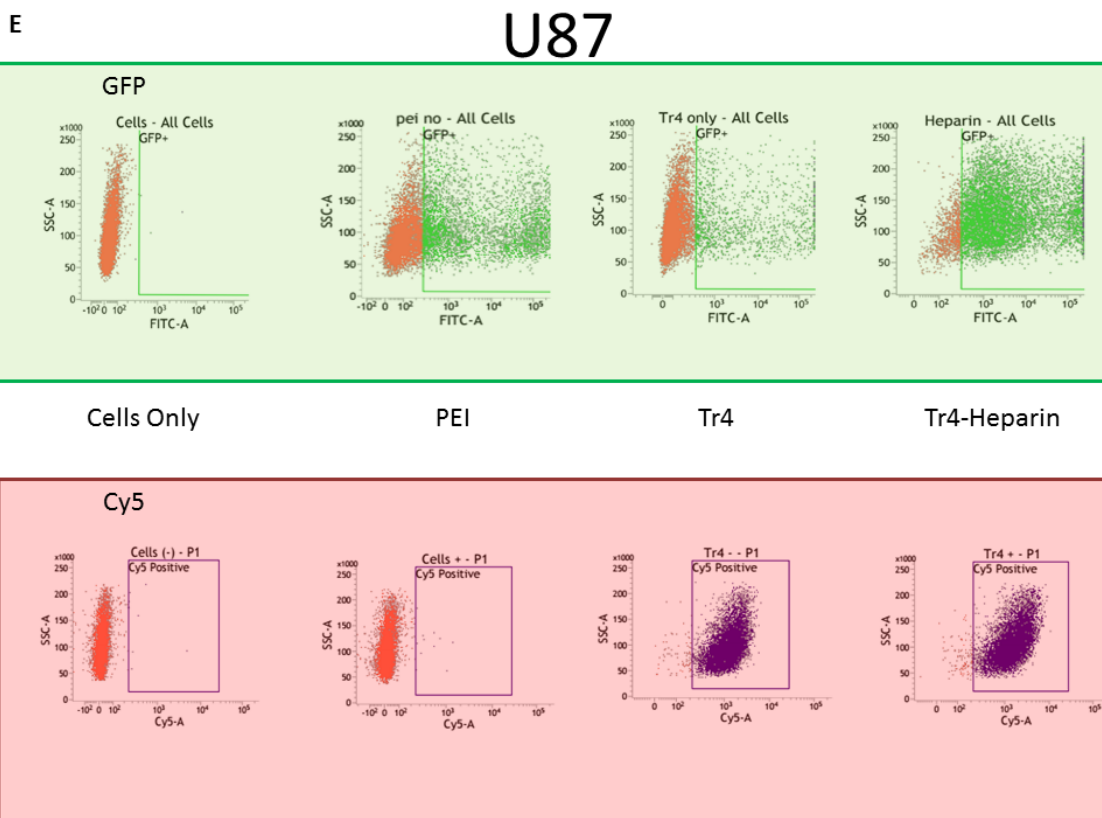
Cy5

D

HepG2

GFP

Cells Only   PEI   Tr4   Tr4-Heparin

Cy5
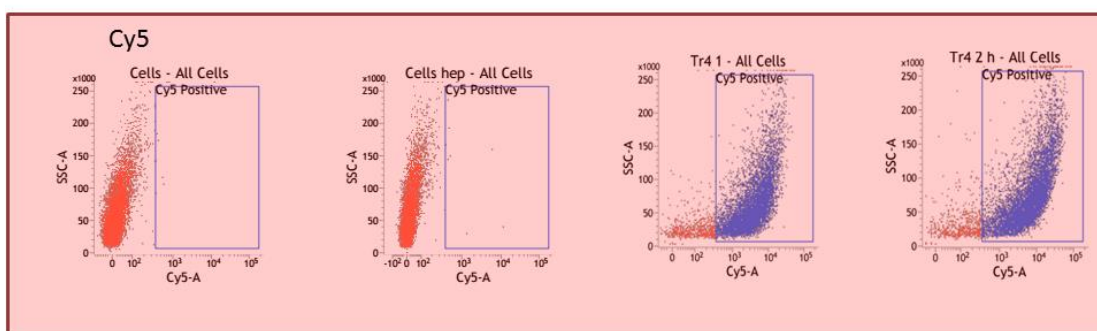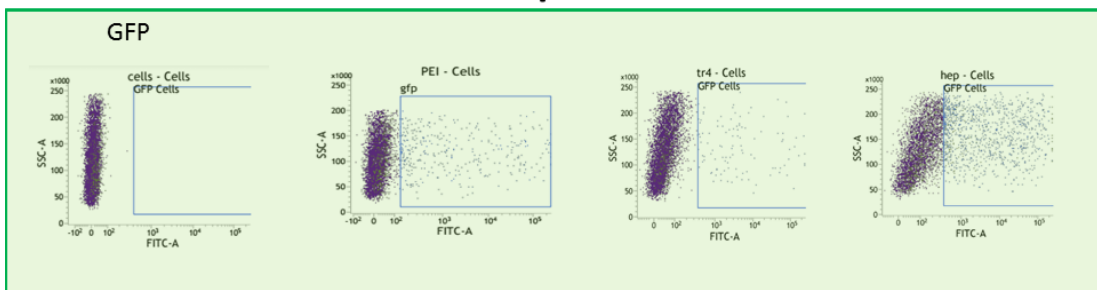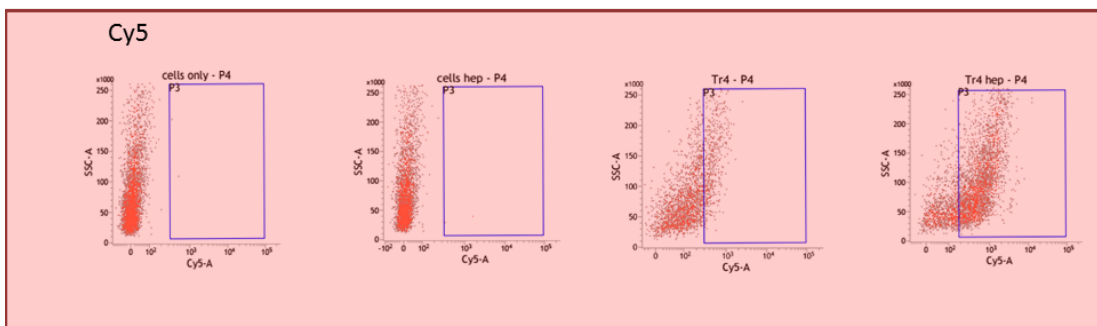
Figure S2.5: A-B) Gating schemes for GFP and Cy5 positive cells. From left to right, definition of all cells followed by live cells, and finally GFP/Cy5 positive cells. C-E) Representative dot plots for GFP+ (top) and Cy5+ (bottom) cells for each cell type from cells only, PEI, Tr4, and Tr4 heparin samples.

Plasmid Sequences.

Plasmids encoding green fluorescent protein were purchased from Aldevron (Fargo, ND). To ensure that the large plasmid contained the same promoter and reporter as the small plasmid, we purchased a large plasmid based on pszGreen containing a noncoding sequence in the backbone of the plasmid.
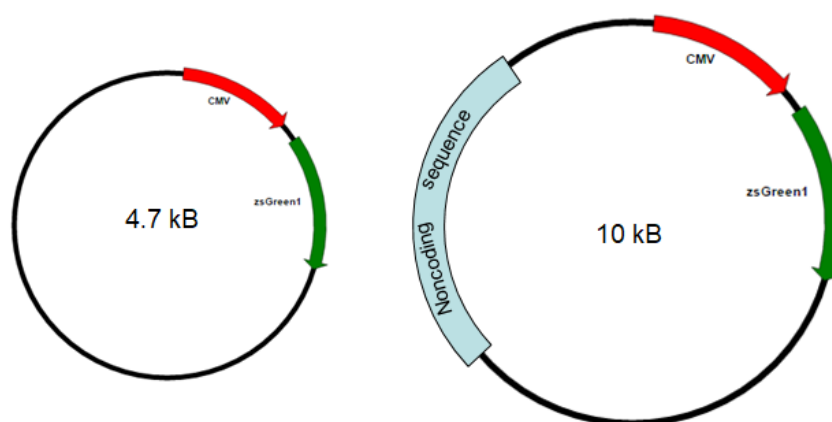

**Figure S3.1**: Plasmid maps for pzsGreen (4.7 kbp) and pzsGreen-10k (10 kbp)

Cell Cycle Analysis

Primary fibroblasts were treated with a double thymidine block prior to transfection. To quantify the effect of the double thymidine block, cells were lifted and stained with Vybrant® DyeCycle[TM] Ruby stain (ThermoFisher Scientific) using the manufacturer's protocol. Three populations of cells with increasing Ruby intensity were identified corresponding to G0/G1, S and G2/M respectively. The thymidine block reduces the number of cells in G0/G1 from 72% to 12% at block release. At block release (when the transfection was started) 66% of the cells are in S or G2/M. This should

guarantee that a much larger fraction of cells will undergo division during the transfection compared to a transfection of an unblocked population.
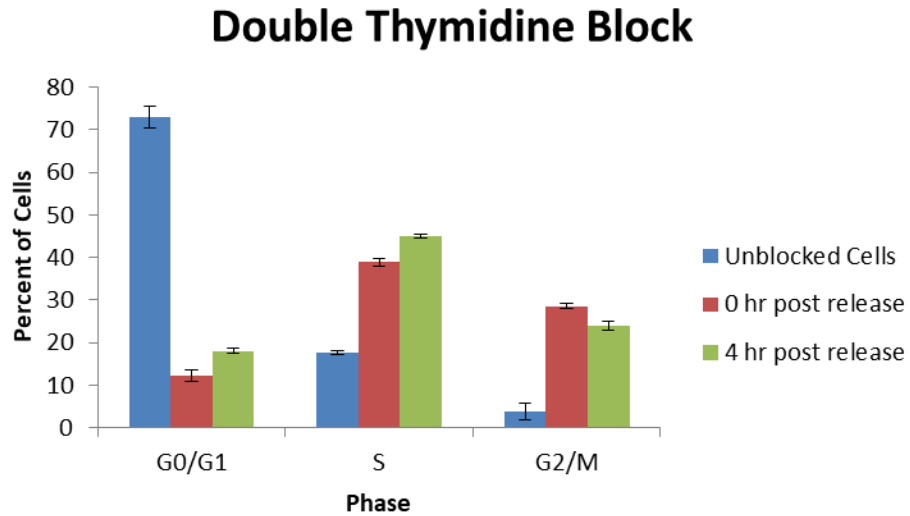
Figure S3.2: Cell cycle analysis of double thymidine blocked primary fibroblasts. Cell cycle determined by Vybrant® DyeCycle^{TM} Ruby stain. Error bars represent the standard deviation of three replicates.
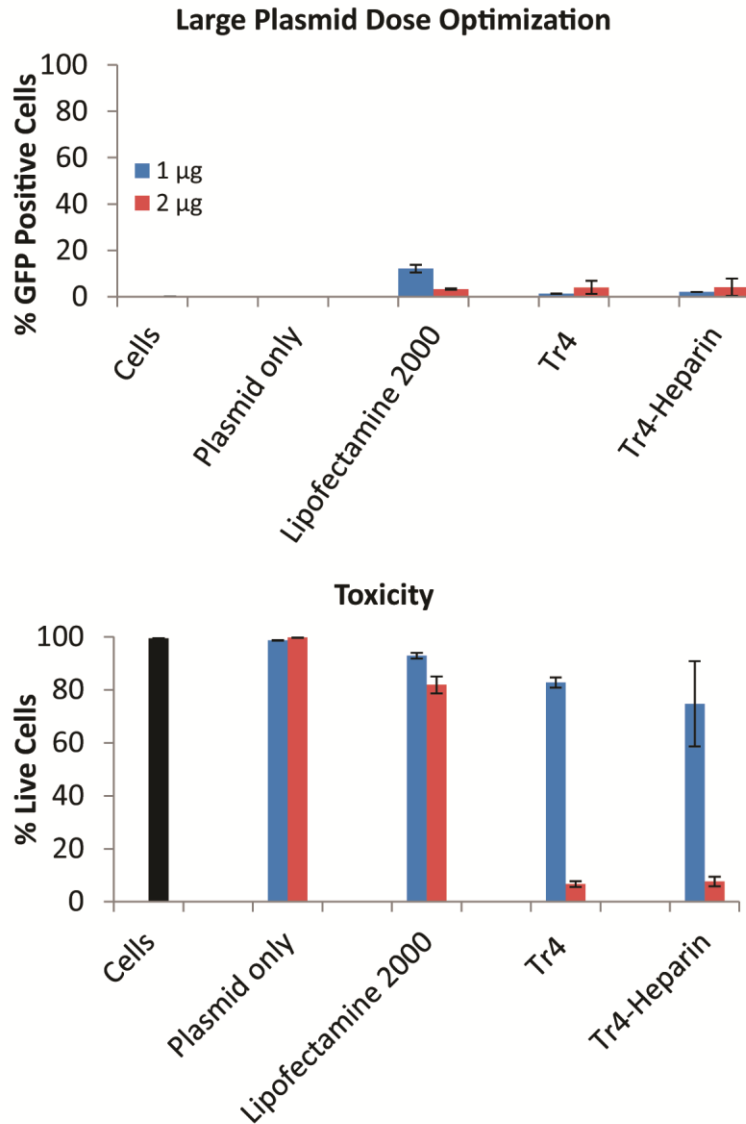
Figure S3.3: Optimization of large plasmid transfection dose in primary fibroblasts.

pDNA Dose Optimization

  To ensure that the optimal dose of large plasmid was being used, we investigated

the effect of increasing plasmid dose with the large plasmid. Cells were treated with 1

and 2 μg per well with the 10 kbp plasmid. All Tr4 polyplexes were formed at and N/P of

40. Lipofectamine 2000 transfections were performed using 5 μl/μg DNA. Keeping the

N/P ratios consistent lead to the use of twice as much polymer for the 2 μg transfections.

Polyplexes were formed in the same final transfection volume (300 μl) for both doses. The results showed that 1 μg per well was the optimal dose for the small plasmid. Increasing the dose to 2 μg/well did not provide any increase in transfection efficiency, but dramatically increased toxicity. The cells transfected with 2 μg/well plasmid DNA were almost entirely dead 48 hrs post transfection, and showed no evidence of GFP fluorescence.

Toxicity of transfection as a function of plasmid size
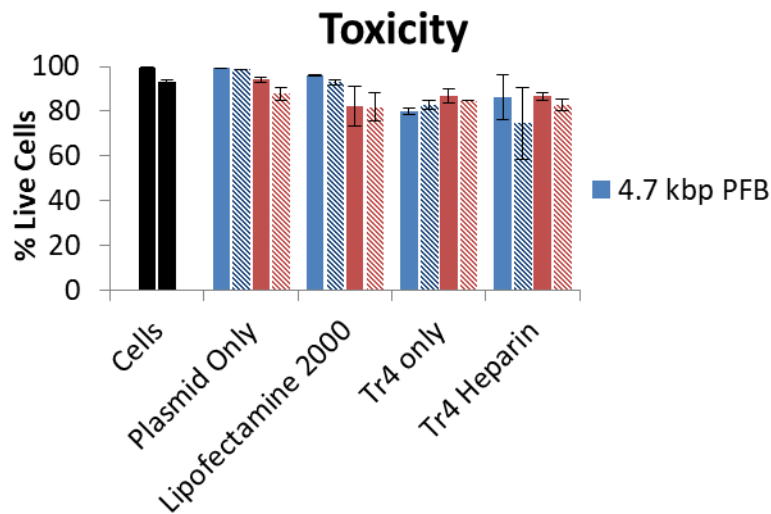

Figure S3.4: Toxicity of transfections in primary fibroblasts and iPSCs as quantified by propidium iodide staining. Error bars represent the standard deviation of 3 replicates. Toxicity was quantified by propidium iodide staining during GFP expression analysis.

Toxicity. Cells were transfected with 4.7 and 10 kbp plasmids formulated as described above. Cells were treated with propidium iodide prior to analysis by flow cytometry. Gates were set based on an untransfected control. No significant difference in toxicity was observed between large and small plasmid transfections in either cell type. Tr4 and Tr4-heparin transfections show approximately 80-85% cell survival for both cell types. Live cells were analyzed for gene expression. In a gene editing experiment, only

live transfected cells would be able to undergo editing. The analysis of only live cells during transfection ensures that only cells that could potentially undergo editing in a practical are shown as positive.

**Tr4 polyplex Z_{ave} size and stability as a function of plasmid size**
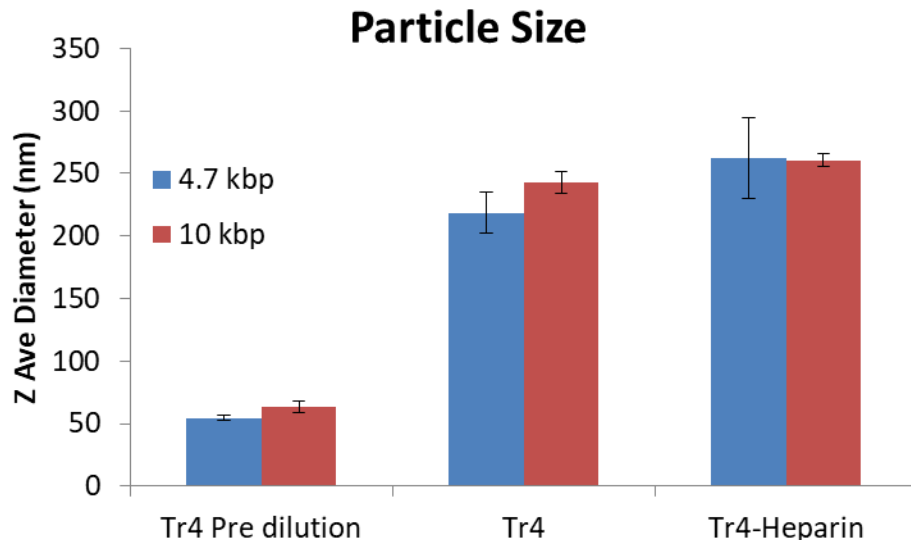
Figure S3.5: Particle size of Tr4 polyplexes as a function of plasmid size quantified by DLS. Error bars represent the standard deviation of 3 replicates. No significant differences were observed as a function of plasmid size.

Polyplexes were formed as described herein. After polyplex formation, the polyplexes were analyzed by DLS using a Malvern Zetasizer Nano ZS (Malvern Instruments, Malvern, UK) with a 4.0 mW 633 nm HeNe laser and a scattering angle of 173°. Polyplexes were formed in water at an N/P of 40 at a pDNA concentration of 0.01 μg/μl. Prior to dilution with media, the size of the polyplexes in water was determined by DLS (Figure S3.5). The polyplexes were then diluted by a factor of 3 with serum free DMEM with or without 10 μg/mL heparin just as they are prior to transfection, and analyzed by DLS (Figure S3.6).

The results can be seen in Figure S3.5. No significant difference can be observed as a function of plasmid size. In pure water, the particles are ~50 nm in diameter. After treatment with cell culture media, they begin to swell or aggregate to ~250 nm. However, particles formed with small and large plasmids increase in same manner.

SI 3.5: Polyplex stability as a function of plasmid size
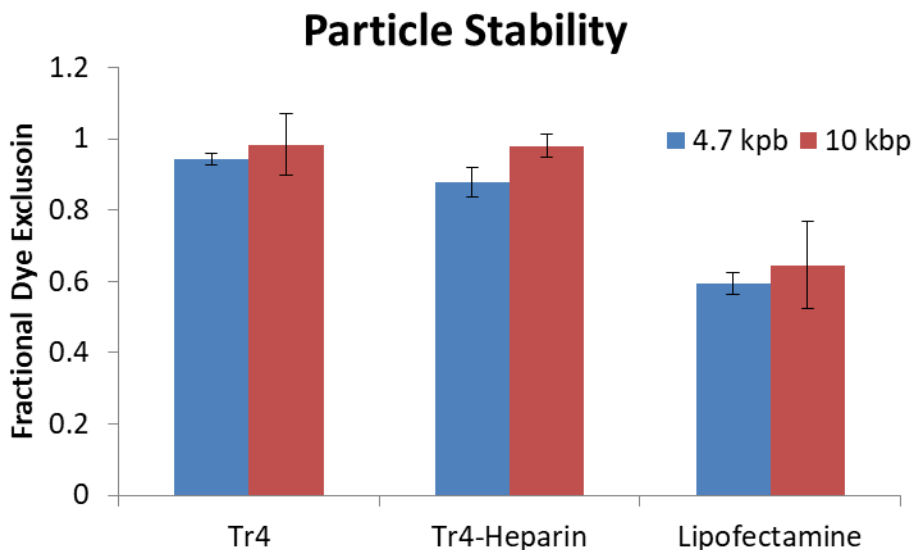
Figure S3.6: Ethidium bromide dye exclusion as a function of plasmid size. Error bars represent the standard deviation of three replicates.

Polyplex stability was assessed using an ethidium bromide dye exclusion assay as previously described. Polyplexes were formed in water at N/P 40 for Tr4 and Tr4-heparin, and with 5 μl lipofectamine/μg DNA. After polyplex formation, polyplex solutions were diluted by a factor of 3 with cell culture media (with or without 10 μg/mL heparin) containing 4 μM EtBr. Samples were then analyzed for EtBr fluorescence (620 nm) compared to DNA alone and a DNA free blank. Dye exclusion was determined using the formula below.

$$Fractional\ Dye\ Exclusion = 1 - \frac{F_{sample} - F_{blank}}{F_{DNA\ only} - F_{blank}}$$

In a solution of free DNA, EtBr can easily intercalate the DNA, leading to increased EtBr fluorescence. In polyplex solutions, complexation of the DNA inhibits EtBr intercalation, and fluorescence is reduced. As can be seen in Figure S3.6, there is no difference between polyplexes formed with small and large plasmid. For Tr4 and Tr4-heparin polyplexes both exhibit almost 100% dye exclusion. Lipofectamine complexes do not completely exclude EtBr, but also show no change with plasmid size.